

Dissertation zur Erlangung des Doktorgrades  
der Fakultät für Chemie und Pharmazie  
der Ludwig-Maximilians-Universität München

# **Synthetic Strategies to Novel Multinary Nitrides of Gallium**

Frauke Charlotte Hintze

aus

München, Deutschland

2013

**Erklärung:**

Die vorliegende Dissertation wurde im Sinne von § 7 der Promotionsordnung vom 28. November 2011 von Herrn Prof. Dr. Wolfgang Schnick betreut.

**Ehrenwörtliche Versicherung:**

Diese Dissertation wurde eigenständig und ohne unerlaubte Hilfsmittel erarbeitet.

München, den 16.05.2013

.....

(Frauke Hintze)

Dissertation eingereicht am 16. Mai 2013

1. Gutachter Prof. Dr. Wolfgang Schnick

2. Gutachter Prof. Dr. Hubert Huppertz

Mündliche Prüfung am 23. Juli 2013



*Meiner Familie*





## **Danksagung**

Herrn Prof. Dr. Wolfgang Schnick möchte ich herzlich danken für die Überlassung des spannenden Forschungsthemas. Die Freiheit seinen eigenen Weg zu finden und das Thema jederzeit frei gestalten zu können ist nicht selbstverständlich. Nicht zuletzt machen die guten Arbeitsbedingungen und die großartige technische Ausrüstung das alles erst möglich.

Herrn Prof. Dr. Hubert Huppertz danke ich für seine Übernahme des Koreferats.

Herrn Prof. Dr. A. Hartschuh, Herrn Prof. Dr. Klapötke, Herrn Prof. Dr. K. Karaghiosoff und Herrn Prof. Dr. H.-C. Böttcher danke ich für die Bereitschaft, als weitere Prüfer zur Verfügung zu stehen.

Christian Minke danke ich besonders für die Aufnahme unzähliger EDX-Spektren und REM-Bilder, auch wenn er bis zu jetzt immer der Stickstoff versteckt hat. Dr. Peter Mayer und Thomas Miller danke ich für die Messungen meiner Kristalle. Wolfgang Wunschheim hat mich in allen technischen Fragestellungen unterstützt und mir damit viel erleichtert. Außerdem waren die Gespräche in illustrierter Mittagsrunde immer erfreulich und sehr unterhaltsam, dafür vielen Dank auch an Catrin Löhnert.

Meinen F-Praktikantinnen und Praktikanten sowie Bachelor Studentinnen und Studenten Veronika Weiß, (Chris)Tine Pösl, Alexander Müller, Peter Zehetmaier, Katrin Rudolf und Derya Bessinger danke ich für ihre tatkräftige Unterstützung. Besonders Tine und Katrin wünsche ich auf ihrem weiteren Weg in der Doktorarbeit alles Gute.

Ein großer Dank geht an meine Laborkollegen Felix Fahnbauer, Dr. Saskia Lupart, Tobias Rosenthal, Dr. Matthias Schneider, Thorsten Schröder und besonders Markus Seibald. Es hat mir viel Spaß gemacht in meinem Séparée von D2.100!

Meinen ehemaligen Betreuern Dr. Martin Zeuner und Dr. Alexander Zurawski bin ich sehr dankbar, sie haben mir den Spaß und die Neugier an der anorganischen Chemie gezeigt und ich freue mich, dass wir Freunde geworden und geblieben sind.

Allen ehemaligen und aktuellen Kollegen der Arbeitsgruppen Schnick, Johrendt, Schmedt auf der Günne, Oeckler, Lotsch und Müller-Buschbaum danke ich für die kollegiale und entspannte Atmosphäre.

Eva Wirnhier und Sandra Lengger haben mich nicht nur in meinem Studium sondern auch während der Doktorarbeit durch ihre Freundschaft sehr unterstützt. Ebenso bin ich meinen (auch nicht chemischen) Freunden, vor allem Diana Geißler, Dr. Marianne Martin, Cornelia Fehlner, Stefanie Gerstner und Andreas Maier für ihre Freundschaft sehr dankbar.

Allen aktuellen und ehemaligen Mitgliedern des Philips- und des Ammonothermal-Teams, Dr. Martin Zeuner, Cora Hecht, Markus Seibald, Dajana Durach, Philipp Pust, Tine Pösl, Jonas Häusler und Sebastian Schmiechen möchte ich für die gute Zusammenarbeit danken, diese beiden Themen haben mir durch euch noch viel mehr Spaß gemacht.

Besonders möchte ich meinen Eltern, Großeltern, Geschwistern sowie Dagmar und Uwe danken. Sie haben mich während meines Studiums und der Doktorarbeit immer unterstützt und mir Rückhalt gegeben. Ihr Vertrauen in mich und meine Fähigkeiten hat mich immer wieder überrascht und mir geholfen.

Ganz besonders möchte ich Sascha danken. Ohne ihn und seinen unerschütterlichen Glauben an mich hätte ich für manche Entscheidung nicht den Mut gehabt und wäre heute vielleicht woanders. Ich freue mich sehr auf unsere gemeinsame Zukunft!

*In der Wissenschaft gleichen wir alle nur den Kindern,  
die am Rande des Wissens hie und da einen Kiesel  
aufheben, während sich der weite Ozean des  
Unbekannten vor unseren Augen erstreckt.*

(Isaac Newton)



---

**Table of Contents**

1. Introduction.....	1
2. Ammonothermal Reaction Procedure .....	9
2.1. Introduction .....	10
2.2. Experimental.....	12
2.3. Results and Discussion .....	18
2.4. Conclusion .....	20
2.5. References .....	22
3. Magnesium Nitrides as Host Lattices for Eu <sup>2+</sup> -Doping .....	24
3.1. Introduction .....	26
3.2. Experimental Section.....	27
3.3. Results and Discussion .....	29
3.3.1. Crystal Structure Description .....	30
3.3.2. DFT Calculations and Soft X-ray Spectroscopy of Mg <sub>3</sub> GaN <sub>3</sub> .....	35
3.3.3. Luminescence Investigations .....	39
3.4. Conclusion .....	42
3.5. References .....	43
4. Ba <sub>3</sub> Ga <sub>3</sub> N <sub>5</sub> – A Novel Host Lattice for Eu <sup>2+</sup> -Doped Luminescent Materials .....	47
4.1. Introduction .....	49
4.2. Experimental .....	50
4.3. Results and Discussion .....	51
4.3.1. Crystal Structure of Ba <sub>3</sub> Ga <sub>3</sub> N <sub>5</sub> .....	51
4.3.2. Luminescence Investigations .....	57
4.3.3. DFT Calculations.....	58
4.4. Conclusion .....	59
4.5. References .....	60
5. Ca <sub>2</sub> Ga <sub>3</sub> MgN <sub>5</sub> – a Highly Condensed Nitridogallate .....	63

## Table of Contents

---

5.1.	Introduction .....	65
5.2.	Results and Discussion .....	66
5.3.	Conclusion .....	71
5.4.	Experimental Section .....	72
5.5.	References .....	74
6.	Nitridogallate Fluoride $\text{LiBa}_5\text{GaN}_3\text{F}_5$ .....	76
6.1.	Introduction .....	78
6.2.	Experimental .....	78
6.3.	Results and Discussion .....	79
6.3.1.	Crystal Structure .....	79
6.3.2.	Band Gap Determination.....	84
6.4.	Conclusion .....	87
6.5.	References .....	88
7.	Novel Nitrido-magnesiometalates of Ga and Al .....	90
7.1.	Introduction .....	92
7.2.	Experimental Section .....	93
7.3.	Results and Discussion .....	95
7.4.	Conclusion .....	102
7.5.	References .....	103
8.	Ammonothermal Synthesis and Crystal Structure of $\text{BaAl}_2(\text{NH}_2)_8 \cdot 2 \text{NH}_3$ .....	105
8.1.	Introduction .....	107
8.2.	Results and Discussion .....	108
8.3.	Conclusions .....	111
8.4.	Experimental Section .....	111
8.5.	References .....	113
9.	Discussion and Outlook.....	114
9.1.	Nitrides.....	114
9.2.	Nitridogallates .....	116

9.3. Outlook .....	118
9.4. References .....	121
10. Summary .....	122
10.1. Ammonothermal reactions .....	122
10.2. Magnesium Nitrides with Luminescence Properties $\text{Mg}_3\text{GaN}_3\text{:Eu}^{2+}$ and $\text{Mg}_3\text{N}_2\text{:Eu}^{2+}$ .....	123
10.3. Ternary Novel Nitridogallate $\text{Ba}_3\text{Ga}_3\text{N}_5$ .....	124
10.4. Quaternary Nitrido-magnesiogallate $\text{Ca}_2\text{Ga}_3\text{MgN}_5$ .....	124
10.5. Nitridogallate Fluoride $\text{LiBa}_5\text{GaN}_3\text{F}_5$ .....	125
10.6. Novel Nitrido-magnesiometalates of Ga and Al .....	126
11. Appendix .....	127
11.1. List of Publications within this thesis .....	127
11.2. Publications published prior to this thesis .....	129
11.3. CSD Numbers .....	129
11.4. Conference contributions .....	130
11.5. Curriculum Vitae .....	131





## 1. Introduction

The chemistry of multinary nitrides is in comparison to oxides and sulfides quite unexplored and still a rather young field of science. In 1998, *Niewa* postulated “that within the next few years, many nitride compounds with new or even unique structures and interesting properties will be discovered”.<sup>[1]</sup> In the same year, *Gregory* wrote, concerning nitride chemistry that “one suspects we have merely scratched the surface of what may yet exist.”<sup>[2]</sup> Both statements turned out to be true since the number of publications with “nitrid” in their topic still undergoes a nearly exponential growth (see Figure 1).

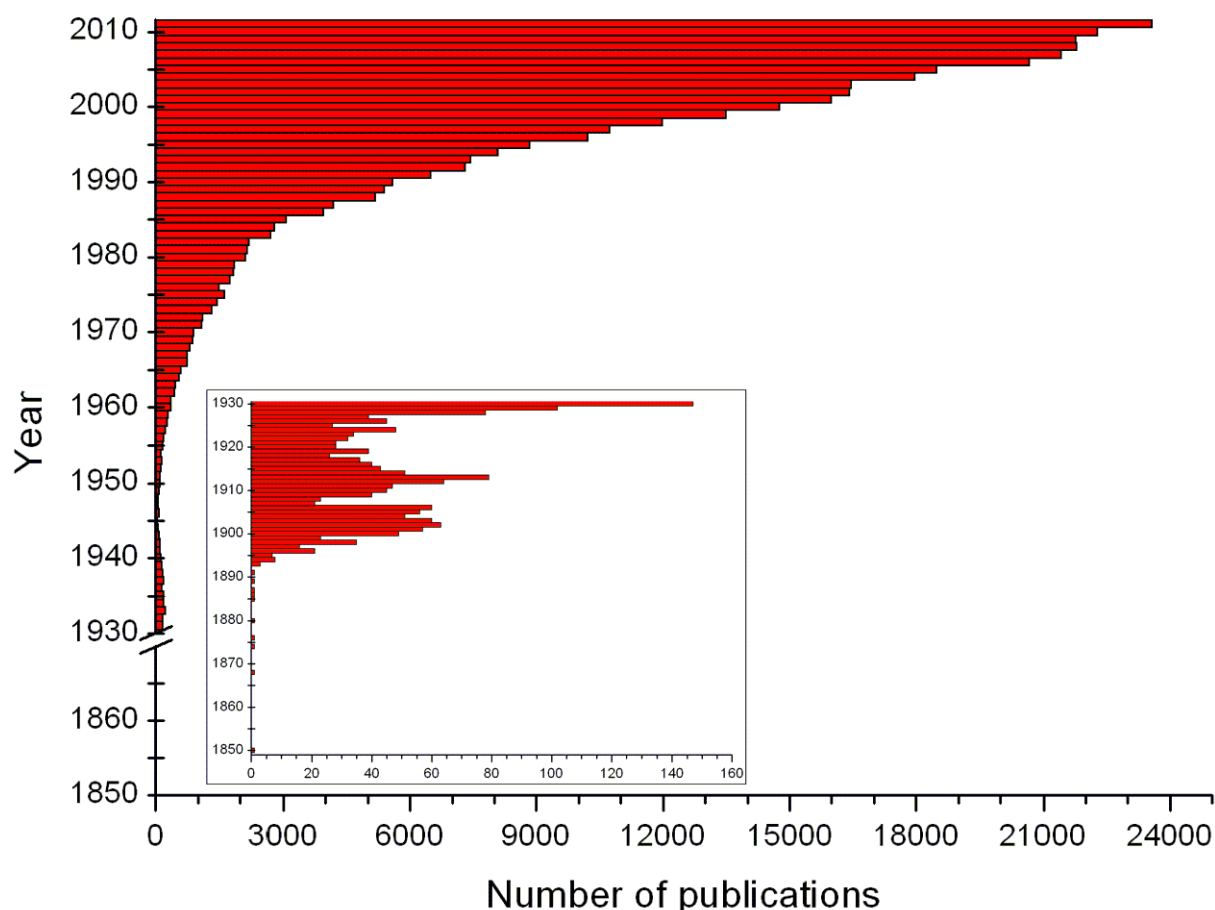


**Figure 1.** Number of publications on the topic “nitrid” until 2011 (Scifinder).

Synthesis of nitride compounds can be performed by classical solid-state methods like high-temperature reactions, high-pressure reaction or metathesis synthesis for example. An important factor for synthesis of nitrides is the strong triple bond in the

$\text{N}_2$  molecule. With a dissociation energy of  $945 \text{ kJ/mol}$ <sup>[3]</sup> for this bond the standard free energy of formation of nitrides is lower in comparison to similar compounds of neighboring elements.<sup>[4]</sup> As a consequence, nitrides are less stable upon heating through the loss of  $\text{N}_2$ . Furthermore, formation of  $\text{N}^{3-}$  requires much more energy than the formation of  $\text{O}^{2-}$ .<sup>[2,4]</sup> This can be easily seen from reaction of alkali metals, all of them react with oxygen but only Li forms a stable nitride ( $\text{Li}_3\text{N}$ ) in nitrogen.<sup>[5]</sup> Therefore, nitrides are comparably rare and build often unusual and unique structure types. For synthesis of nitrides in a solid-state reaction, diffusion of the reactant atoms is necessary to reach an interface between reacting materials and subsequently, these atoms must rearrange into a new structure.<sup>[5]</sup> Diffusion rates in solids are very slow, therefore, higher temperatures are necessary. Increasing the reaction temperature will lead mostly to thermodynamic products, resulting in binary and ternary compounds regarding nitrides. The high stability of those compounds hinders further reactions to multinary compounds. Additionally, the parameter temperature cannot be increased infinitely due to early decomposition of ternary compounds.<sup>[2]</sup> Another way to increase diffusion rates is the introduction of a melt. Therein, also lowering of activation energy for a solid-solid reaction can be observed and kinetically controlled products are accessible.<sup>[6]</sup> Melts can be formed by salts or metals but important prerequisites like a low melting point and a wide temperature area between melting and boiling point are necessary. Additionally, the melt should be easy to remove and not react with starting materials. For synthesis of binary nitrides or higher nitrides with alkaline earth metals, sodium is a widely used fluxing agent.<sup>[7-9]</sup> In combination with sodium azide as nitrogen source, reactions above  $570 \text{ K}$  lead to decomposition of the azide and an increased nitrogen pressure occurs in closed ampoules. For the growth of GaN with sodium-flux method it was shown, that Na can react as enhancing medium for nitride formation. Na is a quite electropositive element with a low ionization energy. If a  $\text{N}_2$  molecule absorbs on the surface of the melt it is supposed that Na transfers an electron to the  $\text{N}_2$  molecule and the antibonding orbital will be occupied. This results in a decrease of bond order and subsequently in a decrease of dissociation energy.<sup>[10,11]</sup> The solubility of nitrogen in liquid sodium can be further increased when alkaline earth elements Sr or Ba are present in the metallic melt.<sup>[11]</sup>

Nitrides can be divided into metallic (i.e. TiN), ionic (i.e. Li<sub>3</sub>N), or covalent (i.e. GaN) compounds,<sup>[12]</sup> or classified as binary, ternary, quaternary, and multinary compounds, depending on the number of constituting elements.<sup>[13]</sup>

Especially the binary nitride GaN has found increasing interest in industrial application as a wide band gap semiconductor.<sup>[14-18]</sup> For semiconductor devices, high quality GaN crystals are required. Therefore, a suitable substrate has to be found and research efforts focused on ammonothermal synthesis for production of high quality GaN substrate.<sup>[19]</sup> In this method, supercritical ammonia is used as reaction medium, generated in high pressure autoclaves at elevated temperatures. By control of filling degree, reactions are reproducible and reaction pressure can be estimated.<sup>[20]</sup> By addition of mineralizing agents, solubility of metals and other starting materials can be increased.<sup>[21,22]</sup> For synthesis of GaN mostly crystal growth techniques and doping of this material has been studied but synthesis of higher nitrides deriving from the binary compound has been widely neglected as yet.<sup>[23-26]</sup>

But not only binary nitrides have found application in industrial devices. In the past years, the compound class of nitridosilicates and oxonitridosilicates grew significantly since a general synthetic approach to these compounds was found using high-temperature synthesis and “Si(NH)<sub>2</sub>” as starting material.<sup>[27-30]</sup> The higher structural variety of nitridosilicates in comparison to oxosilicates is due to the higher connecting ability of N<sup>3-</sup> compared to O<sup>2-</sup>.<sup>[31]</sup> Nitrogen atoms in the crystal structure of nitridosilicates can be connect to one, two, three or even four silicon atoms in tetrahedral building blocks.<sup>[29,32-34]</sup> Additionally, not only corner but also edge sharing can be observed in nitridic structures and the degree of condensation  $\kappa$  (ratio of tetrahedra center to N atoms, i.e. Si : N in nitridosilicates) shows a wider spectrum compared to oxosilicates.<sup>[27]</sup> The structural variety was even extended by addition of Al and or O, resulting in oxonitridosilicates, nitridoalumosilicates or so-called SiAlONs. Recent research also focused on Li-containing nitridosilicates that can be obtained from high-temperature synthesis route or from Li-flux at lower temperatures.<sup>[35,36]</sup> The compound class of nitridosilicates shows interesting properties like high hardness (i.e. SrSi<sub>7</sub>N<sub>10</sub>), Li-ion conductivity (i.e. Li<sub>14</sub>Ln<sub>5</sub>[Si<sub>11</sub>N<sub>19</sub>O<sub>5</sub>]O<sub>2</sub>F<sub>2</sub> with Ln = Ce, Nd), or luminescence (i.e. Ba<sub>2</sub>Si<sub>5</sub>N<sub>8</sub>:Eu<sup>2+</sup>).<sup>[37-39]</sup>

Luminescence can be observed when a host lattice with high covalency is doped by an activator ion like Eu<sup>2+</sup> for example. Recently, Eu<sup>2+</sup>-doped nitridosilicates and

oxonitridosilicates turned out to be highly efficient phosphors for use in phosphor-converted light-emitting diodes (LEDs).<sup>[13,40-42]</sup> To obtain an efficient luminescence the materials host lattices must be chemically and thermally highly stable.<sup>[40,43,44]</sup> Detailed knowledge of structural features like surrounding environment of activator ion, symmetry, coordination, covalence and bond length to anions as well as resulting crystal field strength is necessary for understanding and a possible influence on the color point of emission and the broadness of emission band.<sup>[13,42,45]</sup>

Crystal structures of nitride compounds are mostly described as nitridometalate ions,<sup>[1]</sup> stabilized by electropositive elements like alkaline earth or rare earth. The crystal structures of nitridosilicates are therefore often clarified by description of  $\text{SiN}_4$  tetrahedra sharing corners and/or edges building one-, two-, or three-dimensional anionic substructures, charge balanced by alkali, alkaline earth, or rare-earth atoms. This structural motif of tetrahedra constituted of four nitrogen atoms and a metal/metalloid atom in the center is also known from other ternary or multinary nitrides like nitridoaluminates or nitridogallates. Like nitridosilicates derive from the binary nitride  $\text{Si}_3\text{N}_4$ , the latter mentioned compound classes derives from the binary nitrides  $\text{AlN}$  and  $\text{GaN}$ . Only a small number of ternary nitridogallates with alkaline earth elements was known so far. Only two ternary compounds with Ba, namely  $\text{Ba}_3\text{Ga}_2\text{N}_4$ <sup>[46]</sup> and  $(\text{Ba}_6\text{N})[\text{Ga}_5]$ <sup>[47]</sup> are known whereof the latter shows  $[\text{Ga}_5]^{7-}$  clusters and cannot be described by an anionic nitridic substructure charge balanced with electropositive atoms like in  $\text{Ba}_3\text{Ga}_2\text{N}_4$ . With alkaline earth elements Ca and Sr some more compounds are known, building one-, two, or three-dimensional substructures of  $\text{GaN}_4$  tetrahedra (i.e. 1D:  $\text{Ba}_3\text{Ga}_2\text{N}_4$ , 2D:  $\text{Ca}_3\text{Ga}_2\text{N}_4$ , 3D:  $\text{Sr}_3\text{Ga}_3\text{N}_5$ ).<sup>[9,46]</sup>

Also some quaternary nitridogallates are known, containing additionally Mg or Li for example.<sup>[8,48]</sup> Synthesis of nitridogallates is typically carried out in weld shut tantalum or niobium ampoules using sodium-flux technique with  $\text{NaN}_3$  as nitrogen source.<sup>[49,50]</sup> Temperatures up to 800 °C are reached, comparable low for solid-state synthesis. The structural relation between nitridogallates and nitridosilicates raises the question, if similar properties like those of nitridosilicates, for example luminescence can be expected in the compound class nitridogallates as well. Therefore, not only from structural point of view but also concerning luminescence properties and possible application as optical material, investigations on novel crystal structures and properties of nitridogallates might be interesting.

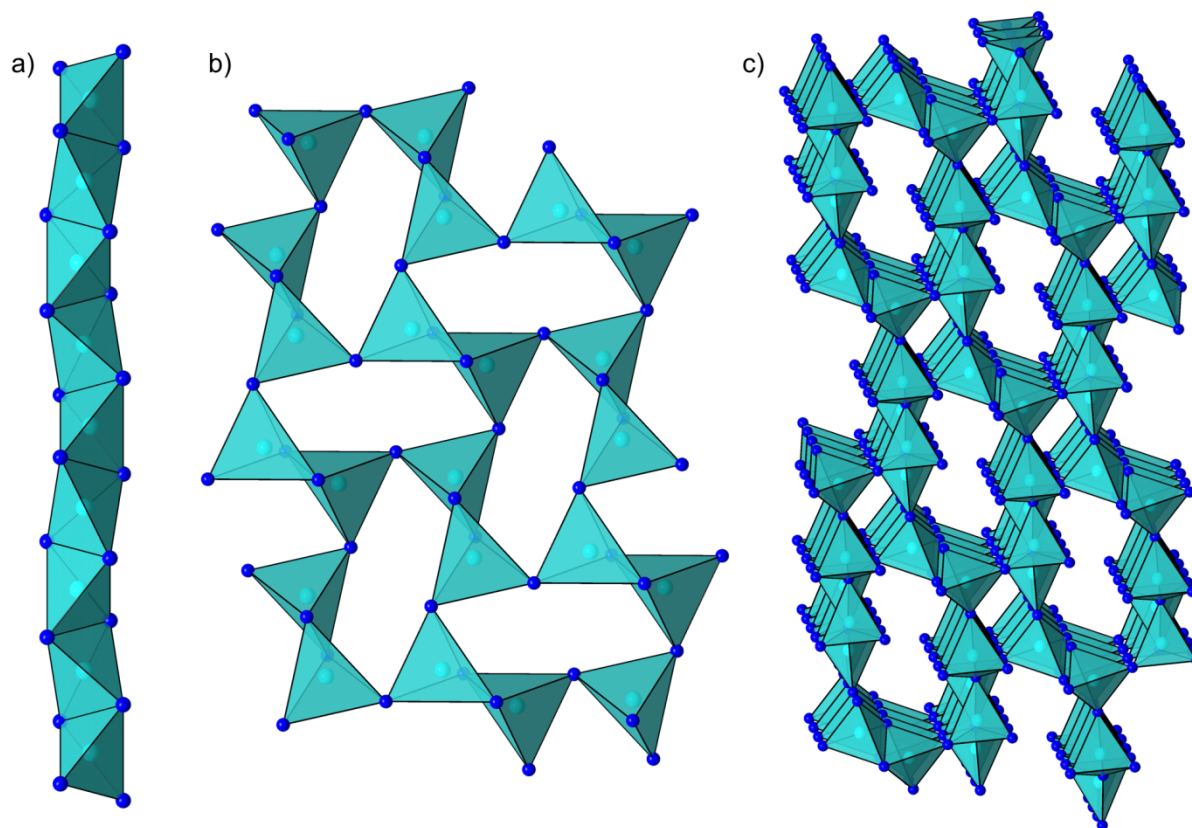


**Figure 2.** Ga atoms light blue, N atoms dark blue; a) one-dimensional chains of edge-sharing  $\text{GaN}_4$  tetrahedra in  $\text{Ba}_3\text{Ga}_2\text{N}_4$ ; b) sheets  $\text{GaN}_4$  units, sharing corners and edges in  $\text{Ca}_3\text{Ga}_2\text{N}_4$ ; c) three-dimensional network of corner- and edge-sharing tetrahedra in  $\text{Sr}_3\text{Ga}_3\text{N}_5$ .

The objective of this thesis was the synthesis, identification and characterization of novel nitrides of gallium. Therefore, synthesis was carried out starting from the metals with sodium azide in a sodium melt in weld shut metal ampoules. Crystal structure elucidation with single-crystal X-ray diffraction was carried out on new compounds. Furthermore, investigations of band gap as well as physical properties like luminescence were performed on several nitridogallates. Additionally, ammonothermal synthesis with high pressure autoclaves is described in detail in the first part of this thesis and application of this method for synthesis of a novel amide compound is reported later. With the reported compounds, not only successful establishment of ammonothermal synthesis but also an extension in the class of nitridogallates was gained. Observation of luminescence properties on several nitridogallates points out their possible application as optical materials.

## References

- [1] R. Niewa, F. J. DiSalvo, *Chem. Mater.* **1998**, 10, 2733.
- [2] D. H. Gregory, *J. Chem. Soc. Dalton Trans.* **1999**, 3, 259.
- [3] E. Riedel, *Anorganische Chemie*, de Gruyter, Berlin, New York, **2004**.
- [4] F. J. DiSalvo, S. J. Clarke, *Curr. Opin. Solid State Mater. Sci.* **1996**, 1, 241.
- [5] F. J. DiSalvo, *Science* **1990**, 247, 649.
- [6] M. Kanatzidis, R. Pöttgen, W. Jeitschenko, *Angew. Chem.* **2005**, 117, 7156; *Angew. Chem. Int. Ed.* **2005**, 43, 6996.
- [7] M. Yano, M. Okamoto, Y. K. Yap, M. Yoshimura, Y. Mori, T. Sasaki, *Diamond Relat. Mater.* **2000**, 9, 512.
- [8] D. G. Park, Y. Dong, F. J. DiSalvo, *Solid State Sci.* **2008**, 10, 1846.
- [9] S. J. Clarke, F. J. DiSalvo, *Inorg. Chem.* **1997**, 36, 1143.
- [10] H. Yamane, D. Kinno, M. Shimada, *J. Mater. Sci.* **2000**, 35, 801.
- [11] H. Yamane, *J. Ceram. Soc. Japan* **2009**, 117, 1021.
- [12] R. Marchand, Y. Laurent, J. Guyader, P. L'Haridon, P. Verdier, *J. Eur. Ceram. Soc.* **1991**, 8, 197.
- [13] R.-J. Xie, N. Hirotsaki, *Sci. Technol. Adv. Mater.* **2007**, 8, 588.
- [14] S. Nakamura, *Science* **1998**, 281, 956.
- [15] S. Nakamura, S. Pearton, G. Fasol, *The Blue Laser Diode*, Springer Verlag, Berlin, **2000**.
- [16] S. Nakamura, *Solid State Commun.* **1997**, 102, 237.
- [17] S. Nakamura, M. Senoh, T. Mukai, *Appl. Phys. Lett.* **1993**, 62, 2390.
- [18] T. Fujii, Y. Gao, R. Sharma, E. L. Hu, S. P. DenBaars, S. Nakamura, *Appl. Phys. Lett.* **2004**, 84, 855.
- [19] T. Hashimoto, K. Fujito, M. Saito, J. S. Speck, S. Nakamura, *Jpn. J. Appl. Phys.* **2005**, 44, L1570.
- [20] H. Jacobs, D. Schmidt, *Curr. Top. Mater. Sci.* **1982**, 8, 381.
- [21] A. Rabenau, *Angew. Chem.* **1985**, 97, 1017; *Angew. Chem. Int. Ed. Engl.* **1985**, 24, 1026.
- [22] R. Juza, H. Jacobs, H. Gerke, *Ber. Bunsenges. Phys. Chem.* **1966**, 70, 1103.
- [23] A. Denis, G. Goglio, G. Demazeau, *Mater. Sci. Eng.* **2006**, R 50, 167.
- [24] M. Bockowski, *Cryst. Res. Technol.* **2007**, 42, 1162.

- [25] R. P. Parikh, R. A. Adomaitis, *J. Cryst. Growth* **2006**, 286, 259.
- [26] S. Krukowski, P. Kempisty, P. Strak, *Cryst. Res. Technol.* **2009**, 44, 1038.
- [27] W. Schnick, H. Huppertz, *Chem. Eur. J.* **1997**, 3, 679.
- [28] M. Zeuner, S. Pagano, W. Schnick, *Angew. Chem.* **2011**, 123, 7898; *Angew. Chem. Int. Ed.* **2011**, 50, 7754.
- [29] T. Schlieper, W. Schnick, *Z. Anorg. Allg. Chem.* **1995**, 621, 1037.
- [30] W. Schnick, H. Huppertz, R. Lauterbach, *J. Mater. Chem.* **1999**, 9, 289.
- [31] H. Huppertz, W. Schnick, *Chem. Eur. J.* **1997**, 3, 249.
- [32] H. Huppertz, W. Schnick, *Angew. Chem.* **1996**, 108, 2115; *Angew. Chem. Int. Ed. Engl.* **1996**, 35, 1983.
- [33] D. Peters, E. F. Paulus, H. Jacobs, *Z. Anorg. Allg. Chem.* **1990**, 584, 129.
- [34] T. Schlieper, W. Milius, W. Schnick, *Z. Anorg. Allg. Chem.* **1995**, 621, 1380.
- [35] S. Pagano, S. Lupart, M. Zeuner, W. Schnick, *Angew. Chem.* **2009**, 121, 6453; *Angew. Chem. Int. Ed.* **2009**, 48, 6335.
- [36] S. Lupart, W. Schnick, *Z. Anorg. Allg. Chem.* **2012**, 638, 2015.
- [37] G. Pilet, H. A. Höpfe, W. Schnick, S. Esmaeilzadeh, *Solid State Sci.* **2005**, 7, 391.
- [38] S. Lupart, G. Gregori, J. Maier, W. Schnick, *J. Am. Chem. Soc.* **2012**, 134, 10132.
- [39] H. A. Höpfe, H. Lutz, P. Morys, W. Schnick, A. Seilmeier, *J. Phys. Chem. Solids* **2000**, 61, 2001.
- [40] R. Mueller-Mach, G. Mueller, M. R. Krames, H. A. Höpfe, F. Stadler, W. Schnick, *Phys. Status Solidi (a)* **2005**, 202, 1727.
- [41] V. Bachmann, C. Ronda, O. Oeckler, W. Schnick, A. Meijerink, *Chem. Mater.* **2009**, 21, 316.
- [42] M. Seibald, T. Rosenthal, O. Oeckler, F. Fahrenbauer, A. Tücks, P. J. Schmidt, W. Schnick, *Chem. Eur. J.* **2012**, 18, 13446.
- [43] T. Jüstel, H. Nikol, C. Ronda, *Angew. Chem.* **1998**, 110, 3250; *Angew. Chem. Int. Ed.* **1998**, 37, 3084.
- [44] H. A. Höpfe, *Angew. Chem.* **2009**, 121, 3626; *Angew. Chem. Int. Ed.* **2009**, 48, 3572.
- [45] Y. Q. Li, G. de With, H. T. Hintzen, *J. Solid State Chem.* **2008**, 181, 515.
- [46] H. Yamane, F. J. DiSalvo, *Acta Crystallogr. Sect. C: Cryst. Struct. Commun.* **1996**, 52, 760.



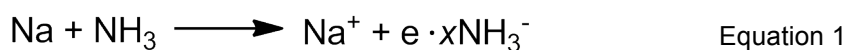
- [47] G. Cordier, M. Ludwig, D. Stahl, P. C. Schmidt, R. Kniep, *Angew. Chem.* **1995**, 107, 1879; *Angew. Chem. Int. Ed. Engl.* **1995**, 34, 1761.
- [48] M. S. Bailey, F. J. DiSalvo, *J. Alloys Compd.* **2006**, 417, 50.
- [49] S. J. Clarke, F. J. DiSalvo, *J. Alloys Compd.* **1998**, 274, 118.
- [50] P. M. Mallinson, Z. A. Gál, S. J. Clarke, *Inorg. Chem.* **2006**, 45, 419.

## 2. Ammonothermal Reaction Procedure

Nitride materials, especially those of third and fourth main group elements are of great interest for application as functional materials. For synthesis of the nitride materials, ammonia can be used as solvent and starting material, for example in ammonothermal synthesis. This method is a solution-based technique, using supercritical  $\text{NH}_3$  as solvent. To achieve a supercritical state, reaction temperatures higher than  $132.5\text{ }^\circ\text{C}$  and reaction pressure more than 113 bar must be realized. Commercial available pressure vessel can be used up to  $600\text{ }^\circ\text{C}$  and pressures of 400 bar. Under these conditions, contaminations with autoclave wall material are observed, increased by use of mineralizing agents. Teflon-inlays can be used to overcome these contaminations but they decrease reaction temperature to  $150\text{ }^\circ\text{C}$  and corresponding lower pressures ( $\sim 220$  bar). For the synthesis of nitride materials, higher pressures are necessary. Therefore, special autoclaves were developed for reaction conditions up to  $600\text{ }^\circ\text{C}$  and 3000 bar. These conditions cannot be realized in any commercial available system. In the following chapter the autoclaves as well as the filling device will be presented in detail. Furthermore, exemplarily synthesis of GaN will be described and discussed.

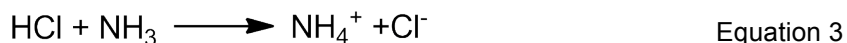
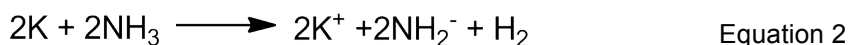
### 2.1. Introduction

Gallium nitride GaN turned out to be one of the most important semiconductors in modern technology.<sup>[1]</sup> Most available GaN based semiconductor devices use GaN deposited by heteroepitaxy. These thin nitride films contain large defect concentrations depending on substrate material.<sup>[2]</sup> For growth of homoepitaxial layers, an almost defect free GaN single crystal would be the ideal substrate.<sup>[3-5]</sup> Standard crystal growth methods (i.e. Czochralski-process) are inapplicable since nitrides would decompose. To avoid this decomposition, synthesis under elevated pressure is favorable. Reactions of liquid Ga with gaseous nitrogen at higher pressure would require extremely high pressures (up to 15000 bar) at temperatures up to 1500 °C. Using Na-flux as solvent, temperature can be lowered to 750 °C.<sup>[6]</sup> Changing reaction gas to ammonia, lower pressures and even lower temperatures are sufficient for synthesis of crystalline nitride materials.<sup>[7]</sup> The solvent ammonia is less polar and less protic in comparison to water but nevertheless, many inorganic compounds are soluble in (liquid) NH<sub>3</sub>. Similar to hydrothermal recrystallization of oxides, single crystals of nitrides are accessible in supercritical ammonia.<sup>[8]</sup> Furthermore, ammonothermal synthesis is a quite controllable and reproducible process. The resulting reaction pressure is dependent on the size of reaction vessel, filling degree and temperature. Ammonia itself can react as three-basic acid to form amides, imides or nitrides, whereas the reaction rates are higher and crystallinity of the products is improved when supercritical ammonia is employed.<sup>[9]</sup> Early investigations of the solubility of metals in ammonia showed that alkali and alkaline-earth metals as well as lanthanides dissolve well in liquid ammonia (ref. eq. 1).<sup>[10-16]</sup>



Nevertheless, other metals and inorganic compounds dissolve poorly and additional reagents are necessary. Mineralizers can increase solubility by formation of complexes between solute and mineralizer.<sup>[5,17,18]</sup> Therefore, higher supersaturation is possible without spontaneous nucleation and reactivity of solution as well as growth rates are increased. Depending on the behavior in ammonia, mineralizers are differentiated as ammonobasic or ammonoacidic. Under ammonobasic reaction conditions amide ions NH<sub>2</sub><sup>-</sup> are formed, for example when alkali metals are dissolved

in  $\text{NH}_3$  (eq. 2). An ammonoacidic mineralizer produces  $\text{NH}_4^+$ -species in the solution like  $\text{HCl}$  or  $\text{NH}_4\text{Cl}$  (eq. 3).



But not only the acidity of the solution is changed by use of mineralizers, also different products can be obtained. For example by synthesis of bulk GaN, the hexagonal form h-GaN is obtained by ammonobasic reaction, metastable cubic zinc-blende modification c-GaN can be synthesized by using ammonoacidic mineralizer.<sup>[3,19-21]</sup>

The ammonothermal synthesis is already known for some time since Jacobs and Juza established this method as a synthesis tool for inorganic syntheses.<sup>[13,14]</sup> At that time, reactions to binary and ternary metal nitrides and imides as well as syntheses of phosphides were carried out.<sup>[13,22-26]</sup> Solid-state chemistry of nitrides was quite unexplored back then and Jacobs and Juza performed pioneer work in this field. Nevertheless, yet ammonothermal synthesis is hardly in use except for synthesis of GaN and AlN materials.

The ammonothermal synthesis imposes high demands on technical equipment. First of all the autoclave material must be inert to reaction mixture and the supercritical ammonia. Therefore, nickel-based alloys are used as autoclave material. But in ammonoacidic conditions, often problems with contamination from autoclave material occur. In this case, liner technology is used but still challenging to find a suitable, cost effective material. Additionally, autoclaves must withstand high pressures and higher temperatures for ammonothermal reaction conditions. Therefore, materials for autoclave design and sealing technology have to equal this challenge. Also the filling of autoclaves has to be optimized. Often, starting materials are sensitive to moisture and air so inert gas atmosphere is required. The control of filling degree is highly important to control the maximum pressure during synthesis and to make these experiments reproducible.

This synthesis tool offers a wide field of reaction variations not only for synthesis of nitrides but also for reactions of more complex systems.<sup>[27]</sup> Here, we present exemplarily ammonothermal synthesis of GaN in specially designed autoclaves,

## 2. Ammonothermal Reaction Procedure

capable to afford reaction conditions of 600 °C and 3000 bar. The autoclave and filling procedure will be described in detail.

### 2.2. Experimental

*Autoclave design.* The autoclave used for ammonothermal reactions is shown in Figure 1. They were developed from engineers at university Erlangen in the group of Prof. Schlücker in a research cooperation. The pressure vessel, cover and screw flange as well as the screws are made up of Inconel 718 (material number 2.4668). The whole autoclave without peripheral devices is 337 mm long with diameter 50 mm and an inner volume of 97 ml. Construction detail of the autoclave without peripheral devices are given in Figures 2-5. As sealing material C-ring sealings of silver-coated Inconel 718 with a spring inside are used (GFD Dichtungen, type MCI-(F7)-732-0026, 20-1s1). From the autoclave to the valve (Dieckers, type 720.1523) an Inconel-pipe is installed. The valve can close the autoclave to the inlet pipe that can be attached via DN 16 flange (Figure 1, a) to the ammonia filling device. Additionally, the valve connects the autoclave to the distribution rack for the bursting disc holder (Figure 1, b) and the pressure transmitter (Figure 1, c). The bursting disc holder (Dieckers, type 720.5022-2) contains a bursting disc (Dieckers, type 7282500-4500) with a bursting pressure of 3300 bar to protect the pressure vessel.



**Figure 1:** Autoclave with peripheral device.

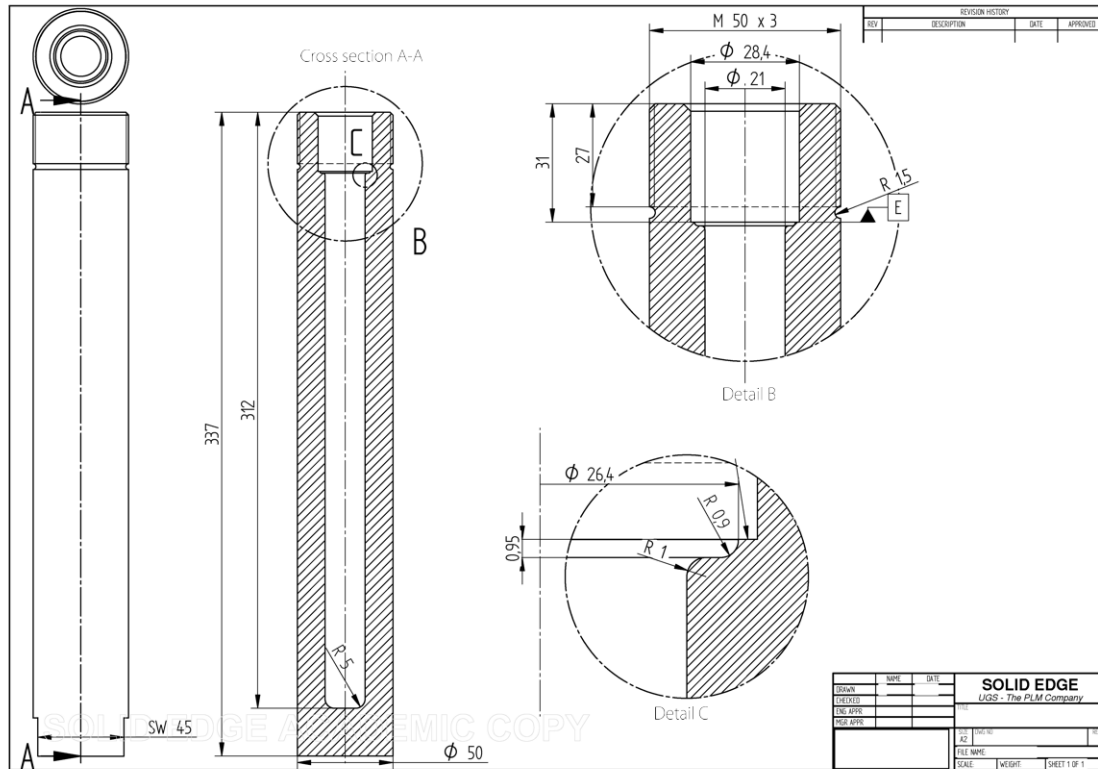


**Figure 2:** Technical drawing of pressure vessel.<sup>[28]</sup>

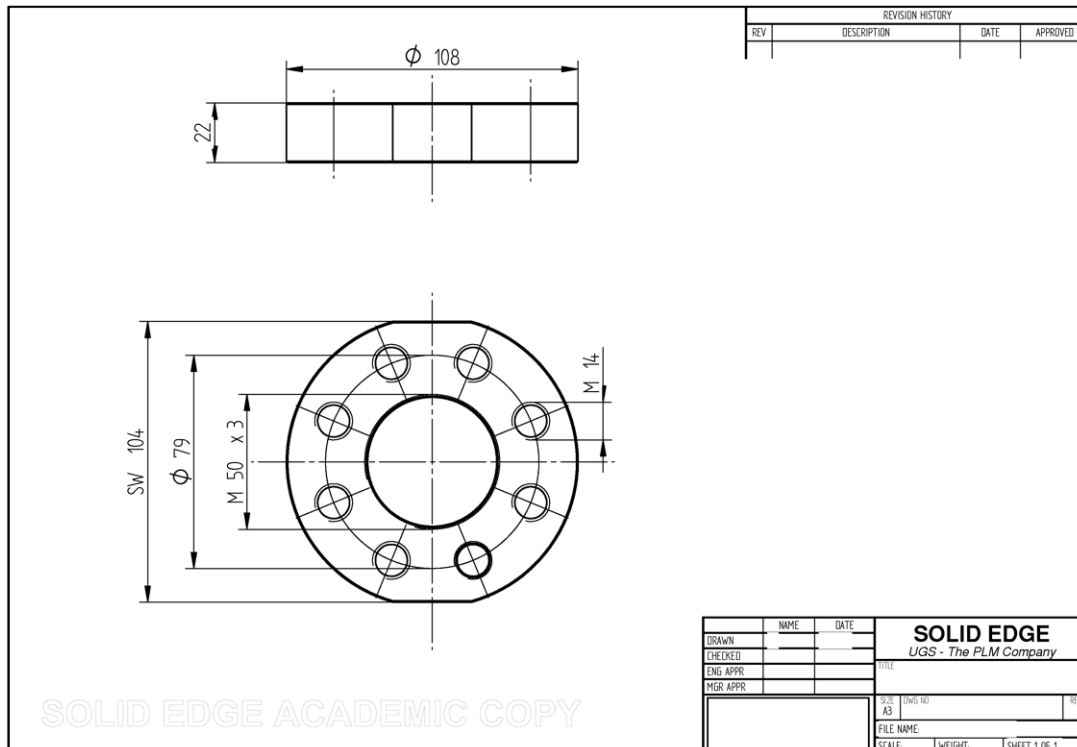


**Figure 3:** Technical drawing of screw flange.<sup>[28]</sup>

## 2. Ammonothermal Reaction Procedure

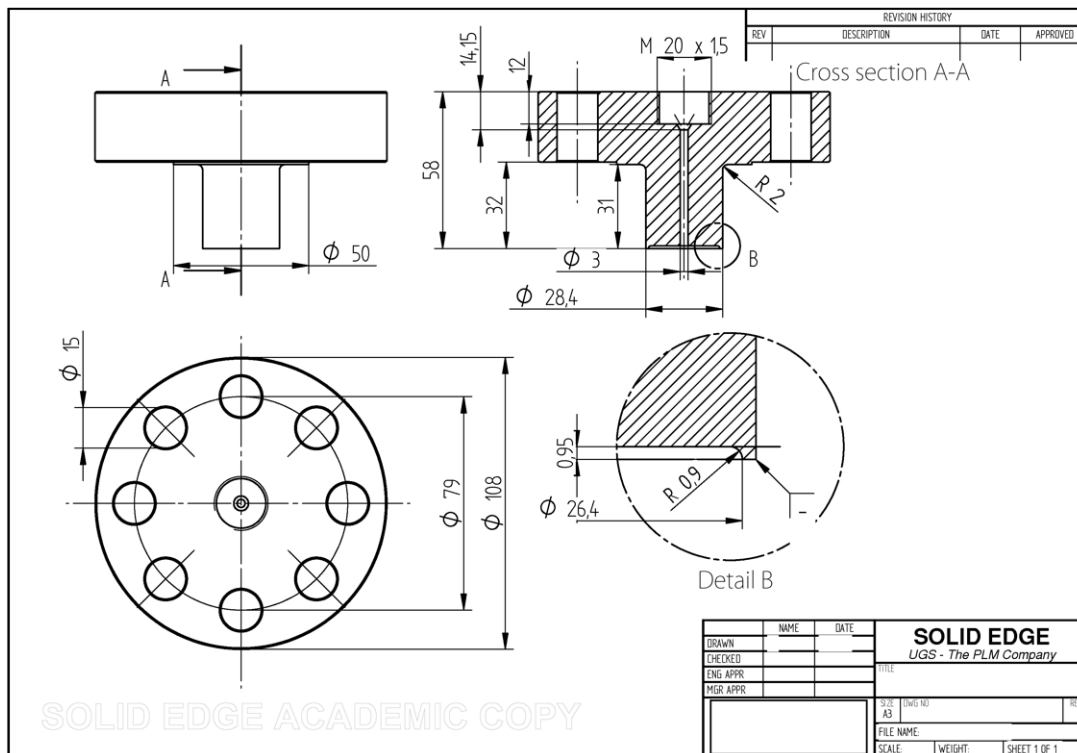


Figure 4: Technical drawing of cover flange.<sup>[28]</sup>

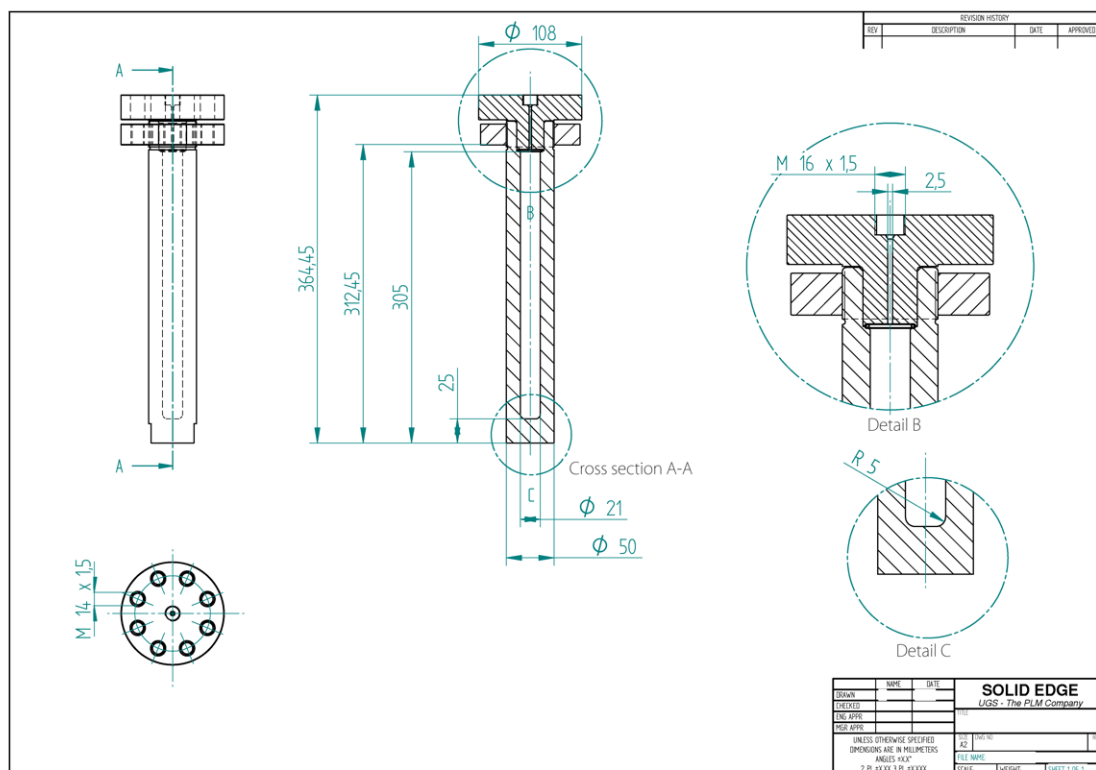
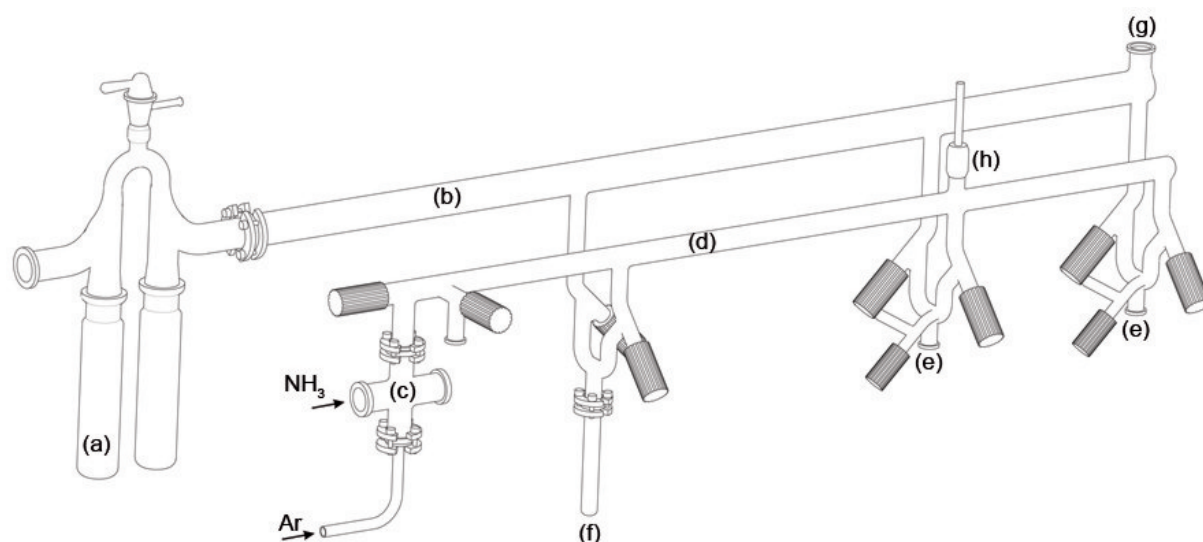


Figure 5: Technical drawing of assembled autoclave.<sup>[28]</sup>

*Ammonia filling device.* For loading the autoclave with ammonia a special filling device was used. The apparatus is built up of glass, using teflon stopcocks to avoid contamination with vacuum grease. The ammonia filling device is schematically shown in Figure 6.



**Figure 6:** Ammonia filling device.

- |                         |                                      |                   |
|-------------------------|--------------------------------------|-------------------|
| (a) double cooling trap | (d) gas line                         | (g) vacuum sensor |
| (b) vacuum line         | (e) taps                             | (h) thermometer   |
| (c) allocator           | (f) glass cylinder with volume scale |                   |

The autoclave can be evacuated and filled with ammonia or argon atmosphere. A rotary vane pump generates the vacuum. Connected via a metal bellow hose (flange DN 16) a double cooling trap (a) is attached (DN 25 flange) in front of the vacuum line (b) to protect the vacuum pump of corrosive gases and contamination with fine dust. The other glass tube can be filled by ammonia or argon, distributed by the allocator (c). From the side below, Ar can be filled in the gas line by opening the Ar-valve and the stopcock on the side of the gas line (d). To obtain the demanded pure gas conditions, Ar is purified by a special gas cartridge (SAES Pure Gas Inc., San Luis Obispo USA, model FT400-902). From the side of the allocator,  $\text{NH}_3$  can be used when the connection to the ammonia gas cylinder is opened. Ammonia is also purified (SAES Pure Gas Inc., San Luis Obispo USA, model MC400-702FV) to remove particularly water and oxygen contaminations. Two taps can thumb the respective gas or vacuum where the autoclave can be flanged (DN 16) (e). Additionally, a glass cylinder with a volume scale (f) is attached to the gas line.



## 2. Ammonothermal Reaction Procedure

---

Therein, ammonia can be condensed to determine the exact ammonia volume. The whole system is protected from overpressure several times. The gas line has a mercury pressure control valve, which is not lockable. Each tap is also secured by such a mercury control valve. Additionally, a mechanical relief pressure valve is attached to the allocator (with a DN 25 flange, opposite to  $\text{NH}_3$  inlet). For control of vacuum a sensor (g) is flanged to the vacuum line. Additionally, a thermometer is attached to the gas line (h). To avoid contaminations with oxygen or air in the autoclave, the front part of gas piping is flushed by dry ammonia before using  $\text{NH}_3$ .

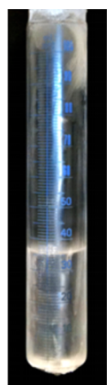


**Figure 7:**  
Glass cylinder  
filled with liquid  
 $\text{NH}_3$ .

For filling an autoclave with a certain amount of  $\text{NH}_3$ , the pressure vessel is flanged to the filling device and evacuated and filled with Ar three times. After the last session, the autoclave as well as the glass cylinder is evacuated. Both, the autoclave and the glass cylinder, are cooled by a mixture of dry ice and ethanol to provide temperatures lower than the boiling point of ammonia ( $-33\text{ }^\circ\text{C}$ ). Under continuous cooling the glass cylinder is then filled with gaseous  $\text{NH}_3$  for several minutes, depending on the desired amount of ammonia, the autoclave can still be evacuated in the meantime. Once enough ammonia is condensed (ref. Figure 7), the link to the ammonia container is closed.

Now the connection between autoclave and glass cylinder is made by opening the autoclave to the gas line. By moderate heating of the liquid ammonia the gas can be evaporated and re-condensed in the cooled autoclave. When all ammonia is condensed in the pressure vessel the autoclave is closed and brought to room temperature, again by moderate heating or defrosting in air. With the maximum temperature of reaction and knowledge of the filling degree, the reaction pressure can be estimated (ref. Figure 8).

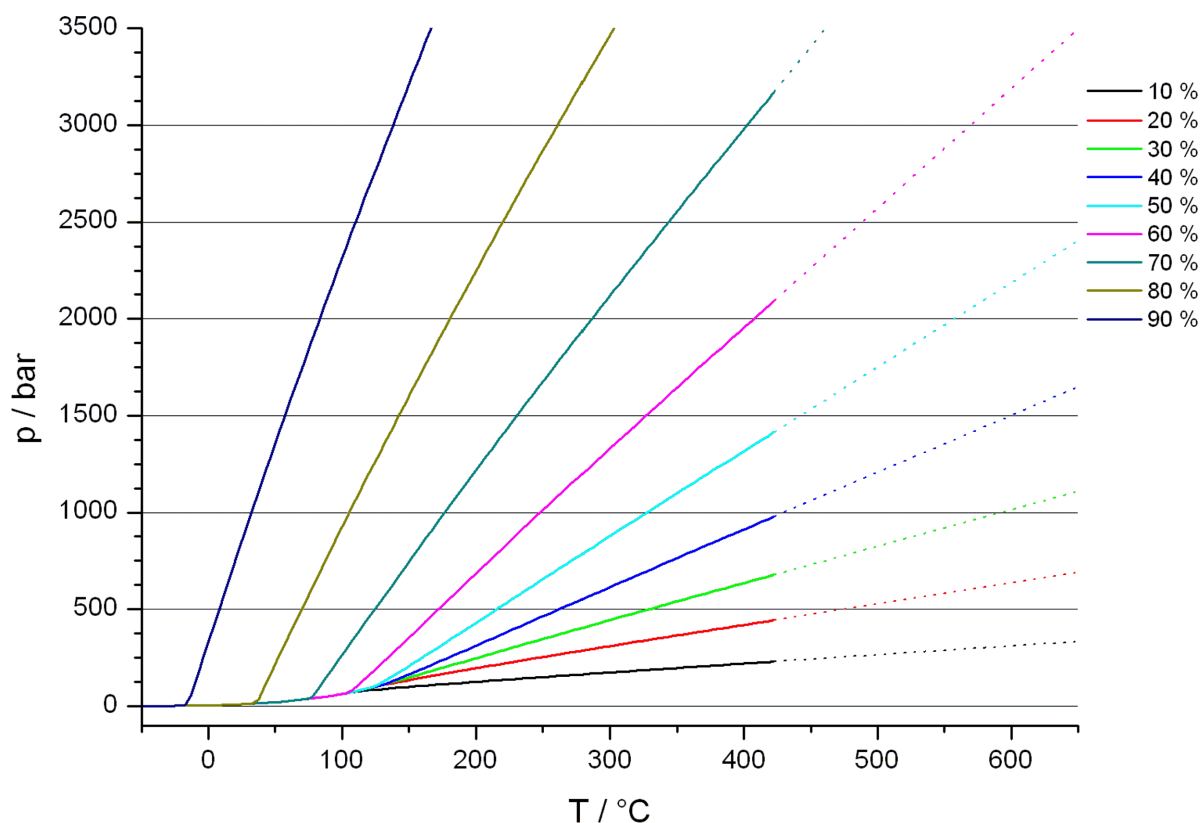


**Figure 8:** Temperature-pressure diagram in dependence on filling degree (in %). Solid lines are based on data from NIST database,<sup>[29]</sup> dotted lines are extrapolated values.

**Synthesis of GaN.** For ammonothermal recrystallisation of GaN powder the autoclave was filled with 1.0 mmol Ga (69.7 mg, Sigma Aldrich, 99.99%) and 1.0 mmol GaN powder (83.7 mg, Sigma Aldrich, 99.99%) in an argon filled glove box (Unilab, MBraun, Garching;  $O_2 < 1$  ppm,  $H_2O < 1$  ppm). A mixture of ammonobasic (Na, 3.0 mmol, Sigma Aldrich, 99.95%) and ammonoacidic ( $NH_4Cl$ , 0.05 mmol, synthesized according to<sup>[30]</sup>) mineralizer was used. After filling the autoclave with starting material mixture the autoclave was closed by cover flange and the eight screws, coated with a BN-suspension lubricant (Henze, HeBoCoat 20E), were inserted and tightened firmly. Outside the glove box, the screws have been tightened in a star pattern with 150 Nm in three 50 Nm steps. Afterwards, the autoclave was connected to ammonia filling device with the DN 16 flange over a metal bellow hose. The autoclave was then cooled down with a dry ice acetone mixture ( $-78$  °C), evacuated and filled with 40 ml (filling degree 41 %) dry, liquid ammonia by condensation as described above. After thawing the autoclave was heated in a tube furnace to 550 °C in 1.5 h, maintained at that temperature for 48 h and subsequently cooled down to 200 °C in 240 h. The cover flange was isolated by several layers of quartz wool to minimize the temperature gradient. Maximum pressure of 1805 bar

was reached during synthesis, after reaction the maintaining pressure was 241 bar. After controlled pressure release the autoclave was evacuated and filled with argon. The screws were loosened and the autoclave was subsequently opened in a glove box under argon atmosphere. The product was obtained as a white crystalline powder.

### 2.3. Results and Discussion

Crystalline GaN powder was filled in a glass capillary (Hilgenberg, 0.2 mm diameter) inside a glove box to prevent products from oxidation. Powder X-ray diffraction data were collected on a Stoe STADI P diffractometer with Cu  $K_{\alpha 1}$ -radiation ( $\lambda = 1.540596 \text{ \AA}$ ). The X-ray diffraction data were first examined by the program package WinXPOW,<sup>[31]</sup> to identify the product phase reflection positions were compared to data of ICSD database, implemented in XPOW Search.<sup>[32]</sup> The crystal structure was refined using the Rietveld method in the TOPAS package.<sup>[33]</sup> The powder product contains hexagonal GaN besides an equal amount of  $\text{NaNH}_2$  as shown in the powder diffractogram in Figure 9.

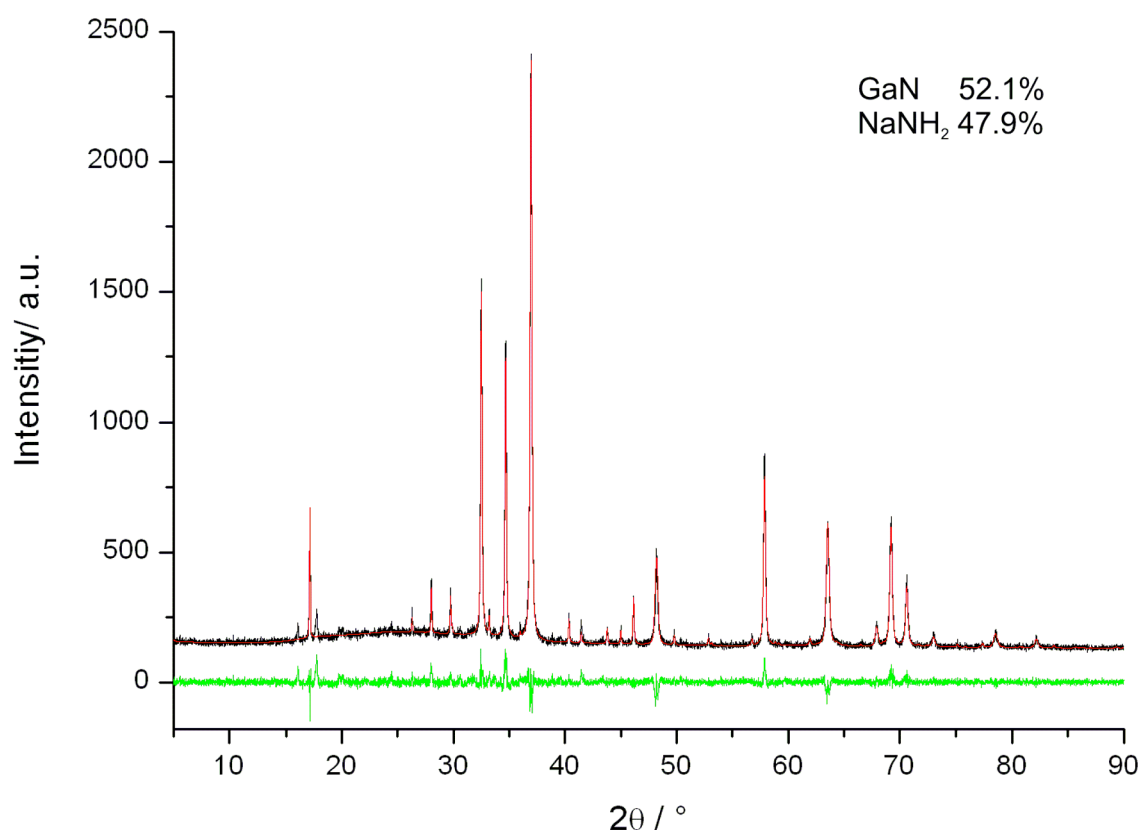


**Figure 9:** Observed and calculated powder diffraction pattern of GaN and  $\text{NaNH}_2$ .

No additional reflections and therefore, no Ga reflections are observed so transformation from Ga into GaN was successful. Due to relatively high amount of Na in the starting reaction mixture,  $\text{NaNH}_2$  was obtained besides crystalline GaN. As indicated above, the hexagonal, wurtzite modification of GaN was achieved due to predominant ammonobasic mineralizer Na. Therein, both atom types, Ga and N, are surrounded by four atoms in a tetrahedral coordination. A picture of crystal structure is presented in Figure 10. The crystal data are summarized in Table 1 and agree well with literature values published before.

**Table 1:** Crystallographic data of GaN.

sum formula	GaN this reaction	GaN literature <sup>[34]</sup>
space group	$P6_3mc$ (no. 186)	$P6_3mc$ (no. 186)
<i>a</i>	3.1893(3) Å	3.18940(1)
<i>c</i>	5.1858(6) Å	5.18614(2)
$R_{\text{Bragg}}$	0.03881	
$R_{\text{wp}}$	0.12944	
GOF	1.154	

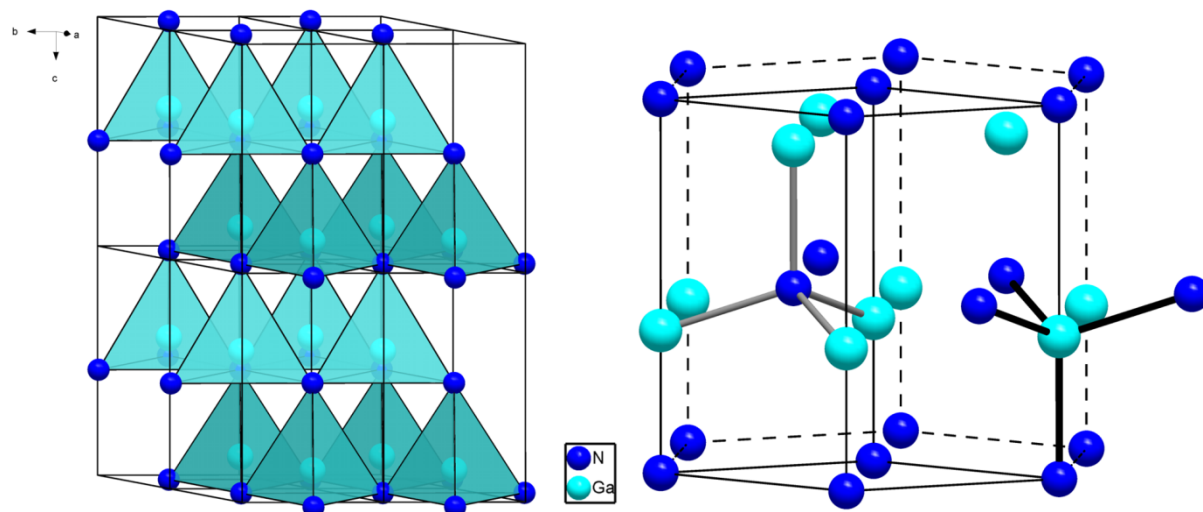


**Figure 10:** Crystal structure of wurtzite GaN, left: shown  $\text{GaN}_4$ -tetrahedra in blue, right: tetrahedral coordination of Ga and N in GaN crystal structure.

The resulting pressure during reaction is higher than expected from filling degree and reaction temperature (ref. Figure 8). This can be related to  $\text{H}_2$  formation during reaction and proved that chemical reaction takes place. Scanning electron microscopy (SEM) was performed on a JEOL JSM 6500 F equipped with a field emission gun at acceleration voltage of 22 kV. Sample composition was investigated by EDX-spectra (Detector Oxford Instruments) on powder sample. The EDX-results

show the presence of Ga (11 atom%), N (12 atom%) and Na (24 atom%) as well as a high content of oxygen (51 atom%) and little amount of Cl (~0.4 atom%) deriving from  $\text{NH}_4\text{Cl}$  as ammonoacidic mineralizer. The oxygen content can be explained by the oxidation sensibility of  $\text{NaNH}_2$  when exposed to air. Although sample storage and preparation for SEM investigation was performed in a glove box under argon, some contact with air cannot be avoided during sample installation on the SEM. By PXRD, h-GaN structure has already been proved. In correlation with EDX-results the existence of GaN in the product can be assumed since the atomic ratio Ga : N is about 1 : 1. Additionally, the Na : O ratio can also be related to the oxidation of  $\text{NaNH}_2$ .

### 2.4. Conclusion

Here, the ammonothermal synthesis of GaN and the instrumental equipment is presented. With the described technique, ammonothermal reactions with pressures up to 3000 bar and temperatures of 600 °C are possible. Furthermore, reactions are reproducible since the amount of  $\text{NH}_3$ , filled in the autoclave can be easily determined by the use of the mentioned ammonia filling device. Nevertheless, the real pressure during reaction cannot be determined before the experiment due to  $\text{H}_2$ -release during reaction. Once all technical equipment is installed, this method is quite “straight forward” for syntheses under supercritical ammonia. Not only synthesis of binary nitrides is possible with this method, also higher nitrides and other nitrogen-containing compounds could be accessible. Furthermore, to optimize the ammonothermal synthesis detailed knowledge of the reaction processes and arising intermediates has to be gained. Another still challenging aspect is the corrosive character of ammonia, especially in the ammonoacidic regime and therefore the need for cost efficient liner material. Currently, Pt liner are used to avoid contaminations with autoclave material but they are expensive.<sup>[17,35]</sup> Additionally, the liner must attach firmly to the inner wall to avoid leakage. Further research efforts have to be made to find a smart solution. With the current heating setup, a temperature gradient cannot be avoided. In some reactions and even for crystal growth such a gradient is essential but up to now the gradient is not defined. Initial assessments indicate a temperature loss through the cover flange of 200 °C which is a third of achieved maximum temperature. Through purposeful choice of temperature

gradient effects like retrograde solubility could be utilized for transport of a special phase for example. Additionally, further investigations on mineralizers is necessary. Often the mineralizing agents are kind of catalytic and still remaining after reaction. Therefore, phase pure products can only be obtained with further purifying steps. Investigations on the acidity in ammonia of common inorganic starting materials in nitride chemistry has been neglected yet. For synthesis of nitridosilicates in supercritical ammonia for example, the behavior of " $\text{Si}(\text{NH})_2$ " would be very interesting. With this knowledge, a one-pot synthesis of nitride of compounds is conceivable, for example in the compound classes of nitridogallates, nitridosilicates or other nitride network based compounds.

### 2.5. References

- [1] T. Fukuda, D. Ehrentaut, *J. Cryst. Growth* **2007**, 305, 304.
- [2] A. Denis, G. Goglio, G. Demazeau, *Mater. Sci. Eng.* **2006**, R 50, 167.
- [3] D. R. Ketchum, J. W. Kolis, *J. Cryst. Growth* **2001**, 222, 431.
- [4] R. Niewa, F. J. DiSalvo, *Chem. Mater.* **1998**, 10, 2733.
- [5] D. Ehrentaut, T. Fukuda, *J. Cryst. Growth* **2010**, 312, 2514.
- [6] T. Sekiguchi, H. Yamane, M. Aoki, T. Araki, M. Shimada, *Sci. Technol. Adv. Mater.* **2002**, 3, 91.
- [7] R. Dwilinski, R. Doradzinski, M. Zajac, *Compound Semiconductor* **2010**, 12.
- [8] Q.-S. Chen, V. Prasad, W. R. Hu, *J. Cryst. Growth* **2003**, 258, 181.
- [9] B. Wang, M. J. Callahan, *Cryst. Growth Des.* **2006**, 6, (6), 1227.
- [10] W. Weyl, *Ann. Physik* **1864**, 197, 601.
- [11] C. A. Kraus, *J. Am. Chem. Soc.* **1907**, 29, 1557.
- [12] G. E. Gibson, W. L. Argo, *J. Am. Chem. Soc.* **1918**, 40, 1327.
- [13] R. Juza, H. Jacobs, *Angew. Chem.* **1966**, 78, 208; *Angew. Chem., Int. Ed. Engl.* **1966**, 5, 247.
- [14] R. Juza, C. Hadenfeldt, *Naturwissenschaften* **1968**, 55, 229.
- [15] J. C. Warf, *Angew. Chem.* **1970**, 82, 397; *Angew. Chem. Int. Ed. Engl.* **1970**, 9, 383.
- [16] C. Hadenfeldt, R. Juza, *Naturwissenschaften* **1969**, 56, 282.
- [17] D. Ehrentaut, Y. Kagamitani, T. Fukuda, F. Orito, S. Kawabata, K. Katano, S. Tereda, *J. Cryst. Growth* **2008**, 310, 3902.
- [18] M. Bockowski, *Cryst. Res. Technol.* **2007**, 42, 1162.
- [19] R. Dwilinski, A. Wyszomolek, J. M. Baranowski, M. Kaminska, R. Doradzinski, J. Garczynski, L. Siersputowski, H. Jacobs, *Acta Phys. Pol. A* **1995**, 88, 833.
- [20] A. P. Purdy, *Chem. Mater.* **1999**, 11, 1648.
- [21] A. P. Purdy, R. J. Jout, C. F. George, *Cryst. Growth Des.* **2002**, 2, 141.
- [22] C. Hadenfeldt, B. Gieger, H. Jacobs, *Z. Anorg. Allg. Chem.* **1974**, 403, 319.
- [23] H. Jacobs, *Z. Anorg. Allg. Chem.* **1971**, 382, 97.
- [24] H. Jacobs, U. Fink, *Z. Anorg. Allg. Chem.* **1977**, 435, 137.
- [25] H. Schlenger, H. Jacobs, *Z. Anorg. Allg. Chem.* **1971**, 385, 177.
- [26] H. Schlenger, H. Jacobs, *Acta Crystallogr., Sect. B.: Struct. Sci.* **1972**, 28, 327.

- [27] R. Niewa, H. Jacobs, *Chem. Rev.* **1996**, 96, 2053.
- [28] N. Alt, *Dissertation*, Friedrich Alexander Universität Erlangen-Nürnberg **2010**.
- [29] <http://webbook.nist.gov/chemistry/fluid/> (2010),
- [30] W. J. Fieser, *Inorg. Syntheses* **1946**, 2, 136.
- [31] WinXPOW, 2.21; STOE & Cie GmbH Darmstadt **2005**.
- [32] WinXPOW Search, 2.08; **2005**.
- [33] A. Coelho, TOPAS-Academic, 4.1; Coelho Software Brisbane, **2007**.
- [34] W. Paszkowicz, S. Podsiadlo, R. Minikayev, *J. Alloys Compd.* **2004**, 382, 100.
- [35] D. Ehrentraut, Y. Kagamitani, A. Yoshikawa, N. Hoshino, H. Itoh, S. Kawabata, K. Fujii, T. Yao, T. Fukuda, *J. Mater. Sci.* **2007**, 43, 2270.



### 3. Magnesium Nitrides as Host Lattices for $\text{Eu}^{2+}$ -Doping

In the previous chapter ammonothermal synthesis of the binary nitride GaN was depicted. In the past decade, many researchers investigated variations of GaN to improve its physical properties. For example InGaN and AlGaN were found with slightly different band gaps compared to GaN but also well suitable for semiconductor application. Furthermore, doping of GaN with Mg was investigated thoroughly. Since the ionic radius of fourfold coordinated  $\text{Mg}^{2+}$  is comparable to fourfold coordinated  $\text{Ga}^{3+}$  it should easily incorporate into the crystal lattice of GaN. Due to different charges of these two ions,  $\text{Mg}^{2+}$  increases p-doping level when introduced to GaN crystal structure. Higher nitrides of Ga are known as nitridogallates and thereof only a small number is known as discussed later. In this chapter we present a novel double nitride containing Ga and Mg which shows an interesting crystal structure as well as luminescence properties upon doping. Additionally, luminescence of  $\text{Eu}^{2+}$ -doped  $\text{Mg}_3\text{N}_2$  is presented.

## Magnesium Double Nitride Mg<sub>3</sub>GaN<sub>3</sub> as New Host Lattices for Eu<sup>2+</sup>-Doping – Synthesis, Structural Studies, Luminescence and Band-Gap Determination

Frauke Hintze, Neil W. Johnson, Markus Seibald, David Muir, Alexander Moewes and Wolfgang Schnick

**Published in:** *Chem. Mater.* **2013** (accepted).

**Keywords:** Gallium Nitride, Double Nitride, Luminescence, Band Gap, Europium

**Abstract:** The double nitride Mg<sub>3</sub>GaN<sub>3</sub> and binary nitride Mg<sub>3</sub>N<sub>2</sub> were synthesized from the elements by reaction with NaN<sub>3</sub> in Na-flux. Reactions were carried out at 760 °C in weld shut Ta-ampoules. Mg<sub>3</sub>GaN<sub>3</sub> was obtained as single crystals (space group  $R\bar{3}m$  (no. 166),  $a = 3.3939(5)$  and  $c = 25.854(5)$  Å,  $Z = 3$ ,  $R1 = 0.0252$   $wR2 = 0.0616$  for 10 refined parameters, 264 diffraction data). This double nitride consists of an uncharged three-dimensional network of MgN<sub>4</sub>- and mixed (Mg/Ga)N<sub>4</sub>-tetrahedra which share common corners and edges. First-principles DFT calculations predict Mg<sub>3</sub>GaN<sub>3</sub> to have a direct band gap of 3.0 eV, a value supported by soft X-ray spectroscopy measurements at the N K-edge. Eu<sup>2+</sup>-doped samples show yellow luminescence when irradiated with UV to blue light ( $\lambda_{\text{max.}} = 578$  nm, FWHM = 132 nm). Doped samples of Mg<sub>3</sub>N<sub>2</sub>:Eu<sup>2+</sup> also show luminescence at room temperature when excited with UV to blue light. The maximum intensity of the emission band is found at 589 nm (FWHM = 145 nm).

#### 3.1. Introduction

Gallium nitride has found broad application in high-performance light-emitting diodes (LEDs) due to its properties as a direct wide band gap semiconductor.<sup>1-5</sup> Recently, crystal growth and doping of GaN have been studied thoroughly.<sup>6-10</sup> On the contrary, investigations of the deriving ternary and higher nitridogallates or gallium nitrides have been scarcely pursued so far. Mg was found to be suited for p-doping in GaN or AlGaN thus increasing hole concentration.<sup>11-13</sup> Mostly, GaN:Mg has been synthesized by MOCVD with bis(cyclopentadienyl) magnesium ( $\text{Cp}_2\text{Mg}$ ) as Mg-source.<sup>14-16</sup> The influence of such doping on the GaN-lattice and its physical properties have been investigated in detail.<sup>17-20</sup> So-called heavily doped GaN:Mg was obtained when Mg concentration was around  $10^{20} \text{ cm}^{-3}$  and resulting photoluminescence bands at 2.8 eV (443 nm) and 3.2 eV (388 nm) were observed.<sup>19,21-23</sup>

Binary magnesium nitride  $\text{Mg}_3\text{N}_2$  has been known for some time, but has been much less in the focus of applications than GaN.<sup>24,25</sup> Nevertheless, in the last few years, some interest in  $\text{Mg}_3\text{N}_2$  has arisen. Its structure in the anti-bixbyite type was further investigated<sup>26,27</sup> and a green photoluminescence was reported in the literature.<sup>28</sup>

During the past decade, ternary and multinary alkaline-earth nitrides emerged as important host lattices for doping with  $\text{Eu}^{2+}$ , exhibiting parity allowed  $4f^6(^7F)5d^1 \rightarrow 4f^7(^8S_{7/2})$  transitions resulting in intense broad-band emission. This is due to the fact that these levels lie in between the band gap as shown by P. Dorenbos,<sup>29,30</sup> exemplarily on important phosphor material  $\text{M}_2\text{Si}_5\text{N}_8:\text{Eu}^{2+}$ .<sup>31</sup> In order to estimate the performance of a luminescent material in phosphor-converted (pc)-LEDs at higher temperatures band-gap investigations are of special interest. These results allow assessment of the thermal quenching behavior.

Some of the afore mentioned nitrides were identified as highly efficient optical luminescence materials and are therefore promising candidates for photon conversion.<sup>32</sup> In this respect, (oxo-)nitridosilicates, nitridoalumosilicates and (oxo-)nitridoalumosilicates have been intensively investigated.<sup>33-39</sup> Recent research has focused on  $\text{Eu}^{2+}$ -doped nitridogallates as host lattices as well.<sup>40</sup> The aforementioned materials are made up of tetrahedra-based anionic (sub-)structures wherein tetrahedra can be connected via common corners or edges, building either isolated polyhedra or one-, two- or three-dimensional structures.<sup>39,41,42</sup> Some of these

materials are suitable as host lattices for  $\text{Eu}^{2+}$  with their emission depending on the coordination of  $\text{Eu}^{2+}$  by the surrounding anions. Basically,  $\text{Eu}^{2+}$  can either substitute other electropositive ions (typically alkaline-earth ions) when the ionic radii are appropriate, or it can occupy interstitial sites.

In this contribution we report on investigation of  $\text{Eu}^{2+}$ -doped  $\text{Mg}_3\text{N}_2\text{:Eu}^{2+}$  as well as the double nitride  $\text{Mg}_3\text{GaN}_3\text{:Eu}^{2+}$  with respect to their synthesis, structure elucidation and luminescence. These nitrides represent interesting new host lattices for  $\text{Eu}^{2+}$ -doping. Furthermore, we explore the electronic partial density of states (pDOS) of the latter and quantify its band gap through calculation and experiment.

## 3.2. Experimental Section

Synthesis of  $\text{Mg}_3\text{GaN}_3$  was carried out in weld shut Ta-ampoules (30 mm length, 10 mm diameter, 0.5 mm wall thickness). All manipulations were done under Ar-atmosphere in a glove box (Unilab, MBraun, Garching;  $\text{O}_2 < 1$  ppm,  $\text{H}_2\text{O} < 1$  ppm). Single crystals were obtained from reaction of 0.38 mmol  $\text{NaN}_3$  (25.0 mg, Acros, 99%), 0.59 mmol Mg (14.3 mg, Alfa Aesar, 99.9%) and 0.58 mmol Ga (40.4 mg, AluSuisse, 99.999%) in 2.19 mmol Na-flux (50.4 mg, Sigma Aldrich, 99.95%). For doping, 2 mol% of  $\text{EuF}_3$  was added. Ca was introduced into the metallic melt with the initial goal of finding new compounds in the system Ca-Ga-Mg-N. However, in these experiments Ca has not been incorporated into the final products but did appear to improve crystallinity. Reactions without additional Ca have been unsuccessful so far.

Synthesis of doped  $\text{Mg}_3\text{N}_2$  was performed analogously in Ta-ampoules sealed under inert-gas conditions in Ar-atmosphere. Single crystals were obtained from reaction of 0.30 mmol  $\text{NaN}_3$  (20.2 mg, Acros, 99%), 0.47 mmol Mg (11.4 mg, Alfa Aesar, 99.9%) and  $0.5 \cdot 10^{-3}$  mmol  $\text{EuF}_3$  (1.2 mg, Sigma Aldrich, 99.99%) as dopant in 2.12 mmol Na-flux (48.7 mg, Sigma Aldrich, 99.95%). According to EDX-measurements, addition of Sr and Ge metal were found to improve crystallinity but were not incorporated into the crystalline product.

Weld shut Ta-ampoules were placed into quartz tubings under vacuum to prevent oxidation of the ampoules. The respective reaction mixtures were then heated in a tube furnace at a rate of  $0.83^\circ\text{C}/\text{min}$  to  $760^\circ\text{C}$ , maintained at that temperature for

### 3. Magnesium Nitrides as Host Lattices for $\text{Eu}^{2+}$ -Doping

---

48 h and then cooled down to 200 °C at a rate of 0.06 °C/min. Subsequently, the furnace was turned off and the Ta-ampoules were opened in a glove box. The Na-flux was removed from the reaction products by sublimation at 320 °C under vacuum for 10 h.

Scanning electron microscopy was performed on a JEOL JSM 6500 F equipped with a field emission gun at an acceleration voltage of 30 kV. Synthesized samples were prepared on adhesive conductive carbon pads and coated with a likewise conductive carbon film. Chemical compositions were confirmed by EDX spectra (detector: Oxford Instruments), each spectrum was recorded on an area limited to one crystal face to avoid influence of possible contaminating phases and to verify that additional Ca or Sr and Ge were not incorporated into the crystalline products.

For X-ray diffraction and luminescence investigations, single crystals of each compound were sealed in glass capillaries under inert conditions.

Single-crystal X-ray diffraction data of  $\text{Mg}_3\text{GaN}_3$  were collected on a Nonius Kappa-CCD diffractometer with graded multilayer X-ray optics and monochromated  $\text{Mo-K}_\alpha$  radiation ( $\lambda = 0.71073 \text{ \AA}$ ). X-ray diffraction data of  $\text{Mg}_3\text{N}_2$  single crystals were collected on a STOE IPDS I diffractometer using monochromated  $\text{Mo-K}_\alpha$  radiation ( $\lambda = 0.71073 \text{ \AA}$ ). Applied absorption corrections were done using WinGX and X-RED.<sup>43,44</sup> The structures were solved by direct methods implemented in SHELXS-97.<sup>45,46</sup> Refinement of crystal structures was carried out with anisotropic displacement parameters for all atoms by full-matrix least-squares calculation on  $F^2$  in SHELXL-97.<sup>46,47</sup> Further details of the structure investigations are available from the Fachinformationszentrum Karlsruhe, D-76344 Eggenstein Leopoldshafen, Germany (fax: +49-7247-808-666; email: crysdata@fiz.karlsruhe.de) on quoting the depository numbers CSD-425108 ( $\text{Mg}_3\text{GaN}_3$ ) and CSD-425109 ( $\text{Mg}_3\text{N}_2$ ), respectively.

N K-edge soft X-ray emission and absorption spectroscopy (XES and XAS, respectively) measurements of  $\text{Mg}_3\text{GaN}_3$  were performed at the XES endstation of the Resonant Elastic and Inelastic X-ray Scattering beamline of the Canadian Light Source located on the University of Saskatchewan campus. The monochromator's resolving power ( $E/\Delta E$ ) was approximately  $1 \times 10^4$ , and it was calibrated such that the lowest energy peak in the *h*-BN absorption spectrum appeared at 402.1 eV in the

bulk-sensitive total fluorescence yield (TFY) mode. All reported Mg<sub>3</sub>GaN<sub>3</sub> absorption measurements were also performed in TFY mode to mitigate the possibility of surface contamination effects. The emission spectrometer, currently undergoing commission, has a theoretical resolving power of  $2 \times 10^3$  at the N K-edge. It uses diffraction gratings in a Rowland circle geometry as dispersive elements, and is fitted with a microchannel plate detector. XES measurements were calibrated relative to the monochromator using a series of elastic peak measurements. The double nitride sample consisted of an agglomeration of single crystals, stored under Ar-atmosphere prior to being mounted on carbon tape. Exposure to ambient conditions was less than ten minutes.

Density functional theory (DFT) calculations of the electronic structure of Mg<sub>3</sub>GaN<sub>3</sub> were performed with the *WIEN2k* software package<sup>48</sup> using the Perdew-Burke-Ernzerhoff generalized gradient approximation (PBE-GGA).<sup>49</sup> The theoretical band gap was calculated with the modified Becke-Johnson (mBJ) exchange-correlation functional,<sup>50</sup> which has been shown to improve calculated band-gap values for most semiconductors.<sup>51</sup> Calculations were performed on a (5×7×12) k-point mesh with a plane-wave cutoff of -8.0 Ryd.

Luminescence investigations were performed on single crystals placed in glass capillaries (diameter 0.2 mm, Hilgenberg) at room temperature. The capillaries were aligned with a Leitz Epiverts microscope. A JobinYvon Traix190 monochromator with 365 nm wavelength was used as excitation source, while a CCD camera (LaVision Dyna Vision) was used to detect the luminescence through a 500 µm slit.

### 3.3. Results and Discussion

The ternary nitride Mg<sub>3</sub>GaN<sub>3</sub> was obtained as a colorless to light yellow powder with light yellow crystals having the appearance of hexagonal plates. EDX analyses have confirmed the sum formula. The crystals were not sensitive to moisture and air, even contact with ethanol or acetone had no influence on the compound.

The existence of a ternary nitride with stoichiometric formula Mg<sub>3</sub>GaN<sub>3</sub> was claimed earlier by *Verdier et al.*, obtained as a green powder from the reaction of GaN and Mg<sub>3</sub>N<sub>2</sub> at 930 °C.<sup>52</sup> The authors reported nonindexed powder data and postulated an

atomic ratio Mg:Ga:N of 3:1:3 but no structural details have been published so far. Here, we were able to obtain this compound as colorless single crystals and to elucidate the crystal structure. Calculated reflection positions and intensities from single-crystal data show accordance to data reported by *Verdier*.

The product of the second reaction route described in the experimental section was obtained as heterogeneous mixture of metallic powder, orange crystals and colorless cube shaped crystals. EDX analysis showed the presence of only Mg and N in the cube shaped crystals, while the orange crystals were found to be  $\text{Sr}(\text{Mg}_3\text{Ge})\text{N}_4$ .<sup>53</sup>

#### **3.3.1. Crystal Structure Description**

The crystal structure of  $\text{Mg}_3\text{Ga}\text{N}_3\text{:Eu}^{2+}$  was solved using single-crystal X-ray diffraction data. The  $\text{Eu}^{2+}$  content was neglected because of its insignificant contribution to the scattering density. Initially, the solution was carried out in space group  $R3m$  (no. 160). After examination with PLATON<sup>54,55</sup> further refinement was performed in space group  $R\bar{3}m$  (no. 166) with  $a = 3.3939(5)$  and  $c = 25.854(5)$  Å. Crystallographic data for  $\text{Mg}_3\text{Ga}\text{N}_3$  are summarized in Table 1. The atomic coordinates and displacement parameters are listed in Table 2 and 3, while selected bond lengths and angles are shown in Table 4.

Similarly to most Ga-N compounds, the structure of  $\text{Mg}_3\text{Ga}\text{N}_3$  is composed of metal centered nitrogen tetrahedra (Fig. 1). Two metal sites are present in the crystal structure whereby one site is occupied by an even number of Mg- and Ga-atoms, while the other is occupied solely by Mg. The distances Mg-N and (Mg/Ga)-N vary in the range 1.9815(6)-2.1915(8) Å and thus are representative for typical Ga-N or Mg-N distances.<sup>40,53,56</sup> The observed bond lengths agree well with the expected sum of the ionic radii, even for the mixed occupied site.<sup>57-59</sup>

**Table 1.** Crystallographic Data for Mg<sub>3</sub>GaN<sub>3</sub>.

	Mg <sub>3</sub> GaN <sub>3</sub>
formula mass/g·mol <sup>-1</sup>	184.68
temperature/K	293(2)
crystal system	trigonal
space group	$R\bar{3}m$ (no. 166)
lattice parameters/Å	$a = 3.3939(5)$ $c = 25.854(5)$
$V/\text{Å}^3$	257.91(7)
formula units/cell	3
crystal size/mm <sup>3</sup>	0.05 · 0.04 · 0.02
abs. coefficient $\mu/\text{mm}^{-1}$	8.321
F (000)	264
diffractometer	Nonius Kappa-CCD
radiation,	Mo-K $\alpha$ ( $\lambda = 0.71073 \text{ Å}$ )
graphite-monochromator	
$\theta$ range/°	4.73– 27.48
measured reflections	275
independent reflections	102
observed reflections	100
refined parameters	10
GOF	1.067
$R$ indices ( $F_o^2 \geq 2\sigma(F_o^2)$ )	$R1 = 0.0252$ $wR2 = 0.0616$
$R$ indices (all data)	$R1 = 0.0255$ $wR2 = 0.0617$



### 3. Magnesium Nitrides as Host Lattices for $\text{Eu}^{2+}$ -Doping

**Table 2.** Atomic coordinates and equivalent isotropic displacement parameters (in  $10^{-4} \text{ pm}^2$ ) of  $\text{Mg}_3\text{GaN}_3$  (e.s.d.'s in parentheses).

site	Wyckoff Position	x	y	z	$U_{\text{eq}}/\text{\AA}^3$
Mg1/Ga1	6c	0	0	0.12999(3)	0.0124(4)
Mg2	6c	0	0	0.29538(7)	0.0092(4)
N1	6c	0	0	0.21474(13)	0.0105(9)
N2	3a	0	0	0	0.0090(11)

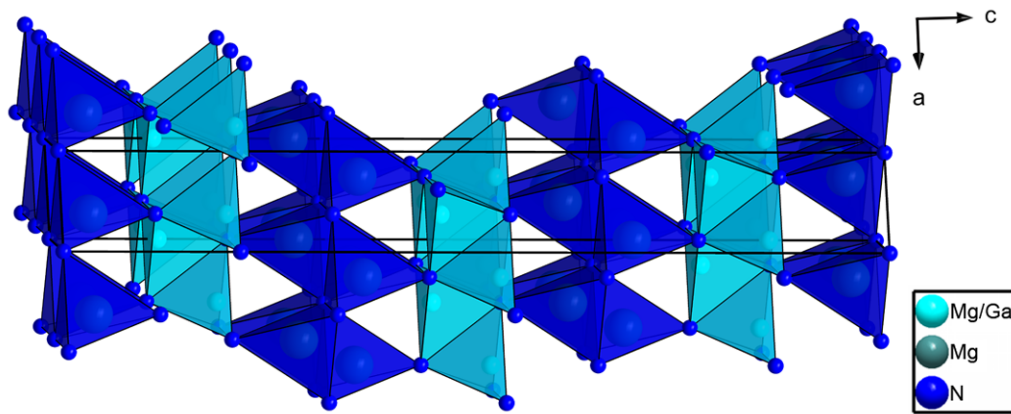


**Figure 1.** Figure 1. Crystal structure of  $\text{Mg}_3\text{GaN}_3$ . Unit cell shown in solid black lines. Sheets of  $(\text{Mg}/\text{Ga})\text{N}_4$ -units (light blue) and  $\text{MgN}_4$ -tetrahedra (dark blue) linked via corners to each other and via edges within the sheets.

The tetrahedra are connected to each other by common corners and edges, building a three-dimensional network. Both tetrahedra  $\text{MgN}_4$  and  $(\text{Mg}/\text{Ga})\text{N}_4$  are connected via edges to themselves and via corners to the other kind. Thereby, sheets of  $\text{MgN}_4$ - and  $(\text{Mg}/\text{Ga})\text{N}_4$ -tetrahedra are built which are linked to each other via vertices and stacked along  $[001]$  (Fig. 1). In their second coordination sphere each metal atom is coordinated by twelve further metal atoms. The mixed  $(\text{Mg}/\text{Ga})$ -site is surrounded by a cuboctahedron, while the pure Mg-site is coordinated with an anti-cuboctahedron.

**Table 3.** Anisotropic displacement parameters (in  $10^{-4} \text{ pm}^2$ ) for  $\text{Mg}_3\text{GaN}_3$  (e.s.d.'s in parentheses).

atom	$U_{11}$	$U_{22}$	$U_{33}$
Mg1/Ga1	0.0081(4)	$U_{11}$	0.0210(6)
Mg2	0.0080(5)	$U_{11}$	0.0116(8)
atom	$U_{23}$	$U_{13}$	$U_{12}$
Mg1/Ga1	0	0	0.00406(19)
Mg2	0	0	0.0040(3)

**Table 4.** Selected bond lengths and angles in Mg<sub>3</sub>GaN<sub>3</sub> (e.s.d.'s in parentheses).

(Mg1/Ga1)-N1	3x	1.9815(6) Å
(Mg1/Ga1)-N2		2.191(4) Å
Mg2-N1	3x	2.1915(8) Å
Mg2-N2		2.085(4) Å

Nitridogallates containing Mg are barely known thus far. The only examples appearing in the literature are Ca<sub>2</sub>Ga<sub>3</sub>MgN<sub>5</sub> and Sr(Mg<sub>2</sub>Ga<sub>2</sub>)N<sub>4</sub>.<sup>42,53</sup> For both compounds, mixed occupation Mg/Ga on the tetrahedral sites has been reported. These tetrahedra exhibit both corner and edge sharing, forming a network that represents the anionic substructure charge balanced by Ca<sup>2+</sup> or Sr<sup>2+</sup>, respectively.

Contrary to this, in the crystal structure of Mg<sub>3</sub>GaN<sub>3</sub> there are no further metal sites beside the ones in the uncharged tetrahedron network. Therefore, the atomic ratio (Mg/Ga) : N, representing the degree of condensation  $\kappa = 4 : 3$ , is much higher than  $\kappa$  of any other known nitridogallate. According to *Liebau*,<sup>60</sup> Mg<sub>3</sub>GaN<sub>3</sub> can be interpreted as a double nitride of Mg and Ga rather than a magnesium nitridogallate as assumed before.<sup>52</sup>

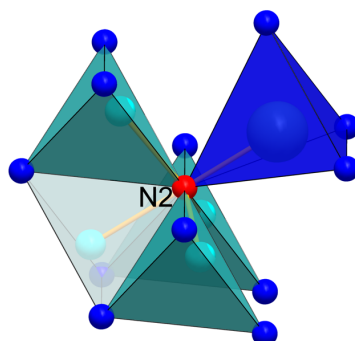
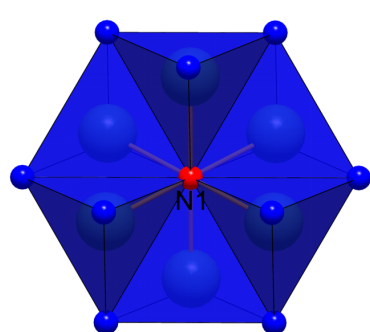
### 3. Magnesium Nitrides as Host Lattices for $\text{Eu}^{2+}$ -Doping

**Table 5.** MAPLE values [kJ/mol] for  $\text{Mg}_3\text{GaN}_3$  and  $\text{Mg}_3\text{N}_2$  and respective deviation  $\Delta$  [%] from theoretical value of constituting nitrides.

$\text{Mg}_3\text{GaN}_3$	calculated MAPLE values	$\Delta$	$\text{Mg}_3\text{N}_2$	calculated MAPLE values	$\Delta$
Mg	2206.12 - 2416.53		Mg	2250.57	
Mg/Ga	3402.19 - 3587.68		N	4757.32 - 4764.33	
N	4528.52 - 5275.71				
$\text{Mg}_3\text{GaN}$	26394.85		$\text{Mg}_3\text{N}_2$	16284.66	
model:			model:		
$\text{Mg}_3\text{N}_2^{27}$			3 $\text{MgSiN}_2^{62}$		
+ $\text{GaN}^{61}$	26772.85	1.41	- $\text{Si}_3\text{N}_4^{63}$	16265.34	0.11

Typical partial MAPLE values [kJ/mol]:  $\text{Ga}^{3+}$ : 4500 - 6000;  $\text{Mg}^{2+}$ : 2100 - 2400;  $\text{N}^{3-}$ : 3000 - 6000.<sup>34,64-66</sup>

An alternate structural description of  $\text{Mg}_3\text{GaN}_3$  can be afforded on the basis of anion-centered polyhedra. There are two distinct nitrogen sites (Fig. 2). N1 is surrounded



by six Mg-atoms in edge-sharing  $\text{MgN}_4$ -units in a slightly distorted octahedron, while N2 is coordinated by five metal atoms in a trigonal bipyramidal configuration, belonging to one  $\text{MgN}_4$ - and four  $(\text{Mg/Ga})\text{N}_4$ -tetrahedra.

**Figure 2.** N-coordination of N-sites in  $\text{Mg}_3\text{GaN}_3$ .

These structural details can be compared to the respective binary nitrides  $\text{Mg}_3\text{N}_2$  and  $\text{GaN}$ . In  $\text{Mg}_3\text{N}_2$  there are two N-sites as well,<sup>27</sup> both of which are sixfold coordinated with one of them showing the same hexagonal arrangement of six  $\text{MgN}_4$ -tetrahedra as N1 in  $\text{Mg}_3\text{GaN}_3$ . In  $\text{GaN}$ , regardless of whether hexagonal or cubic modification<sup>61,67</sup> is realized, nitrogen is coordinated by four  $\text{GaN}_4$ -units in a tetrahedral arrangement. This arrangement is comparable to the surroundings of N2 in  $\text{Mg}_3\text{GaN}_3$ , where the fivefold coordination of the N-atom can also be seen as a tetrahedral arrangement of three  $(\text{Mg/Ga})\text{N}_4$ - and one  $\text{MgN}_4$ -unit with a further  $(\text{Mg/Ga})\text{N}_4$ -tetrahedron. The anion-centered polyhedra illustrate the structural relation to the binary nitrides and support the double nitride character of  $\text{Mg}_3\text{GaN}_3$ .  $\text{Sr}_3\text{GaN}_3$  is known as well and its structure has been described in the literature. Unlike

Mg<sub>3</sub>GaN<sub>3</sub> the Sr compound is made up of Sr<sup>2+</sup> and isolated trigonal planar [GaN<sub>3</sub>]<sup>6-</sup> ions.<sup>68</sup> Contrary, Mg<sub>3</sub>BN<sub>3</sub> has to be classified as a nitridoborate nitride containing even linear [BN<sub>2</sub>]<sup>3-</sup> ions and isolated N<sup>3-</sup> ions besides Mg<sup>2+</sup>.<sup>69</sup> The system Mg/Ga/N has been thoroughly studied in the literature,<sup>11-20</sup> however no other ternary Mg-Ga-N compounds but only quaternary Mg-containing nitridogallates of formula Ca<sub>2</sub>Ga<sub>3</sub>MgN<sub>5</sub> or Sr(Mg<sub>2</sub>Ga<sub>2</sub>)N<sub>4</sub> have been described.<sup>42,53</sup>

There are a number of other double nitrides (e. g. Li<sub>7</sub>PN<sub>4</sub>) made up of edge-sharing LiN<sub>4</sub>- and PN<sub>4</sub>-tetrahedra<sup>70</sup> or phenakite-type BeP<sub>2</sub>N<sub>4</sub> containing an uncharged three-dimensional network of all corner-sharing BeN<sub>4</sub>- and PN<sub>4</sub>-tetrahedra.<sup>71</sup>

Concerning the degree of condensation  $\kappa$  the double nitride Mg<sub>3</sub>GaN<sub>3</sub> ( $\kappa = 4:3$ ) is intermediate between the binary nitrides Mg<sub>3</sub>N<sub>2</sub> ( $\kappa = 3:2$ ) and GaN ( $\kappa = 1:1$ ).

The crystal structure of Mg<sub>3</sub>N<sub>2</sub> was re-refined on the basis of single-crystal X-ray diffraction data. The solution and refinement was performed in cubic space group  $Ia\bar{3}$  (no. 206) with  $a = 9.955(2)$  Å. The refined crystal structure parameters are slightly different from single-crystal data published before,<sup>27</sup> but agree well with literature values from powder X-ray investigations on Mg<sub>3</sub>N<sub>2</sub>.<sup>24-26,72</sup> The results of the crystal structure refinement are listed in the supporting information. Mg<sub>3</sub>N<sub>2</sub> crystallizes in the anti-bixbyite type and is constituted of edge-sharing MgN<sub>4</sub>-tetrahedra.<sup>27</sup> To further confirm the refined crystal structures of Mg<sub>3</sub>GaN<sub>3</sub> and Mg<sub>3</sub>N<sub>2</sub>, MAPLE calculations were performed on both compounds. The electrostatic consistency was proven by comparison of the MAPLE sum with the sum of constituting nitrides. Moreover, MAPLE values for each atom were compared with known MAPLE values from reference data previously reported.<sup>34</sup> Results of MAPLE investigations are listed in Table 5.

### 3.3.2. DFT Calculations and Soft X-ray Spectroscopy of Mg<sub>3</sub>GaN<sub>3</sub>

Given a well-defined, periodic crystal structure, DFT calculations can be used to predict the electronic properties of a material, to explore the chemical bonding that occurs and further refine its structural parameters. In order to perform DFT calculations on Mg<sub>3</sub>GaN<sub>3</sub> (Fig. 1), the mixed occupancy metal sites must be divided evenly into pure Mg- and Ga-sites with periodic ordering. Since the unit cell in

### 3. Magnesium Nitrides as Host Lattices for $\text{Eu}^{2+}$ -Doping

Figure 1 contains six inequivalent mixed sites, a simple way to achieve this would be to assign three of them as Ga-atoms and three as Mg. There are ten unique unit cells that can be created in this manner, all of which predict  $\text{Mg}_3\text{Ga}\text{N}_3$  to be either a metal or a narrow band gap ( $<0.2$  eV) semiconductor when their electronic structure is calculated. Given the colorless nature of the double nitride crystals, such structures can be safely ruled out.

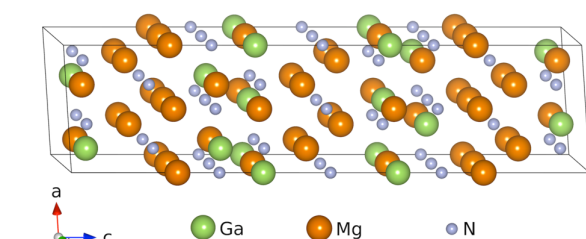


**Figure 3.** A VESTA<sup>70</sup> visualization of the energetically favored crystal structure of  $\text{Mg}_3\text{Ga}\text{N}_3$  with optimal Mg/Ga ordering and crystal symmetry.

In a  $2 \times 2 \times 1$  supercell, all of the aforementioned inequivalent sites are quadrupled, generating six different sets of four equivalent crystal positions. The total energy of the unit cell is found to decrease when each set of equivalent sites is half filled with Mg and half with Ga, and decreases further if each Ga-site is only

coordinated with one more Ga-atom in the second coordination sphere, as shown in Figure 3. Furthermore, when the electronic structure of this particular configuration is calculated, a band gap compatible with colorless  $\text{Mg}_3\text{Ga}\text{N}_3$  crystals is predicted. If this structure is relaxed to minimize internal atomic forces and pressure on the unit cell, the resulting optimized atomic coordinates and lattice constants agree with results of the single-crystal X-ray diffraction experiment. The calculated band gap is not significantly affected by relaxing the crystal structure.

The calculated DOS is shown in the bottom frame of Figure 4. Typically, calculations using the PBE-GGA exchange-correlation functional are found to underestimate the band gap, while mBJ calculations provide more appropriate band gap estimates but have been observed to horizontally contract the surrounding states.<sup>74</sup> For  $\text{Mg}_3\text{Ga}\text{N}_3$ , PBE-GGA calculations returned a band gap of 1.7 eV, while mBJ calculations predicted a more reasonable value of 3.0 eV. To compensate for the shortcomings of both techniques, Figure 4 uses the PBE-GGA calculated DOS but with the conduction states shifted up 1.3 eV to reflect the mBJ band gap.

A band of Ga 3d states can be found from -15 to -11 eV relative to the Fermi energy, in which a narrow peak of states at -13.3 eV comprising primarily of Ga 3d character is surrounded by hybridized Ga 3d and N 2s states. The 6.5 eV wide valence band,

terminating at the Fermi energy, is dominated by N  $2p$  character and contains very little charge associated with Mg or Ga. This suggests that bonding is fairly ionic, with N-atoms peeling away some valence electrons from the metal sites. In fact, each Ga-site only contributes 0.3 e of charge to the DOS in the valence band, essentially giving them a  $3d^{10}$  valency. This could explain the energetic preference for the Mg/Ga-ordering in Figure 4. Any other stoichiometric configuration would include more than one Ga-Ga coordination in the second coordination sphere, which would increase the total energy of the cell through  $d^{10}$ - $d^{10}$  filled-shell Pauli repulsion.

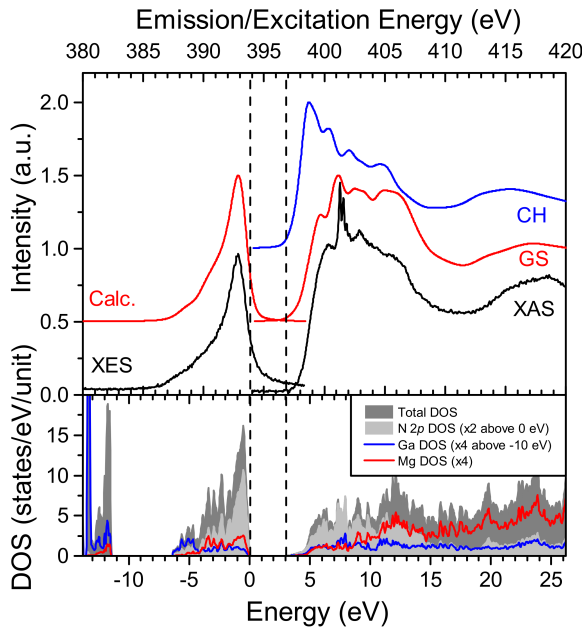


**Figure 4.** The calculated DOS of  $\text{Mg}_3\text{GaN}_3$  (bottom panel). The total DOS for all atoms is shown in dark gray, N  $p$  states are light gray, and total Ga- and Mg-states are blue and red, respectively. Measured and calculated soft X-ray emission (XES) and absorption spectra (XAS, top panel). Measurements are shown in black, ground state (GS) calculations are red, and the core hole (CH) absorption spectrum is blue. Dashed lines represent the band gap edges.

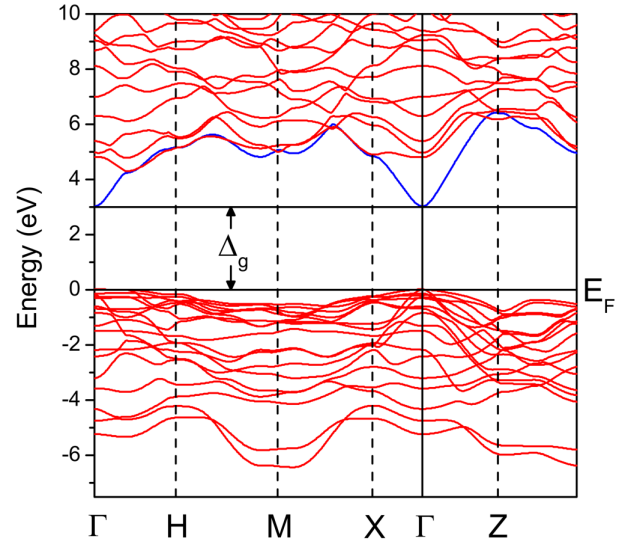


**Figure 5.** The calculated ground-state band structure of  $\text{Mg}_3\text{GaN}_3$ . The blue band is responsible for the weak states near the conduction band minimum. The chosen k-point path is standard for monoclinic unit cells.

The conduction band contains relatively few states from 3 to 5 eV. N  $s$  and  $p$  character dominate the conduction band from 5 to 15 eV, at which point the N  $p$  states begin to recede and N  $s$  and Mg states become more prominent.

Examining the ground-state band structure (Fig. 5), the weak low-energy conduction states are observed to be the result of a single high-curvature band at the

conduction-band minimum. This calculation also reveals that the band gap of  $\text{Mg}_3\text{GaN}_3$  is direct across the  $\Gamma$ -point.

XES and XAS offer an indirect probe of the local partial DOS in the valence and conduction bands, respectively. At the N K-edge, these techniques are predominantly sensitive to N  $p$  states. The measured N  $K_\alpha$  emission and N 1s absorption spectra are shown in the top frame of Figure 4 in black.

Significant core hole lifetime broadening effects prevent any fine details of the emission spectrum from being resolved. There is a single peak at 392 eV (relative to the N 1s core level) with a broad low energy shoulder. The measured XAS has a 3 eV wide onset followed by four resolvable features, including an  $\text{N}_2$  gas absorption spectrum superimposed on the  $\text{Mg}_3\text{GaN}_3$  spectrum between 400.5 and 402 eV. This gas likely originates from within the material, liberated by irradiation before becoming trapped in the pockets between agglomerated crystals.<sup>75</sup> Successive XAS scans show an increase in  $\text{N}_2$  gas buildup, but no other spectral changes due to radiation damage are observed.

The WIEN2k utility XSPEC, which uses the formalism described in ref. 76, is used to estimate ground-state N  $K_\alpha$  emission spectra from the occupied DOS and absorption spectra from the unoccupied DOS. These calculated spectra are shown in the top frame of Figure 4 in red. The calculated XES spectrum agrees well with the measured emission profile in terms of valence band width and overall shape. All three of the  $\text{Mg}_3\text{GaN}_3$  absorption features observed in the XAS measurement are recreated in the calculated absorption spectrum at approximately the same energy, as well as a fourth feature that may have been obscured by the  $\text{N}_2$  gas signal in the measured XAS. There is a slight disagreement in the relative peak heights between the measurement and calculation, which is likely the result of the N 1s core hole introduced in the course of an XAS measurement. Indeed, in calculations with a core hole present, the relative amplitudes of lower energy features are increased (Fig. 4, top panel, blue line). However, such calculations almost invariably overestimate the density of core holes and their effects on the electronic structure, placing too much emphasis on the low energy states and shifting the entire conduction band down in energy. It would be possible to decrease the core hole density by further expanding the supercell or introducing fractional core holes, but such calculations are

computationally expensive, and the observed core hole effect is too small to make this approach worthwhile.

In the region of the valence-band maximum and conduction-band minimum, the measured and calculated spectra are in very good agreement, suggesting experimental confirmation of the predicted 3.0 eV band gap. Furthermore, the excellent overall agreement between the experimental and theoretical soft X-ray spectra lead us to conclude that the structure shown in Figure 3 is the correct choice for  $\text{Mg}_3\text{GaN}_3$ .

### 3.3.3. Luminescence Investigations

Luminescence investigations were performed on  $\text{Eu}^{2+}$ -doped single crystals of both compounds. When irradiated with UV to blue light, crystals of  $\text{Mg}_3\text{GaN}_3:\text{Eu}^{2+}$  show yellowish luminescence at room temperature. The 365 nm excitation yields an emission band peaking at 578 nm with a lumen equivalent of 132 lm/W and CIE color coordinates  $x = 0.491$ ,  $y = 0.498$ . The full width at half maximum (FWHM) was measured to be  $4052 \text{ cm}^{-1}$  (132 nm). The emission spectrum (Fig. 6) shows a tailing on the right and a second order excitation peak that occurs due to instrumental reasons.  $\text{Eu}^{2+}$ -doped samples of  $\text{Mg}_3\text{N}_2$  were equally investigated under room temperature conditions. An emission band with maximum intensity at 589 nm was observed when excited with 365 nm light (Fig. 6).  $\text{Mg}_3\text{N}_2:\text{Eu}^{2+}$  shows a FWHM of  $4056 \text{ cm}^{-1}$  (147 nm) with a lumen equivalent of 317 lm/W and CIE color coordinates  $x = 0.509$  and  $y = 0.480$ . An uncommon green luminescence of non-doped  $\text{Mg}_3\text{N}_2$  powders was reported in literature.<sup>28</sup>

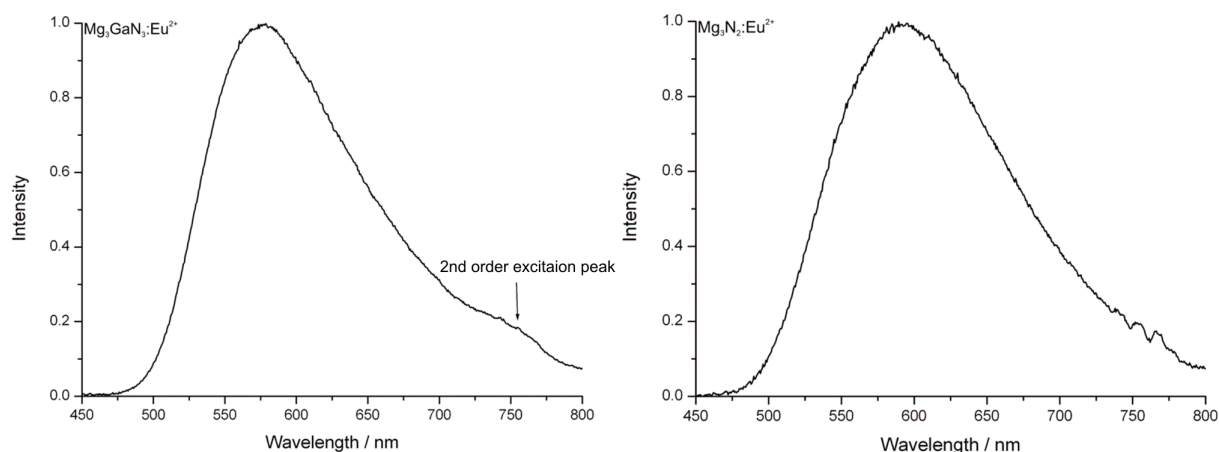


**Figure 6.** Emission spectra of  $\text{Mg}_3\text{Ga}_2\text{N}_6:\text{Eu}^{2+}$  (left) and  $\text{Mg}_3\text{N}_2:\text{Eu}^{2+}$  (right).



### 3. Magnesium Nitrides as Host Lattices for $\text{Eu}^{2+}$ -Doping

In both compounds the question arises as to where the  $\text{Eu}^{2+}$  activator ions are located within the crystal structure. In most nitride host lattices,  $\text{Eu}^{2+}$  is supposed to occupy an alkaline-earth site (e. g.  $\text{Ba}_3\text{Ga}_3\text{N}_5:\text{Eu}^{2+}$  and  $\text{Sr}_2\text{Si}_5\text{N}_8:\text{Eu}^{2+}$ ).<sup>34,40</sup> The ionic radii of sixfold coordinated alkaline-earth ions  $\text{Ba}^{2+}$  (1.35 Å),  $\text{Sr}^{2+}$  (1.18 Å) and  $\text{Ca}^{2+}$  (1.00 Å) fit that of sixfold surrounded  $\text{Eu}^{2+}$  (1.17 Å) although  $\text{Ba}^{2+}$  is slightly larger and  $\text{Ca}^{2+}$  is smaller.<sup>58</sup> Nevertheless, the change of lattice structure caused by this mismatch is often helpful for luminescence due to influence on bond lengths and resulting change in energy-level positions. Presumably, the fourfold coordinated  $\text{Mg}^{2+}$ -site in  $\text{Mg}_3\text{GaN}_3$  with an ionic radius of 0.57 Å is much too small to be occupied by  $\text{Eu}^{2+}$ . The mixed metal site can also be ruled out because it is even smaller than a pure  $\text{Mg}^{2+}$ -site. This leads to the assumption that  $\text{Eu}^{2+}$  is incorporated on interstitial sites of the crystal structure. In the network of  $\text{Mg}_3\text{GaN}_3$  two kinds of octahedral voids (Fig. 7a, b) are present.

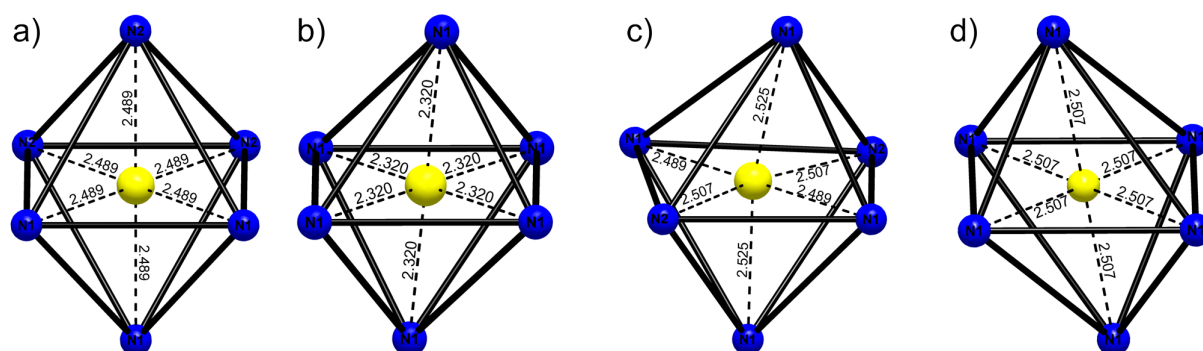


**Figure 7.** Octahedral voids in the crystal structures of  $\text{Mg}_3\text{GaN}_3$  (a and b) and  $\text{Mg}_3\text{N}_2$  (c and d). The yellow spheres are possible Eu-atom positions and the resulting distances to coordinating N are given in Å.

The polyhedra around these voids are linked through edges to themselves and via faces to each other. Both octahedra offer a possible position for  $\text{Eu}^{2+}$ . The positions displayed in yellow color in Figure 7 are thus suitable for  $\text{Eu}^{2+}$  and the observed distances to N-atoms of 2.320-2.489 Å are in good agreement with typical distances for Eu-N found in the literature.<sup>77,78</sup> To the best of our knowledge,  $\text{Mg}_3\text{GaN}_3:\text{Eu}^{2+}$  is the first reported luminescent double nitride.

$\text{Mg}_3\text{N}_2$  crystallizes in an anti-bixbyite type of structure. In this crystal structure there are also two different octahedral voids, but these are edge-sharing in all three spatial directions.  $\text{Eu}^{2+}$  atoms have been introduced onto these sites in order to verify the occurring Eu-N distances (Fig. 7c, d), which range from 2.489 to 2.525 Å. The

highest remaining electron density during structure refinement of  $\text{Mg}_3\text{N}_2:\text{Eu}^{2+}$  lies on a special site (8a) and is therefore exactly in the center of one of these octahedral voids (Fig. 7d). This could be another hint for  $\text{Eu}^{2+}$  being located on this site. Due to the low doping level (2 mol% Eu), no refinement of the occupancy of Eu on this position has been possible.

To reassess if the observed luminescence of  $\text{Mg}_3\text{GaN}_3:\text{Eu}^{2+}$  and  $\text{Mg}_3\text{N}_2:\text{Eu}^{2+}$  could be traced to these voids, known compounds with similar Eu-N distances and coordination numbers have been compared. One example is  $\text{Li}_2\text{CaSiN}_4$  where a sixfold coordinated Ca-site was reported with Ca-N distances ranging from 2.489-2.586 Å.<sup>79</sup> In the doped compound  $\text{Li}_2\text{CaSiN}_4:\text{Eu}^{2+}$  it is assumed that  $\text{Eu}^{2+}$  occupies a  $\text{Ca}^{2+}$ -site. The observed luminescence shows an emission-band maximum at 583-585 nm.<sup>80</sup> In  $\text{Eu}^{2+}$ -doped Li- $\alpha$ -SiAlON the activator  $\text{Eu}^{2+}$  is supposed to occupy the  $\text{Li}^+$ -site.<sup>81</sup> There the coordination number is seven and distances to N/O range from 2.052 to 2.767 Å. The reported luminescence varies between 563 and 586 nm, depending on composition and  $\text{Eu}^{2+}$ -concentration. This is in good agreement with the luminescence data of  $\text{Mg}_3\text{GaN}_3:\text{Eu}^{2+}$  and  $\text{Mg}_3\text{N}_2:\text{Eu}^{2+}$  so we can assume that  $\text{Eu}^{2+}$  occupies an interstitial position in these two nitride networks. To understand the origin and the quality of luminescence properties, detailed knowledge of the local environment of the activator ion is necessary. Recent investigations focused on determination of Eu-contribution in the *M*-sites in  $M_2\text{Si}_5\text{N}_8$  (*M* = Ca, Sr, Ba). With a high concentration of  $\text{Eu}^{2+}$ , a reliable distribution and a preferred site can be determined based on structural refinement methods and composition investigations.<sup>82</sup> These investigations give an indication of the average  $\text{Eu}^{2+}$ -contribution, statistically distributed over the whole crystal, but no information of the local structure of the activator can be achieved. Another recent approach to detect interstitial dopants and elucidate local surrounding of the dopant involved STEM investigations on  $\beta$ -SiAlON. There, a single dopant ion was detected in the atomic channel of the crystal structure.<sup>83</sup> This method seems quite promising when the layer thickness is suitable for such measurements and the crystal structure reveals appropriate requirements. Nevertheless, it is still difficult to determine the real location and the amount of activator ions in such host lattices

#### 3.4. Conclusion

In this study we present a structural description of  $\text{Mg}_3\text{GaN}_3$  based on single crystal X-ray diffraction data, which shows a three-dimensional uncharged network of corner- and edge-sharing  $\text{MgN}_4$ - and mixed  $(\text{Mg}/\text{Ga})\text{N}_4$ -tetrahedra. Since all metal atoms are part of the tetrahedral network,  $\text{Mg}_3\text{GaN}_3$  can be classified as a double nitride, in contrast to known nitridogallates which exhibit an anionic tetrahedra substructure with electropositive counter ions like  $\text{Sr}^{2+}$  or  $\text{Ba}^{2+}$ . To our knowledge the compound  $\text{Mg}_3\text{GaN}_3$  represents the first known stoichiometrically defined ternary compound in the system  $\text{Mg}/\text{Ga}/\text{N}$ . It is found to be a semiconductor with a direct band gap of 3.0 eV across the  $\Gamma$ -point. DFT calculations suggest a periodic ordering in the mixed occupancy metal sites, and the measured soft X-ray spectra confirm these calculations. The band gap of  $\text{Mg}_3\text{GaN}_3$  lies with 3.0 eV in between that of  $\text{Mg}_3\text{N}_2$  (2.8 eV)<sup>84</sup> and  $\text{GaN}$  (3.02–3.20 eV),<sup>85</sup> which further emphasizes the double nitride character of  $\text{Mg}_3\text{GaN}_3$ . Upon doping with  $\text{Eu}^{2+}$  the double nitride shows broad-band emission due to  $4f^6(^7F)5d^1 \rightarrow 4f^7(^8S_{7/2})$  transitions with maximum intensity at 578 nm after excitation at 365 nm. Due to the structural characteristics of  $\text{Mg}_3\text{GaN}_3:\text{Eu}^{2+}$  it is assumed that activator ions are localized in interstitial octahedral voids of the crystal structure.

A likewise luminescent binary nitride,  $\text{Mg}_3\text{N}_2:\text{Eu}^{2+}$  is also investigated. Structural details are known from the literature and presumably  $\text{Eu}^{2+}$  also occupies interstitial sites. After excitation with UV to blue light, this compound shows luminescence with an emission-band maximum at 589 nm with a FWHM of  $4056\text{ cm}^{-1}$  (147 nm).

Both presented nitrides are new host lattices for  $\text{Eu}^{2+}$ -doping and show interesting luminescence properties. The results of this study illustrate the potential of nitrides as host lattices for  $\text{Eu}^{2+}$ -doping once again. It is remarkable that double nitride  $\text{Mg}_3\text{GaN}_3$  is the first representative showing luminescence, to the best of our knowledge. Further optimization of synthesis and the optical properties of these materials must be achieved for them to have possible applications as phosphor materials.

### 3.5. References

- [1] Nakamura, S.; Senoh, M.; Iwasa, N.; Nagahama, S.; Yamada, T.; Mukai, T. *Jpn. J. Appl. Phys.* **1995**, *34*, L1332.
- [2] Nakamura, S. *Solid State Commun.* **1997**, *102*, 237.
- [3] Fujii, T.; Gao, Y.; Sharma, R.; Hu, E. L.; DenBaars, S. P.; Nakamura, S. *Appl. Phys. Lett.* **2004**, *84*, 855.
- [4] Nakamura, S. *Science* **1998**, *281*, 956.
- [5] Nakamura, S.; Pearton, S.; Fasol, G.; *The Blue Laser Diode*, Springer Verlag, Berlin, **2000**.
- [6] Denis, A.; Goglio, G.; Demazeau, G. *Mater. Sci. Eng.* **2006**, *R 50*, 167.
- [7] Bockowski, M. *Cryst. Res. Technol.* **2007**, *42*, 1162.
- [8] Krukowski, S.; Kempisty, P.; Strak, P. *Cryst. Res. Technol.* **2009**, *44*, 1038.
- [9] Wang, B.; Callahan, M. J. *Cryst. Growth Des.* **2006**, *6*, 1227.
- [10] Parikh, R. P.; Adomaitis, R. A. *J. Cryst. Growth* **2006**, *286*, 259.
- [11] Onuma, T.; Uedono, A.; Asamizu, H.; Sato, H.; Kaeding, J. F.; Iza, M.; DenBaars, S. P.; Nakamura, S.; Chichibu, S. F. *Appl. Phys. Lett.* **2010**, *96*, 091913.
- [12] Nakamura, S.; Senoh, M.; Mukai, T. *Jpn. J. Appl. Phys.* **1991**, *30*, L1708.
- [13] Nakamura, S.; Mukai, T.; Senoh, M.; Iwasa, N. *Jpn. J. Appl. Phys.* **1992**, *31*, L139.
- [14] Kuo, C. H.; Chang, S. J.; Su, Y. K.; Wu, L. W.; Sheu, J. K.; Chen, C. H.; Chi, G. C. *Jpn. J. Appl. Phys.* **2008**, *41*, L112.
- [15] Nakano, Y.; Fujishima, O.; Kachi, T. *J. Appl. Phys.* **2004**, *96*, 415.
- [16] Chen, Z.; Fichtenbaum, N.; Brown, D.; Keller, S.; Mishra, U. K.; DenBaars, S. P.; Nakamura, S. *J. Electron. Mater.* **2008**, *37*, 546.
- [17] Zohta, Y.; Iwasaki, Y.; Nakamura, S.; Mukai, T. *Jpn. J. Appl. Phys.* **2001**, *40*, L423.
- [18] Akiyama, T.; Ammi, D.; Nakamura, K.; Ito, T. *Jpn. J. Appl. Phys.* **2009**, *48*, 110202.
- [19] Shahedipour, F.; Wessels, B. W. *Appl. Phys. Lett.* **2000**, *76*, 3011.
- [20] Ehrentraut, D.; Meißner, E.; Bockowski, M.; *Technology of Gallium Nitride Crystal Growth*, Springer, Berlin, Heidelberg, **2010**, Vol. 133.
- [21] Reshchikov, M. A.; Yi, G.-C.; Wessels, B. W. *Phys. Rev. B* **1999**, *59*, 13176.

- [22] Qu, B. Z.; Zhu, Q. S.; Sun, X. H.; Wan, S. K.; Wang, Z. G.; Nagai, H.; Kawaguchi, Y.; Hiramatsu, K.; Sawaki, N. *J. Vac. Sci. Technol. A* **2003**, 21, 838.
- [23] Kaufmann, U.; Kunzer, M.; Maier, M.; Obloh, H.; Ramakrishnan, A.; Santic, B.; Schlotter, P. *Appl. Phys. Lett.* **1998**, 72, 1326.
- [24] Stackelberg, M. von; Paulus, R. *Z. Phys. Chem. (Abt. B)* **1933**, 22, 305.
- [25] David, J.; Laurent, Y.; Lang, J. *Bull. Soc. Fr. Mineral. Cristallogr.* **1971**, 94, 340.
- [26] Partin, D. E.; Williams, D. J.; O'Keefe, M. *J. Solid State Chem.* **1997**, 132, 56.
- [27] Reckeweg, O.; DiSalvo, F. J. *Z. Anorg. Allg. Chem.* **2001**, 627, 371.
- [28] Chengshan, X.; Yujie, A.; Lili, S.; Chuanwei, S.; Huizhao, Z.; Fuxue, W.; Zhaozhu, Y.; Lixia, Q.; Jinhua, C.; Hong, L. *Rare Metal Materials and Engineering* **2007**, 36, 2020.
- [29] Dorenbos, P. *J. Lumin.* **2003**, 104, 239.
- [30] Dorenbos, P. *ECS J. Solid State Sci. Technol.* **2013**, 2, R3001.
- [31] ten Kate, O. M.; Zhang, Z.; Dorenbos, P.; Hintzen, H. T.; van der Kolk, E. J. *Solid State Chem.* **2013**, 197, 209.
- [32] Höpfe, H. A. *Angew. Chem.* **2009**, 121, 3626; *Angew. Chem. Int. Ed.* **2009**, 48, 3648, 3572.
- [33] Li, Y. Q.; Hirosaki, N.; Xie, R. J.; Takeda, T.; Mitomo, M. *J. Solid State Chem.* **2008**, 181, 3200.
- [34] Zeuner, M.; Pagano, S.; Schnick, W. *Angew. Chem.* **2011**, 123, 7898; *Angew. Chem. Int. Ed.* **2011**, 50, 7850, 7754.
- [35] Schnick, W. *Phys. Status Solidi RRL* **2009**, 3, A113.
- [36] Seibald, M.; Oeckler, O.; Celinski, V. R.; Schmidt, P. J.; Tücks, A.; Schnick, W. *Solid State Sci.* **2011**, 13, 1769.
- [37] Kechele, J. A.; Hecht, C.; Oeckler, O.; Günne, J. Schmedt auf der; Schmidt, P. J.; Schnick, W. *Chem. Mater.* **2009**, 21, 1288.
- [38] Shioi, K.; Hirosaki, N.; Xie, R.-J.; Takeda, T.; Li, Y. Q. *J. Mater. Sci.* **2010**, 45, 3198.
- [39] Pagano, S.; Lupart, S.; Zeuner, M.; Schnick, W. *Angew. Chem.* **2009**, 121, 6453; *Angew. Chem. Int. Ed.* **2009**, 48, 6335.
- [40] Hintze, F.; Hummel, F.; Schmidt, P. J.; Wiechert, D.; Schnick, W. *Chem. Mater.* **2012**, 24, 402.

- [41] Clarke, S. J.; DiSalvo, F. J. *Inorg. Chem.* **1997**, 36, 1143.
- [42] Hintze, F.; Schnick, W. Z. *Anorg. Allg. Chem.* **2012**, 638, 2243.
- [43] Farrugia, L. J. *J. Appl. Crystallogr.* **1999**, 32, 837.
- [44] X-RED 32, 1.03 ed., Darmstadt, **2002**.
- [45] SHELXS, Universität Göttingen, **1997**.
- [46] Sheldrick, G. M. *Acta Crystallogr. Sect. A: Found. Crystallogr.* **2008**, 64, 112.
- [47] SHELXL, Universität Göttingen, **1997**.
- [48] Blaha, P.; Schwarz, K.; Madsen, G. K. H.; Kvasnicka, D.; Luitz, J., WIEN2K An Augmented Plane Wave + Local Orbitals Program for Calculating Crystal Properties, Technical University Vienna, **2001**.
- [49] Perdew, J. P.; Burke, K.; Ernzerhof, M. *Phys. Rev. Lett.* **1996**, 77, 3865.
- [50] Becke, A. D.; Johnson, E. R. *J. Chem. Phys.* **2006**, 124, 221101.
- [51] Tran, F.; Blaha, P. *Phys. Rev. Lett.* **2009**, 102, 226401.
- [52] Verdier, P.; Marchand, R.; Lang, J. C. *R. Acad. Sci. Ser. C.* **1970**, 271, 1002.
- [53] Park, D. G.; Dong, Y.; DiSalvo, F. J. *Solid State Sci.* **2008**, 10, 1846.
- [54] Spek, A. L. *Acta Crystallogr. Sect. D: Biol. Crystallogr.* **2009**, 65, 148.
- [55] Sluis, P. Van Der; Spek, A. L. *Acta Crystallogr. Sect. A: Found. Crystallogr.* **1990**, 46, 194.
- [56] Park, D. G.; Gál, Z. A.; DiSalvo, F. J. *J. Alloys Compd.* **2003**, 360, 85.
- [57] Baur, W. H. *Crystallogr. Rev.* **1987**, 1, 59.
- [58] Shannon, R. D. *Acta Crystallogr., Sect. A: Found. Crystallogr.* **1976**, 32, 751.
- [59] Slater, J. C. *J. Chem. Phys.* **1964**, 41, 3199.
- [60] Liebau, F.; *Structural Chemistry of Silicates*, Springer, Berlin, **1985**.
- [61] Roos, M.; Wittrock, J.; Meyer, G.; Fritz, S.; Strähle, J. Z. *Anorg. Allg. Chem.* **2000**, 626, 1179.
- [62] Wintenberger, M.; Tcheou, F.; David, J.; Lang, J. Z. *Naturforsch. B* **1980**, 35, 604.
- [63] Schneider, J.; Frey, F.; Johnson, N.; Laschke, K. Z. *Kristallogr.* **1994**, 209, 328.
- [64] Höppe, H. A., *Doctoral Thesis*, Ludwig-Maximilians-Universität München **2003**.
- [65] Köllisch, K., *Doctoral Thesis*, Ludwig-Maximilians-Universität München **2001**.
- [66] Lauterbach, R., *Doctoral Thesis*, Universität Bayreuth **1999**.
- [67] Saib, S.; Bouarissa, N. *Physica B: Condensed Mater.* **2007**, 387, 377.
- [68] Park, D. G.; Gál, Z. A.; DiSalvo, F. J. *Inorg. Chem.* **2003**, 42, 1779.

- [69] Hiraguchi, H.; Hashizume, H.; Fukunaga, O.; Takenaka, A.; Sakata, M. *J. Appl. Crystallogr.* **1991**, *24*, 286.
- [70] Schnick, W.; Lücke, J. *J. Solid State Chem.* **1990**, *87*, 101.
- [71] Pucher, F. J.; Römer, S. R.; Karau, F. W.; Schnick, W. *Chem. Eur. J.* **2010**, *16*, 7208.
- [72] Orhan, E.; Jobic, S.; Brec, R.; Marchand, R.; Saillard, J. Y. *J. Mater. Chem.* **2002**, *12*, 2475.
- [73] Momma, K.; Izumi, F. *J. Appl. Crystallogr.* **2011**, *44*, 1272.
- [74] Johnson, N. W.; McLeod, J. A.; Moewes, A. *J. Phys.: Condens. Matter* **2011**, *23*, 445501.
- [75] Braun, C.; Börger, S. L.; Boyko, T. D.; Miehe, G.; Ehrenberg, H.; Höhn, P.; Moewes, A.; Schnick, W. *J. Am. Chem. Soc.* **2011**, *133*, 4307.
- [76] Schwarz, K.; Neckel, A.; Nordgren, J. *J. Phys. F: Met. Phys.* **1979**, *9*, 2509.
- [77] Huppertz, H.; Schnick, W. *Acta Crystallogr., Sect. C: Cryst. Struct. Commun.* **1997**, *53*, 1751.
- [78] Zeuner, M.; Pagano, S.; Matthes, P.; Bichler, D.; Johrendt, D.; Harmening, T.; Pöttgen, R.; Schnick, W. *J. Am. Chem. Soc.* **2009**, *131*, 11242.
- [79] Zeuner, M.; Pagano, S.; Hug, S.; Pust, P.; Schmiechen, S.; Scheu, C.; Schnick, W. *Eur. J. Inorg. Chem.* **2010**, *2010*, 4945.
- [80] Zeuner, M., *Doctoral Thesis*, Ludwig-Maximilians-Universität München **2009**.
- [81] Xie, R.-J.; Hirosaki, N.; Mitomo, M.; Sakuma, K.; Kimura, N. *Appl. Phys. Lett.* **2006**, *89*, 241103.
- [82] Kim, Y.-I.; Kim, K. B.; Lee, Y.-H.; Kim, K.-B. *J. Nanosci. Nanotechnol.* **2012**, *12*, 3443.
- [83] Kimoto, K.; Xie, R.-J.; Matsui, Y.; Ishizuka, K.; Hirosaki, N. *Appl. Phys. Lett.* **2009**, *94*, 041908.
- [84] Fang, M. C.; de Groot R. A.; Bruls, R. J.; Hintzen, H. T.; de With, G. *J. Phys.: Condens. Matter* **1999**, *11*, 4833.
- [85] Duan, Y.; Qin, L.; Shi, L.; Tang, G.; Shi, H. *Appl. Phys. Lett.* **2012**, *199*, 022104.

#### 4. $\text{Ba}_3\text{Ga}_3\text{N}_5$ – A Novel Host Lattice for $\text{Eu}^{2+}$ -Doped Luminescent Materials

In the chapter above two luminescent nitrides were reported. Even though  $\text{Mg}_3\text{GaN}_3$  is a ternary compound it is closely related to binary nitrides as discussed before. Herein we present a novel ternary compound  $\text{Ba}_3\text{Ga}_3\text{N}_5$ . This compound is in contrast to the nitrides shown before a nitridogallate since it contains an anionic substructure charge balanced by  $\text{Ba}^{2+}$  in this case. The mentioned anionic substructure is built up of highly condensed  $\text{GaN}_4$ -tetrahedra, sharing edges and additionally corners, building strands running along [010]. In between these strands  $\text{Ba}^{2+}$  ions are intercalated. Upon doping with  $\text{Eu}^{2+}$   $\text{Ba}_3\text{Ga}_3\text{N}_5$  shows also luminescence properties in the orange to red spectral region when irradiated with UV to blue light. This compound represents the first luminescent nitridogallate and reveals an unexpected substructure. In this chapter, synthesis conditions as well as crystal structure investigations and description are presented. Additionally, band gap calculations and luminescence investigations were carried out and are reported in the following.



## **Ba<sub>3</sub>Ga<sub>3</sub>N<sub>5</sub> – a Novel Host Lattice for Eu<sup>2+</sup>-Doped Luminescent Materials with Unexpected Nitridogallate Substructure**

**Frauke Hintze, Franziska Hummel, Peter J. Schmidt, Detlef Wiechert and  
Wolfgang Schnick**

**published in:** *Chem. Mater.* **2012**, 24, 402.

**Keywords:** nitridogallate, Eu<sup>2+</sup>-luminescence, DFT calculations, structure elucidation, band gap

**Abstract:** The alkaline earth nitridogallate Ba<sub>3</sub>Ga<sub>3</sub>N<sub>5</sub> was synthesized from the elements in a sodium flux at 760 °C utilizing weld shut tantalum ampoules. The crystal structure was solved and refined on the basis of single-crystal X-ray diffraction data. Ba<sub>3</sub>Ga<sub>3</sub>N<sub>5</sub> (space group C2/c (no. 15),  $a = 16.801(3)$ ,  $b = 8.330(2)$ ,  $c = 11.623(2)$  Å,  $\beta = 109.92(3)^\circ$ ,  $Z = 8$ ) contains a hitherto unknown structural motif in nitridogallates, namely infinite strands made up of GaN<sub>4</sub>-tetrahedra, each sharing two edges and at least one corner with neighboring GaN<sub>4</sub>-units. There are three Ba<sup>2+</sup>-sites with coordination numbers six or eight, respectively, and one Ba<sup>2+</sup>-position exhibiting a low coordination number 4 corresponding to a distorted tetrahedron. Eu<sup>2+</sup>-doped samples show red luminescence when excited by UV-irradiation at room temperature. Luminescence investigations revealed a maximum emission intensity at 638 nm (FWHM = 2123 cm<sup>-1</sup>). Ba<sub>3</sub>Ga<sub>3</sub>N<sub>5</sub> is the first nitridogallate for which parity allowed broadband emission due to Eu<sup>2+</sup>-doping has been found. The electronic structure of both Ba<sub>3</sub>Ga<sub>3</sub>N<sub>5</sub> as well as isoelectronic but not isostructural Sr<sub>3</sub>Ga<sub>3</sub>N<sub>5</sub> were investigated by DFT methods. The calculations revealed a band gap of 1.53 eV for Sr<sub>3</sub>Ga<sub>3</sub>N<sub>5</sub> and 1.46 eV for Ba<sub>3</sub>Ga<sub>3</sub>N<sub>5</sub>.

### 4.1. Introduction

Gallium nitride GaN is a direct wide band gap semiconductor that has found increasing application in high performance light emitting diodes (LEDs).<sup>1-6</sup> While synthesis, crystal growth and doping of GaN has been studied thoroughly,<sup>7-12</sup> the chemistry of ternary and higher nitridogallates deriving from binary GaN has been widely neglected as yet. In the literature, only a small number of ternary alkaline earth nitridogallates has been described and thereof, only two compounds are containing Ba.<sup>13-18</sup> Most nitridogallates are made up of GaN<sub>4</sub>-tetrahedra which can be connected through both common corners and/or common edges.<sup>13,15,16</sup> Depending on the degree of condensation of the nitridogallate substructure, a broad range of structural motifs has been identified in nitridogallates, including one-dimensional chains of edge-sharing GaN<sub>4</sub>-units (e.g. in Sr<sub>3</sub>Ga<sub>2</sub>N<sub>4</sub>), two-dimensional sheets made up of Ga<sub>2</sub>N<sub>6</sub>-units which are further linked through corners (e.g. in Ca<sub>3</sub>Ga<sub>2</sub>N<sub>4</sub>), or three-dimensional networks built up from vertex- and corner-sharing tetrahedra (e.g. in Sr<sub>3</sub>Ga<sub>3</sub>N<sub>5</sub>).<sup>16</sup> Synthesis of nitridogallates starts typically from the elements employing a sodium flux and increased nitrogen pressure. These synthesis conditions can be achieved easily by thermal decomposition of sodium azide in weld shut Ta or Nb ampoules. The solubility of nitrogen in sodium can be further enhanced by addition of electropositive elements like alkaline earth metals.<sup>18,19</sup> Synthesis of highly condensed nitridogallates (i.e. atomic ratio Ga : N > 1 : 2) has been pursued for a couple of years in order to reach a higher stability against hydrolysis. To accomplish this goal either a higher nitrogen pressure or a lower metal amount is necessary.<sup>18</sup>

During the last decade, ternary and multinary alkaline earth nitrides emerged as important host lattices for doping with Eu<sup>2+</sup> exhibiting parity allowed intense broad band emission due to 4f<sup>6</sup>(<sup>7</sup>F)5d<sup>1</sup> → 4f<sup>7</sup>(<sup>8</sup>S<sub>7/2</sub>) transitions. Several of these nitrides turned out to be excellent optical materials for application in phosphor-converted (pc)-LEDs.<sup>20,21</sup> Nitridosilicates, nitridoalumosilicates and related SiAlONs have been intensively investigated in this respect.<sup>15,21-27</sup> However, these investigations have scarcely been extended to related alkaline earth containing tetrahedra based nitride materials, e.g. nitridogallates or nitridophosphates.

### 4.2. Experimental

Synthesis of Ba<sub>3</sub>Ga<sub>3</sub>N<sub>5</sub> was carried out in a Ta ampoule (30 mm length, 10 mm diameter, 0.5 mm wall thickness). All manipulations were done under argon atmosphere in recirculated glove boxes (Unilab, MBraun, Garching; O<sub>2</sub> < 1 ppm, H<sub>2</sub>O < 1 ppm). Single crystals of Ba<sub>3</sub>Ga<sub>3</sub>N<sub>5</sub> were obtained from a reaction of 0.312 mmol NaN<sub>3</sub> (20.3 mg, Acros, 99 %), 0.060 mmol Ba (8.2 mg, Sigma Aldrich, 99.99 %), 0.005 mmol Sr (0.4 mg, Sigma Aldrich, 99.99 %), 0.062 mmol Mg (1.5 mg, Alfa Aesar, 99.9 %) and 0.252 mmol Ga (17.6 mg, AluSuisse, 99.999 %) in 1.992 mmol Na-flux (45.8 mg, Sigma Aldrich, 99.95 %). For doping purposes 2 mol% of EuF<sub>3</sub> were added. Sr and Mg were introduced to the metallic melt in order to improve crystallinity of the product and for an initially targeted Ba-Mg-Ga-N compound. Reactions without these additional metals were unsuccessful. The filled Ta ampoule was weld shut under argon atmosphere by arc melting and placed into a quartz tubing. The reaction mixture was then heated in a tube furnace (50 °/h) to 760 °C, maintained at that temperature for 48 h and then cooled to 200 °C with a rate of 3.4 °/h. Subsequently, the furnace was turned off. The Ta ampoule was opened in a glove box and Na was separated from the product by sublimation at 320 °C under vacuum (0.1 Pa) for 18 h.

Scanning electron microscopy was performed on a JEOL JSM 6500 F equipped with a field emission gun at an acceleration voltage of 30 kV. To confirm the chemical composition the samples were prepared on adhesive conductive pads and coated with a conductive carbon film. Each EDX spectrum (Oxford Instruments) was recorded with the analyzed area limited to one crystal face to avoid influence of possible contaminating phases.

Single-crystal X-ray diffraction data were collected on a STOE IPDS I diffractometer with graphite monochromated Mo-K $\alpha$  radiation (0.71073 Å). A numerical absorption correction was applied using X-RED.<sup>28</sup> The structure was solved using direct methods implemented in SHELXS-97.<sup>29</sup> Refinement of the structure was carried out with anisotropic displacement parameters for all atoms by full-matrix least-squares calculation on F<sup>2</sup> in SHELXL-97.<sup>29</sup>

Density-functional theory (DFT) band structure calculations were carried out with the WIEN2k program package,<sup>30</sup> using full potential linearized augmented plane wave

(LAPW)<sup>31</sup> method and the generalized gradient approximation by Perdew, Burke and Ernzerhof (PBE-GGA)<sup>32</sup> with a separation energy for core and valence states of -8 Ry. The energy and charge convergence criteria were chosen to be 10<sup>-5</sup> Ry/cell and 10<sup>-4</sup> e/cell, respectively, and 92 to 105 irreducible *k*-points were used with a cutoff for plane waves  $R_{\text{mt}}K_{\text{max}} = 7.0$ .

Luminescence investigations were performed on single crystals placed in a capillary (diameter 0.2 mm, Hilgenberg) at room temperature. The capillaries were aligned with a Leitz Epivert microscope. Excitation source was a JobinYvon Traix190 monochromator with 365 nm wavelength. As detector a CCD camera (LaVision DynaVision) was used. For recording the emission spectra a 500 µm slit was chosen.

### 4.3. Results and Discussion

The heterogeneous reaction product was obtained as a light-orange powder with metallic impurities. Under the microscope, the title compound was observed in form of orange crystals with a lathy shape. The crystals were sensitive to moisture and air. EDX analyses revealed an atomic ratio Ba : Ga : N = 1.0 : 1.0 : 1.6 that agrees well with the composition of Ba<sub>3</sub>Ga<sub>3</sub>N<sub>5</sub>. No other elements were detected, although Sr and Mg were present in the starting material mixture and synthesis was performed in a sodium melt. For X-ray diffraction and luminescence investigations single crystals were placed in sealed capillaries to protect them from oxidation and hydrolysis.

#### 4.3.1. Crystal Structure of Ba<sub>3</sub>Ga<sub>3</sub>N<sub>5</sub>

The crystal structure of Ba<sub>3</sub>Ga<sub>3</sub>N<sub>5</sub> was solved by using single-crystal X-ray diffraction data. The solution and refinement was performed in the monoclinic space group C2/c (no. 15) with  $a = 16.801(3)$ ,  $b = 8.330(2)$ ,  $c = 11.623(2)$  Å and  $\beta = 109.92(3)^\circ$ . The crystallographic data of Ba<sub>3</sub>Ga<sub>3</sub>N<sub>5</sub> are summarized in Table 1. The atomic coordinates and anisotropic displacement parameters are listed in Table 2 and 3. Selected bond lengths and angles are shown in Table 4.

#### 4. Ba<sub>3</sub>Ga<sub>3</sub>N<sub>5</sub> – a Novel Host Lattice for Eu<sup>2+</sup>-Doped Luminescent Materials

**Table 1.** Crystallographic Data for Ba<sub>3</sub>Ga<sub>3</sub>N<sub>5</sub>.

	Ba <sub>3</sub> Ga <sub>3</sub> N <sub>5</sub>
formula mass/g·mol <sup>-1</sup>	691.21
temperature/K	293(2)
crystal system	monoclinic
space group	C2/c (No. 15)
cell parameters/Å	$a = 16.801(3)$ $b = 8.330(2)$ $c = 11.623(2)$
$\beta/^\circ$	109.92(3)
$V/\text{\AA}^3$	1529.3(5)
formula units/cell	8
crystal size/mm <sup>3</sup>	0.04 · 0.04 · 0.06
X-ray density/g·cm <sup>-3</sup>	6.004
abs. coefficient $\mu/\text{mm}^{-1}$	25.553
F (000)	2368
diffractometer, radiation	Stoe IPDS, I Mo-K $\alpha$ ( $\lambda = 0.71073 \text{ \AA}$ )
absorption correction	numerical <sup>28</sup>
$\theta$ range/ $^\circ$	2.58 – 30.42
measured reflections	7973
independent reflections	2305
observed reflections	1616
refined parameters	102
GOF	1.008
R indices ( $F_o^2 \geq 2\sigma(F_o^2)$ )	$R1 = 0.0523$ , $wR2 = 0.1301$
R indices (all data)	$R1 = 0.0781$ , $wR2 = 0.1458$

#### 4. Ba<sub>3</sub>Ga<sub>3</sub>N<sub>5</sub> – a Novel Host Lattice for Eu<sup>2+</sup>-Doped Luminescent Materials

**Table 2.** Atomic coordinates and equivalent isotropic displacement parameters (in 10<sup>-4</sup> pm<sup>2</sup>) of Ba<sub>3</sub>Ga<sub>3</sub>N<sub>5</sub><sup>a</sup>.

Atom	Site	x	y	z	$U_{eq}/\text{\AA}^3$
Ba1	4e	½	0.15547(14)	¼	0.02076(26)
Ba2	4e	½	0.66165(14)	¼	0.02063(26)
Ba3	8f	0.31113(6)	0.41011(12)	0.11565(8)	0.02632(25)
Ba4	8f	0.29451(5)	0.87596(11)	0.16389(8)	0.02251(23)
Ga1	8f	0.57973(9)	0.43546(19)	0.05727(13)	0.01844(31)
Ga2	8f	0.40244(9)	0.24488(18)	0.95047(13)	0.01784(30)
Ga3	8f	0.57938(9)	0.06821(18)	0.99844(13)	0.01861(31)
N1	8f	0.4548(2)	0.0747(13)	0.8829(10)	0.0174(20)
N2	8f	0.4699(7)	0.3998(14)	0.0792(10)	0.0185(20)
N3	8f	0.3417(8)	0.4055(13)	0.8251(11)	0.0208(21)
N4	8f	0.3484(7)	0.1039(15)	0.0399(11)	0.0205(21)
N5	8f	0.06365(7)	0.2677(14)	0.0016(11)	0.0197(21)

<sup>a</sup> e.s.d.'s in parentheses

**Table 3.** Anisotropic displacement parameters (in 10<sup>-4</sup> pm<sup>2</sup>) for Ba<sub>3</sub>Ga<sub>3</sub>N<sub>5</sub><sup>a</sup>.

Atom	$U_{11}$	$U_{22}$	$U_{33}$	$U_{23}$	$U_{13}$	$U_{12}$
Ba1	0.0225(5)	0.0195(5)	0.0187(5)	0	0.0053(4)	0
Ba2	0.0207(5)	0.0202(5)	0.0209(5)	0	0.0072(3)	0
Ba3	0.0207(4)	0.0345(5)	0.0235(4)	0	0.0072(3)	0
Ba4	0.0199(4)	0.0249(4)	0.0229(4)	0.0021(3)	0.0075(3)	0.0009(3)
Ga1	0.0182(6)	0.0178(7)	0.0189(6)	0.0011(5)	0.0057(5)	0.0008(5)
Ga2	0.0186(6)	0.0170(6)	0.0174(6)	0.0002(5)	0.0055(5)	0
Ga3	0.0177(7)	0.0181(7)	0.0192(7)	0	0.0052(5)	0
N1	0.022(5)	0.018(5)	0.017(5)	0	0.015(4)	0
N2	0.019(5)	0.019(5)	0.017(5)	0	0.005(4)	0
N3	0.028(6)	0.010(5)	0.0120(5)	0	0.003(4)	0
N4	0.014(5)	0.023(5)	0.024(5)	0	0.003(4)	0
N5	0.017(5)	0.022(5)	0.025(5)	0	0.013(4)	0

<sup>a</sup> e.s.d.'s in parentheses

According to its formula,  $\text{Ba}_3\text{Ga}_3\text{N}_5$  exhibits a high degree of condensation  $\kappa = 3 : 5$  (i.e. the atomic ratio Ga : N). In accordance with most known nitridogallates,<sup>15,16,33</sup>  $\text{Ba}_3\text{Ga}_3\text{N}_5$  is built up from  $\text{GaN}_4$ -tetrahedra (Figure 1, Figure 2). The latter, centered

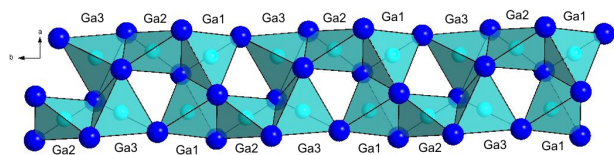


**Figure 1.** Highly condensed strands of  $\text{GaN}_4$ -tetrahedra running along [010].

either by Ga1 or Ga3 exhibit cis-edge sharing while those around Ga2 show trans-edge sharing. The basic structural motif of the anionic substructure is thus formed by three edge-sharing tetrahedra (Ga1, Ga2, Ga3). By further cis-edge sharing, these units are connected to analogous units in opposite orientation (Ga3, Ga2, Ga1) forming infinite chains running along [010]. The strongly folded chains exhibit further corner-sharing of pairs of  $\text{GaN}_4$ -tetrahedra around Ga1 and Ga3, respectively, resulting in three-rings. Thus, the high degree of condensation ( $\kappa = 3 : 5$ ) is a result of

the dominance of edge-sharing over corner-sharing and there are no N-atoms which are terminally bound to Ga. The latter observation is rather untypical for strand-like arrangements of tetrahedra. Moreover, nitrogen atoms  $\text{N}^{[2]}$  and  $\text{N}^{[3]}$  occur in atomic ratio 3 : 2 which are bound to two or three Ga atoms, respectively.

As mentioned above, there are only two other ternary Ba nitridogallates.  $\text{Ba}_3\text{Ga}_2\text{N}_4$ <sup>15</sup> contains edge-sharing single chains of  $\text{GaN}_4$ -tetrahedra, which are not connected to each other while  $\text{Ba}_6\text{Ga}_5\text{N}$  is a barium gallide nitride containing  $[\text{Ga}_5]^{7-}$  clusters.<sup>14</sup> In the field of alkaline earth nitridogallates, only  $\text{Sr}_3\text{Ga}_3\text{N}_5$ <sup>16</sup> and  $\beta\text{-Ca}_3\text{Ga}_2\text{N}_4$ <sup>13</sup> show a high degree of condensation of the anionic substructure, resulting in three-dimensional networks. Taking quaternary compounds into account, only in  $\text{Sr}(\text{Ga}_2\text{Mg}_2)\text{N}_4$  a higher degree of condensation of the (Ga/Mg) $\text{N}_4$ -tetrahedra can be observed, building a three-dimensional network as well.<sup>34</sup> Some nitridogallates build either chains<sup>16</sup> or sheets<sup>16,33</sup> of  $\text{GaN}_4$ -tetrahedra. A number of alkaline earth nitridogallates contain no  $\text{GaN}_4$ -tetrahedra at all but show non-condensed trigonal planar  $\text{GaN}_3$ -units.<sup>17,18,35</sup>

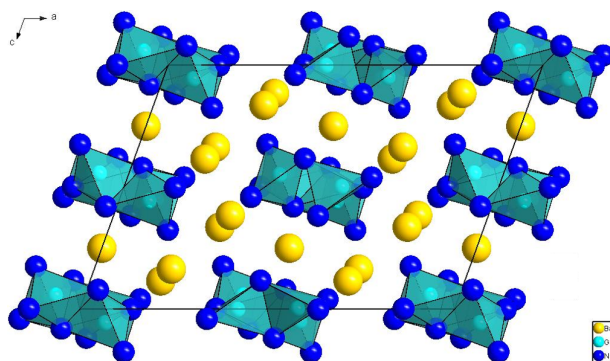


**Figure 2.** Crystal structure of  $\text{Ba}_3\text{Ga}_3\text{N}_5$ , viewing direction along [010].  $\text{Ba}^{2+}$  yellow,  $\text{N}^{3-}$  dark blue,  $\text{Ga}^{3+}$  inside the shown tetrahedra (light blue).

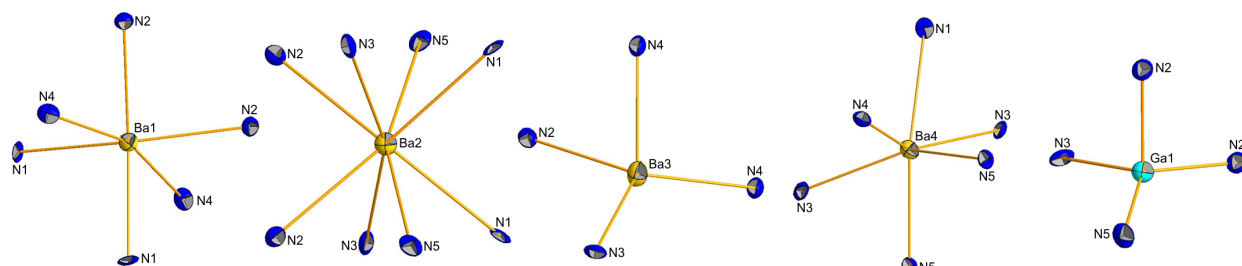
**Table 4.** Selected bond lengths (Å) and angles (°) in Ba<sub>3</sub>Ga<sub>3</sub>N<sub>5</sub><sup>a</sup>.

Ba1-	N1	2.727(10) · 2	Ba4-	N1	3.038(12)	N1-Ba1-N1	90.7(5)
	N2	2.767(11) · 2		N3	2.937(11)	N4-Ba1-N4	163.0(5)
	N4	2.898(11) · 2		N4	2.719(12)	N3-Ba3-N2	104.2(4)
Ba2-	N1	2.930(12) · 2	Ba3-	N4	2.677(11)	N4-Ba4-N3	146.1(4)
Ga1-	N2	1.970(12)	Ga3-	N1	2.047(11)		
	N2	2.048(11)		N1	2.067(12)		
	N3	2.034(12)		N4	2.024(12)		
	N5	1.923(11)		N5	1.913(12)		

<sup>a</sup> e.s.d.'s in parentheses

In Ba<sub>3</sub>Ga<sub>3</sub>N<sub>5</sub>, there are four crystallographically different Ba<sup>2+</sup>-sites which coordination numbers vary from 4 to 8 (Figure 3). The four-fold coordination represents a distorted tetrahedron with rather short distances Ba3-N of 2.677 and 2.775 Å. Ba1 and Ba4 are coordinated by six nitrogen atoms in a distorted octahedron. A higher coordination number of eight is observed around Ba2. The resulting irregular quadratic prism contains a particularly elongated Ba2-N3 distance (3.119 Å). This distance is slightly longer than expected from the sum of the ionic radii (2.88-3.0 Å) while the value for Ba3-N is smaller.<sup>36,37</sup>

All other Ba-N bond lengths are in good agreement with the sum of the ionic radii. Typically, alkaline earth ions are coordinated by four or six nitrogen atoms in nitridogallates or nitridosilicates.<sup>15,16,38,39</sup> In contrast, the coordination number eight of an alkaline earth ion in nitridogallates or (oxo)nitridosilicates is only known for LiSrGaN<sub>2</sub><sup>33</sup>, Sr(Mg<sub>2</sub>Ga<sub>2</sub>)N<sub>4</sub><sup>34</sup> and BaSi<sub>2</sub>O<sub>2</sub>N<sub>2</sub><sup>25</sup> so far.

**Figure 3.** Coordination of metal ions in Ba<sub>3</sub>Ga<sub>3</sub>N<sub>5</sub>. Atoms are shown in ellipsoids with 50 % probability.



An alternative description to the crystal structure may be achieved by introducing anion centered polyhedra. In  $\text{Ba}_3\text{Ga}_3\text{N}_5$ , most of the five nitrogen sites are coordinated by six metal atoms: N1 and N2 are each coordinated by three Ba and three Ga atoms, respectively. The six-fold coordination of N3 and N4 consists of two Ga and four Ba atoms. N2 and N4 are surrounded by quite regular octahedra, with typical distances Ga-N (2.006 Å - 1.974 Å) and Ba-N (2.726 Å - 2.886 Å).<sup>15,16</sup> The polyhedron around N1 is quite irregular, due to the short distance N1-Ba1 of 2.727 Å. The anisotropic displacement ellipsoid of N1 is elongated markedly pointing towards Ba1. The polyhedron around N3 is an octahedron which is distorted due to the long bond Ba2-N resulting in a squared pyramid.

Surprisingly, the crystal structure of the analogous Sr-compound is completely different.  $\text{Sr}_3\text{Ga}_3\text{N}_5$ <sup>16</sup> was described recently from *Clarke et al.*. It was synthesized in a Na-flux at 760 °C. The orange-yellow compound crystallizes in triclinic space group  $P\bar{1}$ . In this compound, a three-dimensional network of corner- and edge-sharing  $\text{GaN}_4$ -tetrahedra typical for such a high  $\kappa$ -value was reported. In contrast, the anionic substructure of  $\text{Ba}_3\text{Ga}_3\text{N}_5$  contains a hitherto unknown structural motif as described above. In both compounds corner- and edge-sharing can be observed but in the Ba-compound edge-sharing is more dominant.

Calculations of the Madelung part of the lattice energy were carried out in order to confirm the crystal structure of  $\text{Ba}_3\text{Ga}_3\text{N}_5$ .<sup>40,41</sup> The results of these MAPLE<sup>42</sup> calculations are summarized in Table 5. The partial MAPLE values for all atoms are in good agreement with reference data reported before.<sup>43</sup> To verify the electrostatic consistency of the refined crystal structure, the calculated MAPLE sum of  $\text{Ba}_3\text{Ga}_3\text{N}_5$  was compared with total MAPLE values of constituting binary and ternary nitrides. One model contains a well known nitridosilicate, the other model contains the hypothetical binary nitride  $\text{Ba}_3\text{N}_2$ .<sup>44,45</sup>

**Table 5.** Partial MAPLE and total MAPLE values [in kJ/mol] of  $\text{Ba}_3\text{Ga}_3\text{N}_5$ .

	calculated MAPLE value	$\Delta$ / %
Ba	1628.06-1824.34	
Ga	4930.00-5090.14	
N	4379.99-4821.36	
$\text{Ba}_3\text{Ga}_3\text{N}_5$	41503.34	
3 GaN		
+ 1.5 $\text{Ba}_2\text{Si}_5\text{N}_8$		
- 2.5 $\text{Si}_3\text{N}_4$	43830.36	0.75
$\text{Ba}_3\text{N}_2$ <sup>[44,45]</sup>		
+ GaN	43683.77	0.41

Both models differ only slightly from the calculated value for  $\text{Ba}_3\text{Ga}_3\text{N}_5$ . With these results the electrostatic consistency is proven and the refined crystal structure is confirmed.

#### 4.3.2. Luminescence Investigations

$\text{Eu}^{2+}$ -doped samples of the title compound show red luminescence under UV-irradiation. Luminescence investigations were performed on single crystals of  $\text{Ba}_3\text{Ga}_3\text{N}_5\text{:Eu}^{2+}$  ( $\text{Eu}^{2+}$  content ca. 2 mol%) sealed in glass capillaries. All measurements show comparable results so an exemplary spectrum of one crystal is shown in Figure 4. 365 nm excitation yield an emission band peaking at

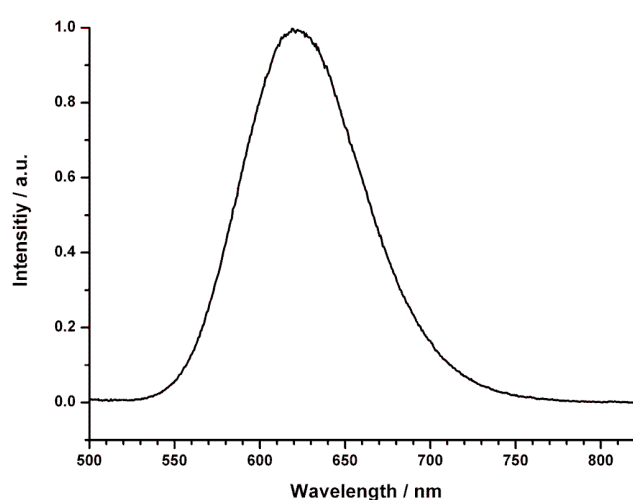


**Figure 4.** Emission spectrum of  $\text{Eu}^{2+}$ -doped  $\text{Ba}_3\text{Ga}_3\text{N}_5$ , excitation at 365 nm.

#### 4. $\text{Ba}_3\text{Ga}_3\text{N}_5$ – a Novel Host Lattice for $\text{Eu}^{2+}$ -Doped Luminescent Materials

638 nm with a lumen equivalent of 173 lm/W and CIE color coordinates  $x = 0.644$ ,  $y = 0.347$ . The emission band is quite narrow with a full width at half maximum (FWHM) of  $2123 \text{ cm}^{-1}$  (84.7 nm).

Due to the strong red shift of the emission band, we expect the emission originating from  $\text{Eu}^{2+}$  in octahedral coordination,<sup>49</sup> as found for the Ba1 and the Ba4 site. A comparison with other known red emitters is difficult, because to our knowledge this is the first time a luminescent Eu-doped nitridogallate is reported. Compared with other nitridic phosphor materials (e.g.  $\text{Sr}_2\text{Si}_5\text{N}_8:\text{Eu}^{2+}$ ),<sup>22,23,50-52</sup>  $\text{Ba}_3\text{Ga}_3\text{N}_5:\text{Eu}^{2+}$  shows emission in the same spectral region. For  $\text{Sr}_2\text{Si}_5\text{N}_8:\text{Eu}^{2+}$  (2 mol% Eu) an emission maximum around 620 nm is reported and also the color coordinates ( $x, y = 0.638, 0.359$ ) and emission width (FWHM  $\sim 1950 \text{ cm}^{-1}$ ) are comparable.<sup>53</sup> Other reported  $\text{Eu}^{2+}$ -doped Ba-compounds (e.g.  $\text{Ba}_{1.89}\text{Eu}_{0.11}\text{Si}_5\text{N}_8$ )<sup>54</sup> show an emission around 600 nm.

##### 4.3.3. DFT Calculations

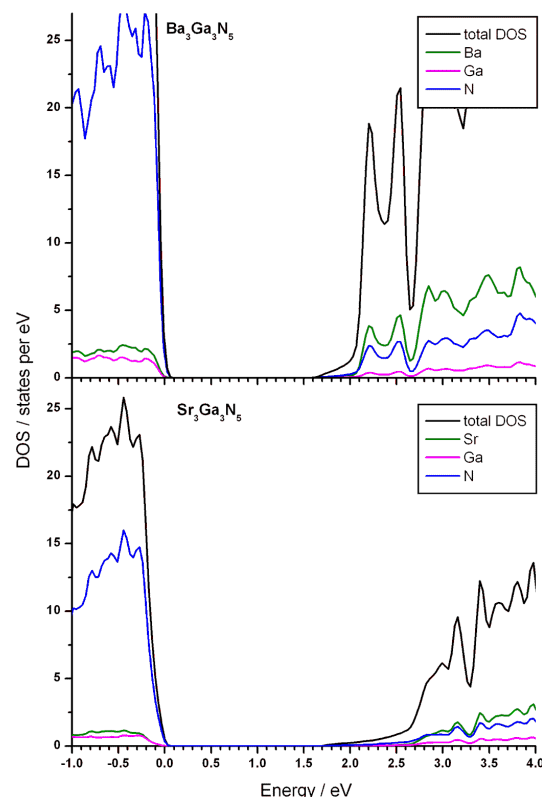


**Figure 5.** Calculated Density of States (DOS) of  $\text{Ba}_3\text{Ga}_3\text{N}_5$  (above) and  $\text{Sr}_3\text{Ga}_3\text{N}_5$  (down). Displayed are the respective overall DOS and the single contributions of the elements.

Calculation of the electronic structures for  $\text{Ba}_3\text{Ga}_3\text{N}_5$  and isoelectronic  $\text{Sr}_3\text{Ga}_3\text{N}_5$  were carried out. As WIEN2k allows only settings with a monoclinic angle  $\gamma$  the calculation of  $\text{Ba}_3\text{Ga}_3\text{N}_5$  was performed in monoclinic space group  $B2/b$ . Therefore, the crystal parameters were transformed accordingly. Figure 5 shows the resulting density of states (DOS) of  $\text{Ba}_3\text{Ga}_3\text{N}_5$  and  $\text{Sr}_3\text{Ga}_3\text{N}_5$ . The title compound shows an electronic band gap of 1.46 eV while the Sr-compound shows a slightly larger value of 1.53 eV. Due to the insufficient description of the exchange correlation potential in DFT calculations the calculated band gaps are usually smaller than the real ones. In both compounds the highest occupied states are mainly influenced by

nitrogen contributions (over 60 %) whereas the lowest unoccupied states are dominated by nitrogen and Ba/Sr contributions. A similar result was reported earlier for LiBa<sub>5</sub>GaN<sub>3</sub>F<sub>5</sub> where the transition also occurs from a nitrogen dominated state in a hybrid nitrogen metal state.<sup>43</sup>

#### 4.4. Conclusion

In this contribution, a new ternary Ba nitridogallate, the third known at all, was reported. This compound exhibits a novel structural feature of GaN<sub>4</sub>-tetrahedra that build up highly condensed strands along [010]. The coordination of the Ba atoms varies from a low coordination number of four to a higher coordination of eight nitrogen atoms. Employing anion centered polyhedra for structure description, four nitrogen sites are sixfold coordinated. The N5 site is surrounded by five cations, building a squared pyramid. Confirmation of the crystal structure was accomplished by MAPLE calculations. In contrast, the crystal structure of the isoelectronic compound Sr<sub>3</sub>Ga<sub>3</sub>N<sub>5</sub><sup>16</sup> shows a connection of GaN<sub>4</sub>-tetrahedra in all three directions, resulting in a three-dimensional anionic network. Luminescence investigations of Eu<sup>2+</sup>-doped samples of the title compound show a strongly red-shifted peak emission at 638 nm with FWHM of 2123 cm<sup>-1</sup>. The fact that yet Ba<sub>3</sub>Ga<sub>3</sub>N<sub>5</sub> has only been obtained as a side phase, limits the further development of Ba<sub>3</sub>Ga<sub>3</sub>N<sub>5</sub>:Eu<sup>2+</sup> as a LED phosphor. Nevertheless, the promising luminescence properties of this compound are a strong incentive to further optimize its synthesis. DFT calculations of Ba<sub>3</sub>Ga<sub>3</sub>N<sub>5</sub> and the isoelectronic Sr-compound were done to determine the band gap resulting in a value 1.46 eV for the Ba-compound (1.53 eV for Sr<sub>3</sub>Ga<sub>3</sub>N<sub>5</sub>). The transition takes place from a nitrogen state to a hybrid metal (Sr or Ba) nitrogen state.

The results of this investigation illustrate the potential of nitridogallates as host lattices for Eu<sup>2+</sup> doped luminescent materials. Both, from a structural point of view but also concerning their materials properties, there are similarities between nitridosilicates and nitridogallates.

#### 4.5. References

- [1] S. Nakamura, M. Senoh, N. Iwasa, S. Nagahama, T. Yamada, T. Mukai, *Jpn. J. Appl. Phys.* **1995**, 34, L1332.
- [2] T. Fujii, Y. Gao, R. Sharma, E. L. Hu, S. P. DenBaars, S. Nakamura, *Appl. Phys. Lett.* **2004**, 84, 855.
- [3] S. Nakamura, *Solid State Commun.* **1997**, 102, 237.
- [4] S. Nakamura, *Science* **1998**, 281, 956.
- [5] S. Nakamura, S. Pearton, G. Fasol, *The Blue Laser Diode*; Springer Verlag: Berlin, **2000**.
- [6] S. Nakamura, M. Senoh, T. Mukai, *Appl. Phys. Lett.* **1993**, 62, 2390.
- [7] A. Denis, G. Goglio, G. Demazeau, *Mater. Sci. Eng., R* **2006**, 50, 167.
- [8] M. Bockowski, *Cryst. Res. Technol.* **2007**, 42, 1162.
- [9] S. Krukowski, P. Kempisty, P. Strak, *Cryst. Res. Technol.* **2009**, 44, 1038.
- [10] R. Niewa, F. J. DiSalvo, *Chem. Mater.* **1998**, 10, 2733.
- [11] B. Wang, M. J. Callahan, *Cryst. Growth Des.* **2006**, 6, 1227.
- [12] R. P. Parikh, R. A. Adomaitis, *J. Cryst. Growth* **2006**, 286, 259.
- [13] S. J. Clarke, F. J. DiSalvo, *J. Alloys Compd.* **1998**, 274, 118.
- [14] G. Cordier, M. Ludwig, D. Stahl, P. C. Schmidt, R. Kniep, *Angew. Chem.* **1995**, 107, 1879; *Angew. Chem. Int. Ed. Engl.* **1995**, 34, 1761.
- [15] H. Yamane, F. J. DiSalvo, *Acta Crystallogr. Sect. C: Cryst. Struct. Commun.* **1996**, 52, 760.
- [16] S. J. Clarke, F. J. DiSalvo, *Inorg. Chem.* **1997**, 36, 1143.
- [17] G. Cordier, P. Höhn, R. Kniep, A. Rabenau, *Z. Anorg. Allg. Chem.* **1990**, 591, 58.
- [18] D. G. Park, Z. A. Gál, F. J. DiSalvo, *Inorg. Chem.* **2003**, 42, 1779.
- [19] P. E. Rauch, A. Simon, *Angew. Chem.* **1992**, 104, 1505; *Angew. Chem. Int. Ed. Engl.* **1992**, 31, 1519.
- [20] W. Schnick, *Phys. Status Solidi RRL* **2009**, 3, A113.
- [21] M. Zeuner, S. Pagano, W. Schnick, *Angew. Chem.* **2011**, 123, 7898; *Angew. Chem. Int. Ed.* **2011**, 50, 7754.
- [22] M. Zeuner, F. Hintze, W. Schnick, *Chem. Mater.* **2009**, 21, 336.
- [23] M. Zeuner, P. J. Schmidt, W. Schnick, *Chem. Mater.* **2009**, 21, 2467.

- [24] J. A. Kechele, C. Hecht, O. Oeckler, J. Schmedt auf der Gönne, P. J. Schmidt, W. Schnick, *Chem. Mater.* **2009**, *21*, 1288.
- [25] J. A. Kechele, O. Oeckler, F. Stadler, W. Schnick, *Solid State Sci.* **2009**, *11*, 537.
- [26] K. Shioi, N. Hirotsuki, R.-J. Xie, T. Takeda, Y. Q. Li, *J. Mater. Sci.* **2010**, *45*, 3198.
- [27] Y. Q. Li, N. Hirotsuki, R.-J. Xie, T. Takeda, M. Mitomo, *J. Solid State Chem.* **2008**, *181*, 3200.
- [28] *X-RED 32*, Version 1.03; *Data Reduction for STADI 4 and IPDS*, Darmstadt, 2002.
- [29] G. M. Sheldrick, *Acta Crystallogr. Sect. A: Found. Crystallogr.* **2008**, *64*, 112.
- [30] P. Blaha, K. Schwarz, G. K. H. Madsen, D. Kvasnicka, J. Luitz, *WIEN2K*, Version 10.1; *An Augmented Plane Wave + Local Orbitals Program for Calculating Crystal Properties*, Technical University Vienna, 2001.
- [31] K. Schwarz, P. Blaha, *Comput. Mat. Sci.* **2003**, *28*, 259.
- [32] J. P. Perdew, K. Burke, M. Ernzerhof, *Phys. Rev. Lett.* **1996**, *77*, 3865.
- [33] D. G. Park, Z. A. Gál, F. J. DiSalvo, *J. Alloys Compd.* **2003**, *353*, 107.
- [34] D. G. Park, Y. Dong, F. J. DiSalvo, *Solid State Sci.* **2008**, *10*, 1846.
- [35] P. M. Mallinson, Z. A. Gál, S. J. Clarke, *Inorg. Chem.* **2006**, *45*, 419.
- [36] R. D. Shannon, *Acta Crystallogr., Sect. A: Found. Crystallogr.* **1976**, *32*, 751.
- [37] W. H. Baur, *Crystallogr. Rev.* **1987**, *1*, 59.
- [38] Z. A. Gál, P. M. Mallinson, H. J. Orchard, S. J. Clarke, *Inorg. Chem.* **2004**, *43*, 3998.
- [39] H. Yamane, F. J. DiSalvo, *J. Alloys Compd.* **1996**, *240*, 33.
- [40] R. Hoppe, *Angew. Chem.* **1970**, *82*, 7; *Angew. Chem. Int. Ed. Engl.* **1970**, *9*, 25.
- [41] R. Hoppe, *Angew. Chem.* **1966**, *78*, 52; *Angew. Chem. Int. Ed. Engl.* **1966**, *5*, 95.
- [42] R. Hübenthal, *MAPLE*, Version 4; *Programm zur Berechnung des Madelunganteils der Gitterenergie*, Universität Gießen, 1993.
- [43] F. Hintze, W. Schnick, *Solid State Sci.* **2010**, *12*, 1368.
- [44] S. R. Römer, T. Dörfler, P. Kroll, W. Schnick, *Phys. Status Solidi (b)* **2009**, *246*, 1604.

- [45] E. Orhan, S. Jobic, R. Brec, R. Marchand, J. Y. Saillard, *J. Mater. Chem.* **2002**, 12, 2475.
- [46] H. Höpfe, *Dissertation*, Ludwig-Maximilians-Universität München **2003**.
- [47] K. Köllisch, *Dissertation*, Ludwig-Maximilians-Universität München **2001**.
- [48] R. Lauterbach, *Dissertation*, Universität Bayreuth **1999**.
- [49] J. J. Zuckermann, *J. Chem. Educ.* **1965**, 42, 315.
- [50] Y. Q. Li, J. E. J. van Steen, J. W. H. van Krevel, G. Botty, A. C. A. Delsing, F. J. DiSalvo, G. de With, H. T. Hintzen, *J. Alloys Compd.* **2006**, 417, 273.
- [51] R. Mueller-Mach, G. Mueller, M. R. Krames, H. A. Höpfe, F. Stadler, W. Schnick, T. Jüstel, P. Schmidt, *Phys. Status Solidi (a)* **2005**, 202, 1727.
- [52] X. Piao, T. Horikawa, H. Hanzawa, K. Machida, *Appl. Phys. Lett* **2006**, 88, 161908.
- [53] X. Piao, K. Machida, T. Horikawa, B. Yun, *J. Lumin.* **2010**, 130, 8.
- [54] H. A. Höpfe, H. Lutz, P. Morys, W. Schnick, A. Seilmeier, *J. Phys. Chem. Solids* **2000**, 61, 2001.

## 5. $\text{Ca}_2\text{Ga}_3\text{MgN}_5$ – a Highly Condensed Nitridogallate

Hitherto, novel ternary compounds deriving from binary GaN have been presented. Although only a small number of ternary nitridogallates is known, the number of known quaternary compounds is even less. In the following a novel quaternary nitridogallate, namely  $\text{Ca}_2\text{Ga}_3\text{MgN}_5$  will be reported. The anionic substructure is again built up of tetrahedral units but here we observe a mixed occupation with Mg and Ga on the tetrahedral site. These miscellaneously occupied tetrahedra are sharing corners and edges whereby a three dimensional network results. In the voids of this network, Ca-atoms are incorporated. The crystal structure of  $\text{Ca}_2\text{Ga}_3\text{MgN}_5$  can be compared to the well known structure of  $\text{Sr}_2\text{Si}_5\text{N}_8$  but reveals a higher condensation in the anionic substructure. Synthesis as well as crystal structure elucidation and a detailed comparison to the crystal structure of  $\text{Sr}_2\text{Si}_5\text{N}_8$  is presented.



## $\text{Ca}_2\text{Ga}_3\text{MgN}_5$ – a Highly Condensed Nitridogallate

Frauke Hintze and Wolfgang Schnick

**published in:** *Z. Anorg. Allg. Chem.* **2012**, 638, 2243.

**Keywords:** Calcium; Highly condensed; Magnesio-nitridogallate

**Abstract:** The nitridogallate  $\text{Ca}_2\text{Ga}_3\text{MgN}_5$  was obtained from reaction of the elements in sodium flux with Na-azide at 760 °C in weld shut Nb-ampoules. Crystal structure solution and refinement was carried out on the basis of single-crystal X-ray diffraction data.  $\text{Ca}_2\text{Ga}_3\text{MgN}_5$  (space group C2/m (no. 12),  $a = 11.160(2)$ ,  $b = 3.2965(7)$ ,  $c = 8.006(2)$  Å, and  $\beta = 109.93(3)^\circ$ ,  $Z = 2$ ) shows an anionic substructure made up of mixed (Mg/Ga) $\text{N}_4$  tetrahedra which are sharing both common vertices and edges building a three-dimensional network. The crystal structure of  $\text{Ca}_2\text{Ga}_3\text{MgN}_5$  is related to known alkaline earth nitridosilicates ( $M^{\text{II}}_2\text{Si}_5\text{N}_8$ ,  $M^{\text{II}} = \text{Sr}, \text{Ba}$ ), but is significantly higher condensed due to additional edge-sharing in the anionic substructure.

### 5.1. Introduction

Gallium nitrides have found increasing interest in the past. The binary compound GaN is a direct semiconductor with a wide bandgap and has been widely applied for manufacturing of high performance light-emitting diodes (LEDs).<sup>[1-6]</sup> Investigation of this compound has mainly focused on synthesis, crystal growth, and doping.<sup>[7-11]</sup> However, the chemistry of ternary and higher alkaline earth nitridogallates has been more or less neglected so far. In the literature only a small number of ternary nitridogallates have been reported and only a few compounds contain the alkaline earth element calcium.<sup>[12-14]</sup> Regarding quaternary nitridogallates, only six compounds are known.  $\text{Sr}(\text{Mg}_2\text{Ga}_2)\text{N}_4$  exhibits a mixed tetrahedral position (Mg/Ga),<sup>[15]</sup> the other ones are either Li-containing compounds (e.g.  $\text{LiCaGaN}_2$ ),<sup>[16,17]</sup> subnitrides (e.g.  $\text{Ba}_2\text{GeGaN}$ ),<sup>[18,19]</sup> or oxonitrides (e.g.  $\text{Sr}_4\text{GaN}_3\text{O}$ ).<sup>[20]</sup>

Most syntheses of nitridogallates start from the elements utilizing liquid sodium as flux and employing sealed Ta- or Nb-ampoules. Therein, an increased nitrogen pressure is attained by decomposition of an azide. The solubility of nitrogen in sodium can be increased by addition of alkaline earth metals or other electropositive metals.<sup>[21]</sup> Recently, highly condensed nitridogallates with an atomic ratio Ga:N > 1:2 came into the focus due to their higher stability against hydrolysis.<sup>[12]</sup>

Nitridogallates are mostly built up of  $\text{GaN}_4$  tetrahedra that may be connected through common corners and/or edges forming 1D- (e.g. in  $\text{Sr}_3\text{Ga}_2\text{N}_4$ ), 2D- (e.g. in  $\text{Ca}_3\text{Ga}_2\text{N}_4$ ) or 3D-substructures (e.g. in  $\text{Ba}_3\text{Ga}_3\text{N}_5$ ).<sup>[12,22]</sup> Besides, non condensed (0D) building units have been found as well (e.g. discrete  $\text{GaN}_3$  units in  $\text{LiBa}_5\text{GaN}_3\text{F}_5$ ).<sup>[23,24]</sup> The observation of tetrahedral building units illustrates the structural similarities between nitridogallates and nitridosilicates. The latter compounds also contain tetrahedral-based substructures with differing dimensionality and degree of condensation.<sup>[25]</sup> Here, we present the novel nitridogallate  $\text{Ca}_2\text{Ga}_3\text{MgN}_5$  which exhibits a highly condensed anionic substructure related to known nitridosilicate structures of  $M^{\text{II}}_2\text{Si}_5\text{N}_8$  ( $M^{\text{II}} = \text{Sr}, \text{Ba}$ ).<sup>[26]</sup>

## 5.2. Results and Discussion

The reaction product was obtained as a heterogeneous mixture of crystals and metallic impurities. Under the microscope the title compound was observed as yellow rods. The crystals were not sensitive to moisture or air. An atomic ratio of  $\text{Ca}:\text{Ga}:\text{Mg}:\text{N} = 2.3:3.2:1.6$  resulted from EDX-analysis and agrees passable with the composition of  $\text{Ca}_2\text{Ga}_3\text{MgN}_5$ . Except a negligible amount of oxygen no other elements were detected by EDX analysis and thus separation of the product from the Na-melt was complete.

### *Crystal Structure of $\text{Ca}_2\text{Ga}_3\text{MgN}_5$*

The crystal structure of  $\text{Ca}_2\text{Ga}_3\text{MgN}_5$  was solved by using single-crystal X-ray diffraction data. The solution and refinement was performed in the monoclinic space group  $C2/m$  (no. 12) with  $a = 11.160(2)$ ,  $b = 3.2965(7)$ ,  $c = 8.006(2)$  Å, and  $\beta = 109.93(3)^\circ$ . The crystallographic data of  $\text{Ca}_2\text{Ga}_3\text{MgN}_5$  are summarized in Table 1. The atomic coordinates and displacement parameters are listed in Table 2 and 3, selected bond lengths are shown in Table 4. Free refinement of the occupancy of the tetrahedra positions resulted in 83 % Ga on (Mg1/Ga1)-site and 56 % Ga on (Mg2/Ga2)-site. To reach electrostatic neutrality an occupancy of 90 % Ga on (Mg1/Ga1) and 60 % Ga on (Mg2/Ga2) were held through further refinement. Most known nitridogallates are built up of  $\text{GaN}_4$  tetrahedra. Regarding quaternary phases in this compound class, only  $\text{Sr}(\text{Mg}_2\text{Ga}_2)\text{N}_4$  is known from the literature with a mixed occupation of Ga and Mg in the tetrahedra position.<sup>[15]</sup> An analogous situation was observed for  $\text{Ca}_2\text{Ga}_3\text{MgN}_5$ . In the latter we found two crystallographic tetrahedra positions, both occupied simultaneously by Mg and Ga (see Figure 1). A mixed

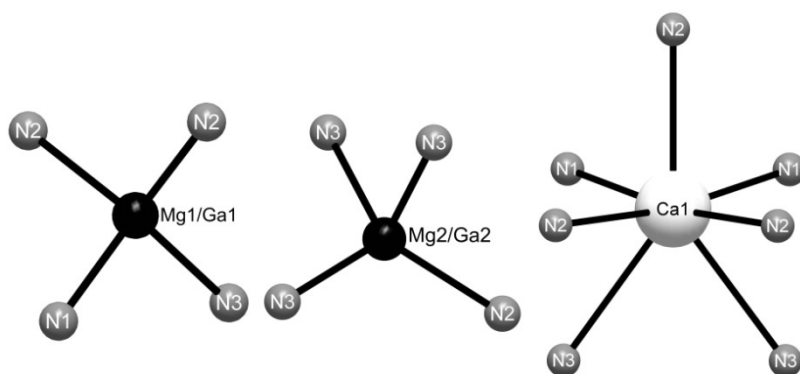


**Figure 1.** Polyhedra of mixed Mg/Ga-sites and the single  $\text{Ca}^{2+}$ -site.

occupation of one site by Ga and Mg is possible since the ionic radii of the fourfold coordinated ions are quite similar (0.57 Å and 0.47 Å for  $\text{Mg}^{+2}$  and  $\text{Ga}^{3+}$ , respectively).<sup>[27]</sup> The distances (Mg/Ga)-N

range from 1.9467(6) to 2.118(3) Å and agree well with the sum of the ionic radii<sup>[27,28]</sup> and vary in the range of known Ga-N or Mg-N distances, respectively.<sup>[15]</sup>

**Table 1.** Crystallographic Data for  $\text{Ca}_2\text{Ga}_3\text{MgN}_5$ .

	$\text{Ca}_2\text{Ga}_3\text{MgN}_5$
formula mass/g·mol <sup>-1</sup>	383.68
temperature/K	293(2)
crystal system	monoclinic
space group	$C2/m$ (no. 12)
cell parameters/Å	$a = 11.160(2)$
	$b = 3.2965(7)$
	$c = 8.006(2)$
$\beta/^\circ$	109.93(3)
$V/\text{Å}^3$	276.9(2)
formula units per cell	2
abs. coefficient $\mu/\text{mm}^{-1}$	16.353
F (000)	360
diffractometer	Nonius Kappa
	CCD
radiation,	Mo-K $\alpha$
graphite-monochromator	( $\lambda = 0.71073$ Å)
$\theta$ range/ $^\circ$	3.88 – 27.42
measured reflections	1208
observed reflections	1186
independent reflections	371
refined parameters	26
GOF	1.081
R indices ( $F_o^2 \geq 2\sigma(F_o^2)$ )	$R1 = 0.0206$
	$wR2 = 0.0494$
R indices (all data)	$R1 = 0.0231$
	$wR2 = 0.0487$

## 5. $\text{Ca}_2\text{Ga}_3\text{MgN}_5$ – a Highly Condensed Nitridogallate

**Table 2.** Atomic coordinates and equivalent isotropic displacement parameters (in  $10^{-4} \text{ pm}^2$ ) of  $\text{Ca}_2\text{Ga}_3\text{MgN}_5^a$ .

Atom	Wyckoff-site	x	y	z	$U_{\text{eq}}/\text{\AA}^3$
Ca1	4i	0.33614(7)	0	0.3748(1)	0.0073(2)
Mg1/Ga1	4i	0.03750(4)	0	0.27970(5)	0.0062(2)
Mg2/Ga2	4i	0.16587(5)	$\frac{1}{2}$	0.04721(7)	0.0063(2)
N1	2c	0	0	$\frac{1}{2}$	0.0050(8)
N2	4i	0.1434(3)	$\frac{1}{2}$	0.2844(4)	0.0082(6)
N3	4i	0.8654(3)	0	0.1017(4)	0.0100(6)

<sup>a</sup> e.s.d.'s in parentheses

**Table 3.** Anisotropic displacement parameters (in  $10^{-4} \text{ pm}^2$ ) for  $\text{Ca}_2\text{Ga}_3\text{MgN}_5^a$ .

Atom	$U_{11}$	$U_{22}$	$U_{33}$	$U_{23}$	$U_{13}$	$U_{12}$
Ca1	0.0056(3)	0.0052(4)	0.0110(4)	0	0.0026(3)	0
Mg1/Ga1	0.0054(3)	0.0057(2)	0.0079(3)	0	0.0026(2)	0
Mg2/Ga2	0.0095(3)	0.0039(3)	0.0069(3)	0	0.0049(3)	0
N1	0.006(2)	0.003(2)	0.007(2)	0	0.004(2)	0
N2	0.009(2)	0.007(2)	0.009(2)	0	0.004(2)	0
N3	0.004(2)	0.011(2)	0.013(2)	0	0	0

<sup>a</sup> e.s.d.'s in parentheses

**Table 4.** Selected bond lengths ( $\text{\AA}$ ) and angles ( $^\circ$ ) in  $\text{Ca}_2\text{Ga}_3\text{MgN}_5^a$ .

Ca1-	N1	2.412(1) · 2	N2-(Mg1/Ga1)-N2	109.3(2)
	N2	2.609(2) · 2	N1-(Mg1/Ga1)-N2	106.8(1)
(Mg1/Ga1)-	N1	1.947(6)	N2-(Mg2/Ga2)-N3	105.6(2)
	N2	2.021(2) · 2	N3-(Mg2/Ga2)-N3	111.5(2)
	N3	1.963(3)	N1-Ca1-N2	169.7(7)
(Mg2/Ga2)-	N2	1.998(3)	N2-Ca1-N2	93.4(1)
	N3	1.994(2) · 2	N1-Ca1-N2	96.9(1)
	N3	2.118(3)		

<sup>a</sup> e.s.d.'s in parentheses

In the crystal structure the tetrahedra are connected both through common corners and edges building a three-dimensional network. Along  $[010]$  the network forms hexagonal channels of *sechser*-rings and quadratic channels of *vierer*-rings. In each

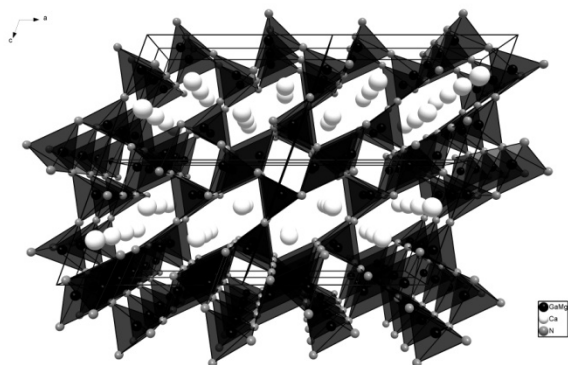


**Figure 2.**  $2 \times 2 \times 2$  cell of  $\text{Ca}_2\text{Ga}_3\text{MgN}_5$ , view along  $[010]$ .

*sechser*-ring two Ca atoms are located, the quadrangular channels are not filled. In viewing direction  $[010]$  each ring type is neighboring itself horizontally and alternating vertically (Figure 2). The tetrahedra around  $\text{Mg1/Ga1}$  are connected solely through common vertices to four other tetrahedra. The tetrahedra around  $\text{Mg2/Ga2}$  are

connected both through common corners and edges. The edge-sharing can only be observed between  $(\text{Mg2/Ga2})\text{N}_4$  units, the corner connection is observed to further  $(\text{Mg1/Ga1})\text{N}_4$  tetrahedra. The  $(\text{Mg2/Ga2})\text{N}_4$  tetrahedra are thus building highly condensed strands running along  $[010]$  and are bridged by  $(\text{Mg1/Ga1})\text{N}_4$  units (see Figure 3). These sheets are stacked along  $[001]$  and are connected through vertex-sharing  $\text{Mg1/Ga1}$  tetrahedra, building a three-dimensional network. As stated above there is only one other quaternary Mg and Ga containing nitridogallate known so far, namely  $\text{Sr}(\text{Mg}_2\text{Ga}_2)\text{N}_4$ ,<sup>[15]</sup> exhibiting a three-dimensional network of corner and

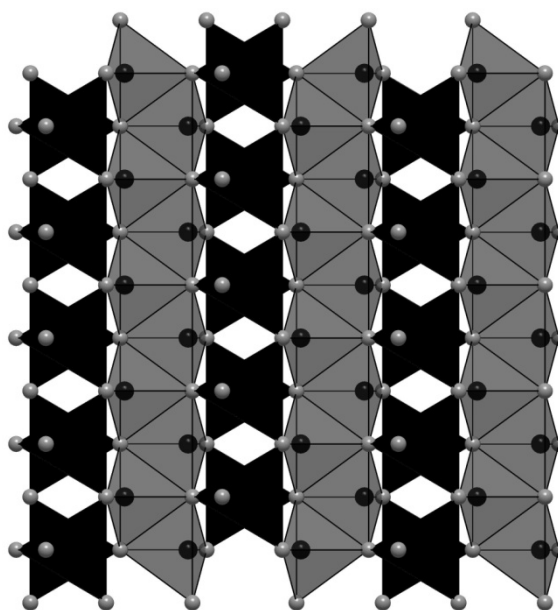


**Figure 3.** Sheet of  $(\text{Mg/Ga})\text{N}_4$  tetrahedra, black tetrahedra show corner linked  $\text{Mg1/Ga1}$  units, the gray tetrahedra are the edge-sharing  $\text{Mg2/Ga2}$  units.

edge-sharing tetrahedra with mixed  $(\text{Mg/Ga})$ -occupancy. In  $\text{Ca}_2\text{Ga}_3\text{MgN}_5$  the degree of condensation  $\kappa$  (i. e. the atomic ratio  $(\text{Mg,Ga}) : \text{N}$ ) is  $4 : 5$  which is even higher than  $\kappa = 4 : 4$  in  $\text{Sr}(\text{Mg}_2\text{Ga}_2)\text{N}_4$ . These quaternary compounds, containing Mg solely on tetrahedra position can be classified as magnesio-nitridogallates.<sup>[29]</sup> To emphasize that Mg is belonging to the tetrahedral network, the sum formula can also be formulated as  $\text{Ca}_2[\text{Ga}_3\text{MgN}_5]$ .

The single  $\text{Ca}^{2+}$ -site in  $\text{Ca}_2\text{Ga}_3\text{MgN}_5$  is surrounded by seven nitrogen atoms with Ca-N bond lengths ranging from 2.4117(7) to 2.845(3) Å. These distances are in good agreement with known values in other Ca-nitridogallates and the calculated sum of the ionic radii.<sup>[12,13,27,28]</sup> With respect to the angles around  $\text{Ca}^{2+}$  the geometrical arrangement can be described as a distorted capped octahedron (Figure 1).

An alternative description of the crystal structure can be attained on the basis of anion centered polyhedra. In  $\text{Ca}_2\text{Ga}_3\text{MgN}_5$  all three nitrogen sites are surrounded by six cations in octahedral coordination. These octahedra are constituted by two to four Ca-atoms and four to two Mg/Ga-atoms, respectively. The octahedra are edge- and corner-sharing building a dense three-dimensional network with empty quadrangular channels running along [010]. The described crystal structure of  $\text{Ca}_2\text{Ga}_3\text{MgN}_5$  is related to the one of  $M^{\text{II}}_2\text{Si}_5\text{N}_8$  ( $M^{\text{II}} = \text{Sr}, \text{Ba}$ ).<sup>[30]</sup> The mentioned structural motifs, considering cation centered polyhedra, like quadrangular channels and channels of *sechser*-rings occur in  $M^{\text{II}}_2\text{Si}_5\text{N}_8$  as well (see Figure 4).

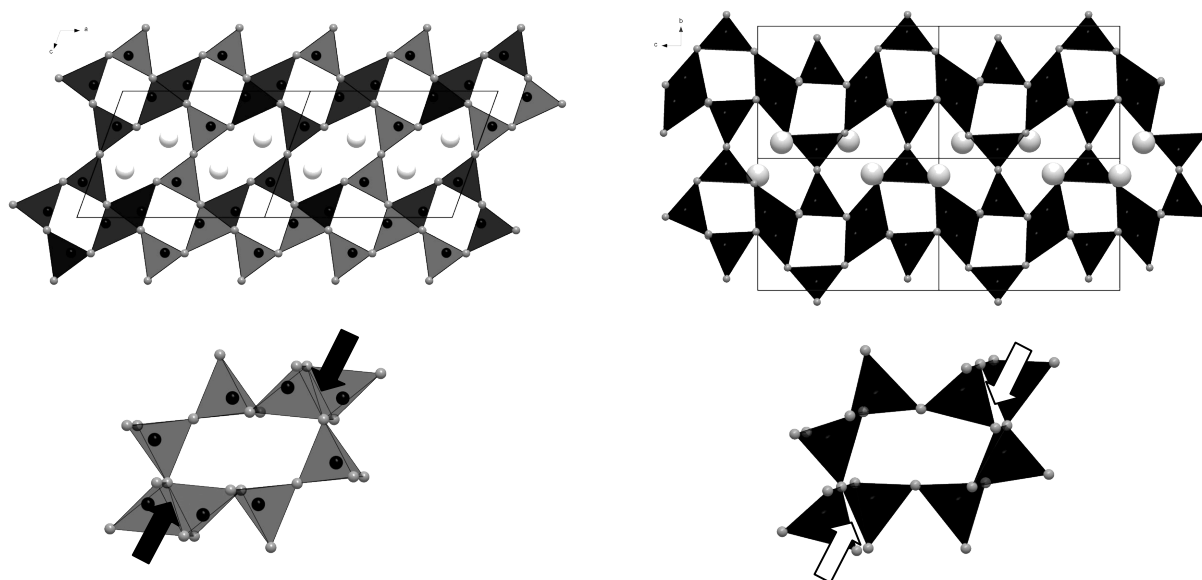


**Figure 4.** Structure detail of  $\text{Ca}_2\text{Ga}_3\text{MgN}_5$  with *sechser*- and *vierer*-rings (left above) and single *sechser*-ring with edge-sharing (left below). On the right (above) a structural detail of  $\text{Sr}_2\text{Si}_5\text{N}_8$  with *sechser*- and *vierer*-rings is illustrated, right below a *sechser*-ring of the  $\text{Sr}_2\text{Si}_5\text{N}_8$  crystal structure is displayed. The arrows in the *sechser*-rings below show the difference in those structural motifs, in  $\text{Ca}_2\text{Ga}_3\text{MgN}_5$  (right) edge-sharing can be observed, in  $\text{Sr}_2\text{Si}_5\text{N}_8$  (left) only corner-sharing occurs.

Furthermore, the hexagonal channels are also filled with two alkaline earth ions. These channels of *sechser*-rings are also neighboring to each other but the orientation of inclination is alternating. Therefore, in  $\text{Sr}_2\text{Si}_5\text{N}_8$  the *vierer*-rings are situated in a wavelike array. Nevertheless, both crystal structures differ in the connection between the tetrahedra. In  $M^{\text{II}}_2\text{Si}_5\text{N}_8$  no edge-sharing occurs whereas in  $\text{Ca}_2\text{Ga}_3\text{MgN}_5$  the  $(\text{Mg2/Ga2})\text{N}_4$  tetrahedra are highly condensed by connection via edges and vertex-sharing to  $(\text{Mg1/Ga1})\text{N}_4$  units as already mentioned. This is also shown in the different degrees of condensation ( $\kappa = 5:8$  for  $M^{\text{II}}_2\text{Si}_5\text{N}_8$  and  $\kappa = 4:5$  for  $\text{Ca}_2\text{Ga}_3\text{MgN}_5$ ). Accordingly, the crystal structure of  $\text{Ca}_2\text{Ga}_3\text{MgN}_5$  can be viewed as a higher condensed variant of the  $M^{\text{II}}_2\text{Si}_5\text{N}_8$  structure as illustrated in Figure 4.

To confirm the crystal structure of  $\text{Ca}_2\text{Ga}_3\text{MgN}_5$  the Madelung part of the lattice energy has been calculated (Table 5). A deviation of only 0.16 % between the sum of the respective MAPLE values of  $\text{Ca}_2\text{Ga}_3\text{MgN}_5$  and the constituting binary and ternary nitrides verifies the electrostatic consistency of the refined structure. Moreover, partial MAPLE values for each atom were compared with known MAPLE values and agree well with reference data reported before.<sup>[31]</sup>

**Table 5.** MAPLE values [kJ/mol] for  $\text{Ca}_2\text{Ga}_3\text{MgN}_5$  and deviation  $\Delta$  [%] from model value.

	calculated MAPLE value	$\Delta$
Ca	2037.03	
Mg/Ga	3810.05-4875.74	
N	4573.48-5081.69	
$\text{Ca}_2\text{Ga}_3\text{MgN}_5$	45853.45	
model $\text{Ca}_3\text{Ga}_2\text{N}_4$ <sup>[12]</sup>		
+ $\text{CaMgN}_2$ <sup>[32]</sup>		
+ $\text{GaN}$ <sup>[33]</sup>		
- $\frac{1}{3} \text{Mg}_3\text{N}_2$ <sup>[34]</sup>		
- $\frac{2}{3} \text{Ca}_3\text{N}_2$ <sup>[35]</sup>	45925.53	0.16

Typical partial MAPLE values [kJ/mol]:  $\text{Ca}^{2+}$ :1940-2650;  $\text{Ga}^{3+}$ :4500-6000;  $\text{Mg}^{2+}$ : 2100-2400;  $\text{N}^{3-}$ :3000-6000.<sup>[31,36-38]</sup>

### 5.3. Conclusion

In this contribution we present the novel quaternary compound  $\text{Ca}_2\text{Ga}_3\text{MgN}_5$ . All Mg-atoms are part of the tetrahedral network. According to *Liebau* the quaternary compound can be thus classified as magnesio-nitridogallate and the sum formula should be formulated  $\text{Ca}_2[\text{Ga}_3\text{MgN}_5]$ .<sup>[29]</sup> One Sr-containing magnesio-nitridogallate



$\text{Sr}(\text{Ga}_2\text{Mg}_2)\text{N}_4$  has already been reported in literature so  $\text{Ca}_2\text{Ga}_3\text{MgN}_5$  is the second example known so far.<sup>[15]</sup> The crystal structure is constituted of corner- and edge-sharing tetrahedra. These building units have a mixed occupation of Mg and Ga on the tetrahedral site due to similarities in ionic radii. The (Mg/Ga) $\text{N}_4$  tetrahedra are building *vierer*- and *sechser*-rings stacked along [010] building hexagonal and quadratic channels. The Ca-atoms are located inside these channels of *sechser*-rings, the quadrangular channels are not filled. This crystal structure is related to the well known crystal structure of  $M^{\text{II}}_2\text{Si}_5\text{N}_8$  ( $M^{\text{II}} = \text{Sr}, \text{Ba}$ ). In the latter also filled hexagonal and unfilled quadratic channels are reported. The arrangement of the *sechser*- and *vierer*-rings to each other are slightly different. Furthermore, in  $M^{\text{II}}_2\text{Si}_5\text{N}_8$  no edge- but only corner sharing of the  $\text{SiN}_4$  tetrahedra is observed. Therefore, the crystal structure of  $\text{Ca}_2\text{Ga}_3\text{MgN}_5$  is higher condensed than that of  $M^{\text{II}}_2\text{Si}_5\text{N}_8$  which can also be seen from the higher degree of condensation  $\kappa = 4 : 5$  for  $\text{Ca}_2\text{Ga}_3\text{MgN}_5$  (cf.  $M^{\text{II}}_2\text{Si}_5\text{N}_8$   $\kappa = 5 : 8$ ).

This example illustrates the strong relationship between nitridogallates and nitridosilicates. Due to different charges of the atoms in the tetrahedra center  $\text{Si}^{4+}$  compared to  $\text{Ga}^{3+}$  or  $(\text{Ga/Mg})^{2.5+}$  the condensation of the anionic substructure varies. Incorporation of additional Mg-atoms in the tetrahedral network influences the structural variety. Introducing Mg in some or all tetrahedral position impacts the charge and the covalency of the anionic substructure. Therefore, the band gap and other physical parameter are expected to be different from nitridogallates.

Nitridosilicates emerged as highly efficient optical materials when doped with  $\text{Eu}^{2+}$ , applicable as phosphors in phosphor-converted (pc-)LEDs. Also nitridogallates were investigated as host lattices for  $\text{Eu}^{2+}$ -doping recently.<sup>[22]</sup> The demonstrated structural relation of magnesio-nitridogallates to nitridosilicates is a strong incentive for further investigation of this compound class. Magnesio-nitridogallates could also be interesting candidates as host lattices for  $\text{Eu}^{2+}$ -doping and possible phosphor materials for application in pc-LEDs.

### 5.4. Experimental Section

Synthesis of  $\text{Ca}_2\text{Ga}_3\text{MgN}_5$  was carried out in Nb-ampoules (30 mm length, 10 mm diameter, 0.5 mm wall thickness). All manipulations were done under argon atmosphere in a glove box (Unilab, MBraun, Garching;  $\text{O}_2 < 1$  ppm,  $\text{H}_2\text{O} < 1$  ppm).

Single crystals were obtained from reaction of 0.312 mmol  $\text{NaN}_3$  (20.3 mg, Acros, 99%), 0.063 mmol Ca (2.5 mg, sigma Aldrich, 99.9%) 0.064 mmol Mg (1.5 mg, Alfa Aesar, 99.9%) and 0.245 mmol Ga (17.1 mg, AluSuisse, 99.999%) in 1.99 mmol Na-flux (45.7 mg, Sigma Aldrich, 99.95%). The filled Nb-ampoule was shut by arc melting under Ar atmosphere and placed in a quartz tubing under vacuum to prevent oxidation of the ampoule. The reaction mixture was then heated in a tube furnace with 50.0 °C/h to 760 °C, maintained at that temperature for 48 h and cooled down to 200 °C with a rate of 3.4 °C/h. Subsequently, the furnace was turned off and the Nb-ampoule was opened in a glove box. To separate Na from the reaction product the opened ampoule was heated to 320 °C under vacuum to sublime the Na-melt.

Scanning electron microscopy was performed on a JEOL JSM 6500 F equipped with a field emission gun at a maximum acceleration voltage of 30 kV. Synthesized samples were prepared on adhesive conductive carbon pads and coated with a conductive carbon film. The chemical composition was confirmed by EDX investigations (Oxford instruments), each recorded on an area limited to one crystal face to avoid influence of possible contaminating phases. Single-crystal X-ray diffraction data were collected on a Nonius Kappa-CCD diffractometer with graded multilayer X-ray optics and Mo  $\text{K}\alpha$  radiation ( $\lambda = 0.71073 \text{ \AA}$ ). The structure was solved using direct methods implemented in SHELXS-97.<sup>[39,40]</sup> Refinement of the crystal structure was carried out with anisotropic displacement parameters for all atoms by full-matrix least-squares calculation on  $F^2$  in SHELXL-97.<sup>[40,41]</sup>

Further details of the structure investigations are available from the Fachinformationszentrum Karlsruhe, D76344 Eggenstein Leopoldshafen, Germany (fax: +49-7247-808-666; email: [crysdata@fiz.karlsruhe.de](mailto:crysdata@fiz.karlsruhe.de)) on quoting the depository number CSD-425083.

## 5.5. References

- [1] S. Nakamura, *Solid State Commun.* **1997**, 102, 237.
- [2] S. Nakamura, *Science* **1998**, 281, 956.
- [3] S. Nakamura, S. Pearton, G. Fasol, *The Blue Laser Diode*, Springer Verlag, Berlin, **2000**.
- [4] S. Nakamura, M. Senoh, N. Iwasa, S. Nagahama, T. Yamada, T. Mukai, *Jpn. J. Appl. Phys.* **1995**, 34, L1332.
- [5] S. Nakamura, M. Senoh, T. Mukai, *Appl. Phys. Lett.* **1993**, 62, 2390.
- [6] T. Fujii, Y. Gao, R. Sharma, E. L. Hu, S. P. DenBaars, S. Nakamura, *Appl. Phys. Lett.* **2004**, 84, 855.
- [7] A. Denis, G. Goglio, G. Demazeau, *Mater. Sci. Eng.* **2006**, R 50, 167.
- [8] M. Bockowski, *Cryst. Res. Technol.* **2007**, 42, 1162.
- [9] S. Krukowski, P. Kempisty, P. Strak, *Cryst. Res. Technol.* **2009**, 44, 1038.
- [10] B. Wang, M. J. Callahan, *Cryst. Growth Des.* **2006**, 6, 1227.
- [11] R. P. Parikh, R. A. Adomaitis, *J. Cryst. Growth* **2006**, 286, 259.
- [12] S. J. Clarke, F. J. DiSalvo, *Inorg. Chem.* **1997**, 36, 1143.
- [13] S. J. Clarke, F. J. DiSalvo, *J. Alloys Compd.* **1998**, 274, 118.
- [14] G. Cordier, P. Höhn, R. Kniep, A. Rabenau, *Z. Anorg. Allg. Chem.* **1990**, 591, 58.
- [15] D. G. Park, Y. Dong, F. J. DiSalvo, *Solid State Sci.* **2008**, 10, 1846.
- [16] M. S. Bailey, F. J. DiSalvo, *J. Alloys Compd.* **2006**, 417, 50.
- [17] D. G. Park, Z. A. Gál, F. J. DiSalvo, *J. Alloys Compd.* **2003**, 353, 107.
- [18] S. J. Clarke, F. J. DiSalvo, *J. Alloys Compd.* **1997**, 259, 158.
- [19] D. G. Park, F. J. DiSalvo, *Bull. Korean Chem. Soc.* **2009**, 30, 1379.
- [20] P. M. Mallinson, Z. A. Gál, S. J. Clarke, *Inorg. Chem.* **2006**, 45, 419.
- [21] P. E. Rauch, A. Simon, *Angew. Chem.* **1992**, 104, 1505; *Angew. Chem. Int. Ed. Engl.* **1992**, 31, 1519.
- [22] F. Hintze, F. Hummel, P. J. Schmidt, D. Wiechert, W. Schnick, *Chem. Mater.* **2012**, 402.
- [23] F. Hintze, W. Schnick, *Solid State Sci.* **2010**, 12, 1368.
- [24] D. G. Park, Z. A. Gál, F. J. DiSalvo, *Inorg. Chem.* **2003**, 42, 1779.
- [25] S. Pagano, S. Lupart, M. Zeuner, W. Schnick, *Angew. Chem.* **2009**, 121, 6453; *Angew. Chem. Int. Ed.* **2009**, 48, 6335.

- [26] T. Schlieper, W. Schnick, *Z. Anorg. Allg. Chem.* **1995**, 621, 1037.
- [27] R. D. Shannon, *Acta Crystallogr., Sect. A: Found. Crystallogr.* **1976**, 32, 751.
- [28] W. H. Baur, *Crystallogr. Rev.* **1987**, 1, 59.
- [29] F. Liebau, *Structural Chemistry of Silicates*, Springer, Berlin, **1985**.
- [30] T. Schlieper, W. Milius, W. Schnick, *Z. Anorg. Allg. Chem.* **1995**, 621, 1380.
- [31] M. Zeuner, S. Pagano, W. Schnick, *Angew. Chem.* **2011**, 123, 7898; *Angew. Chem. Int. Ed.* **2011**, 50, 7754.
- [32] V. Schultz-Coulon, W. Schnick, *Z. Naturforsch.* **1995**, 50b, 619.
- [33] M. Roos, J. Wittrock, G. Meyer, S. Fritz, J. Strähle, *Z. Anorg. Allg. Chem.* **2000**, 626.
- [34] O. Reckeweg, F. J. DiSalvo, *Z. Anorg. Allg. Chem.* **2001**, 627, 371.
- [35] S. Horstmann, E. Irran, W. Schnick, *Z. Anorg. Allg. Chem.* **1998**, 624, 620.
- [36] H. Höppe, *Dissertation*, Ludwig-Maximilians-Universität München **2003**.
- [37] K. Köllisch, *Dissertation*, Ludwig-Maximilians-Universität München **2001**.
- [38] R. Lauterbach, *Dissertation*, Universität Bayreuth **1999**.
- [39] SHELXS, G. M. Sheldrick Universität Göttingen, **1997**.
- [40] G. M. Sheldrick, *Acta Crystallogr. Sect. A: Found. Crystallogr.* **2008**, 64, 112.
- [41] SHELXL, G. M. Sheldrick Universität Göttingen, **1997**.

## 6. Nitridogallate Fluoride $\text{LiBa}_5\text{GaN}_3\text{F}_5$

In the previous described syntheses of nitridogallates, all reactions were carried out with an increased nitrogen pressure by decomposition of  $\text{NaN}_3$  in a sodium flux. As recent researches in our group showed, the use of Li as fluxing agents is also very promising. Therefore, a mixed melt of Na and Li was used in the next description. By the use of additional Li, this element was incorporated in the crystal structure. For the initial target of doping with Eu as described before,  $\text{EuF}_3$  was added to the starting materials mixture as well. By the presence of  $\text{Li}^+$  and the thermodynamically preferred binding to  $\text{F}^-$ , both elements are present in the product but not as side phase.  $\text{LiF}_6$ -octahedrons are part of the crystal structure, building strands by vertex sharing running along [010]. The Ga surrounding in this compound differs from the so far described nitridogallates since here, isolated  $\text{GaN}_3$ -units are observed. In addition to crystal structure elucidation, investigations on the band gap were carried out through calculations and measurements on single crystals.

## A Novel Nitridogallate Fluoride $\text{LiBa}_5\text{GaN}_3\text{F}_5$ – Synthesis, Crystal Structure and Band Gap Determination

Frauke Hintze, Wolfgang Schnick

**published in:** *Solid State Sci.* **2010**, 12, 1368.

**Keywords:** Nitridogallate; crystal structure; electronic structure; optical measurements; sodium flux.

**Abstract:**  $\text{LiBa}_5\text{GaN}_3\text{F}_5$  was obtained as red crystals by reaction of Ba, Ga,  $\text{NaN}_3$  and  $\text{EuF}_3$  in a Na/Li flux at 760 °C in weld-shut tantalum crucibles. The crystal structure (*Pnma* (no. 62),  $a = 15.456(3)$ ,  $b = 5.707(1)$ ,  $c = 12.259(3)$  Å,  $Z = 4$ ) was solved on the basis of single-crystal X-ray diffraction data. In the solid there are trigonal planar  $[\text{GaN}_3]^{6-}$  ions and zigzag chains of vertex sharing  $\text{LiF}_6$  octahedrons surrounded by  $\text{Ba}^{2+}$  ions. Optical measurements and calculations of the electronic structure revealed a band gap of  $\leq 1.9$  eV. According to the calculations, the observed transition occurs from a nitrogen state into a hybrid Ba/N state.

## 6.1. Introduction

Ternary nitrides of Ga in combination with alkaline earth metals (e.g. Sr, Ba) are known since a couple of years,<sup>[1-4]</sup> but only a small number of quaternary examples have been reported recently.<sup>[5-7]</sup> Most of these compounds have been synthesized in sodium melts which due to addition of alkaline earth metals exhibit an increased solubility of nitrogen.<sup>[8]</sup> Syntheses were performed in closed niobium crucibles, utilizing additional azides as nitrogen source.  $\text{Sr}_3\text{GaN}_3$ ,  $\text{Sr}_6\text{GaN}_5$ ,<sup>[2]</sup>  $\text{Sr}_4\text{GaN}_3\text{O}$  and  $\text{Sr}_4\text{GaN}_3(\text{CN}_2)$ <sup>[5]</sup> contain non condensed (“isolated”)  $[\text{GaN}_3]^{6-}$  while  $\text{Ba}_3\text{Ga}_2\text{N}_4$  and  $\text{Sr}_3\text{Ga}_2\text{N}_4$  are made up of trans edge sharing  $\text{GaN}_4$  tetrahedrons building infinite chains.<sup>[1,4]</sup> Two- or three-dimensional networks of vertex sharing  $\text{GaN}_4$  tetrahedrons have been found in  $\text{Ca}_3\text{Ga}_2\text{N}_4$ ,  $\text{Sr}_3\text{Ga}_3\text{N}_5$ <sup>[4]</sup> and  $\text{LiSrGaN}_2$ ,<sup>[6]</sup> respectively. Thus, structural motifs similar to nitridosilicates (e.g.  $\text{BaSi}_7\text{N}_{10}$ ;  $\text{Eu}_2\text{SiN}_3$ )<sup>[9,10]</sup> occur in the nitridogallates mentioned above. Recently, we have reported about synthetic approaches to control the dimensionality of nitridosilicates employing lithium melts.<sup>[11]</sup> In comparison with nitridosilicates, the field of nitridogallates is more unexplored but utilization of the lithium flux technique may lead to a larger structural variety analogously to our experience with nitridosilicates.

## 6.2. Experimental

The synthesis of  $\text{LiBa}_5\text{GaN}_3\text{F}_5$  was carried out in Ta crucibles (30 mm length, 9.5 mm diameter, 0.5 mm wall thickness). Under argon atmosphere (glove box Unilab,



**Figure 1.** SEM micrograph of  $\text{LiBa}_5\text{GaN}_3\text{F}_5$  crystals.

MBraun), 0.35 mmol (22.8 mg)  $\text{NaN}_3$  (Acros, 99 %), 0.138 mmol (9.6 mg) Ga (AluSuisse, 99.999 %), 0.549 mmol (75.4 mg) Ba (Sigma Aldrich, 99.99 %) and 0.027 mmol (5.7 mg)  $\text{EuF}_3$  (Sigma Aldrich, 99.99 %) were mixed and filled into the Ta crucible. For the flux 2.174 mmol (50.0 mg) Na (Sigma Aldrich, 99.95 %) and 0.145 mmol (1.0 mg) Li (Sigma Aldrich, 99.9 %) were added. The Ta crucible was sealed under argon by arc welding. To protect the Ta crucible from oxidation, it was

placed into a silica tube under argon atmosphere. In a tube furnace the crucible was heated to 760 °C with a rate of 50 °C h<sup>-1</sup>. The temperature was maintained for 48 h and then lowered with 3.7 °C h<sup>-1</sup> to 200 °C. Once the temperature reached 200 °C, the furnace was turned off and cooled down to room temperature. The Ta crucible was opened and Na was separated from the reaction products by evaporation at 320 °C under vacuum (0.1 Pa) for 18 h. From the inhomogeneous gray product, red needle-shaped single crystals (200 - 600 µm) were isolated (cf. Figure 1), enclosed in glass capillaries and sealed under argon atmosphere. X-ray diffraction data were collected at room temperature with a STOE IPDS I diffractometer. A numerical absorption correction using the programs XRED<sup>[12]</sup> and XSHAPE<sup>[13]</sup> was applied. The crystal structure was solved by using direct methods with SHELXS.<sup>[14]</sup> The refinement of the structure was carried out by the method of least-squares using SHELXL.<sup>[14]</sup> The chemical composition was confirmed by energy dispersive X-ray spectroscopy (EDX) using a JSM-6500F scanning microscope (Jeol) provided with a Si/Li EDX detector (Oxford Instruments, model 7418). Optical spectra of  $\text{LiBa}_5\text{GaN}_3\text{F}_5$  were measured with a modified microcrystal spectrophotometer CARY 17 (Spectra Services, ANU Canberra, Australia).<sup>[15-17]</sup> Calculations of the band gap were carried out with the program package WIEN2K<sup>[18]</sup> utilizing the structural data from the single-crystal structure refinement.

### 6.3. Results and Discussion

#### 6.3.1. Crystal Structure

The crystal structure was solved and refined in orthorhombic space group *Pnma* (no. 62) with  $a = 15.456(3)$ ,  $b = 5.707(1)$  and  $c = 12.259(3)$  Å. The crystallographic data of  $\text{LiBa}_5\text{GaN}_3\text{F}_5$  is summarized in Table 1, the atomic coordinates and the isotropic displacement parameters are listed in Table 2. In the crystal  $\text{LiBa}_5\text{GaN}_3\text{F}_5$  zigzag chains of vertex sharing  $\text{LiF}_6$  octahedrons running along [010] (cf. Figure 2). Perpendicular to these chains, Ba atoms are arranged in layers. Likewise perpendicular to [010] “isolated” trigonal planar  $[\text{GaN}_3]^{6-}$  ions are found.



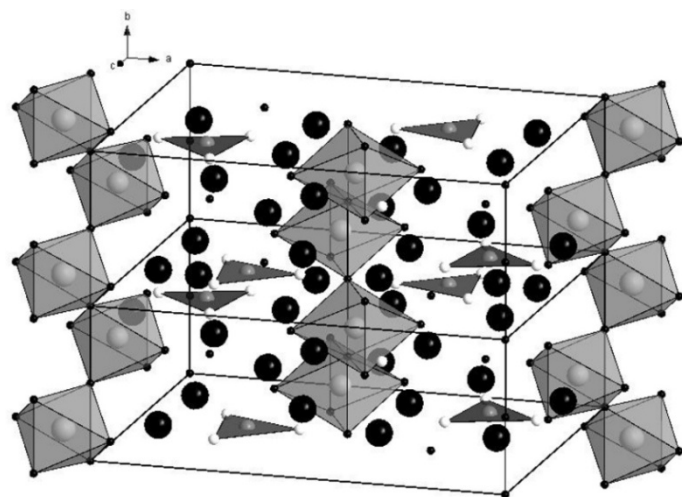


**Figure 2.** Crystal structure of  $\text{LiBa}_5\text{GaN}_3\text{F}_5$ . Big black circles  $\text{Ba}^{2+}$ , small black  $\text{F}^-$ , big gray  $\text{Li}^+$ , white  $\text{N}^{3-}$  and small gray  $\text{Ga}^{3+}$ . The  $\text{LiF}_6$  octahedrons (highlighted in gray) are vertex sharing and build zigzag chains running along the b-axis.

**Table 1.** Crystallographic data of  $\text{LiBa}_5\text{GaN}_3\text{F}_5$ .

Formula	$\text{LiBa}_5\text{GaN}_3\text{F}_5$
Crystal system	orthorhombic
Space group	$Pnma$ (no. 62)
Lattice parameters ( $\text{\AA}$ )	$a = 15.456(3)$ , $b = 5.707(1)$ , $c = 12.259(3)$
Cell volume ( $\text{\AA}^3$ )	1081.3(4)
Formula units per unit cell	4
Density ( $\text{g} \cdot \text{cm}^{-3}$ )	5.531
$\mu$ ( $\text{mm}^{-1}$ )	20.41
T (K)	293(2)
F(000)	1520
Profile range	$5.8 \leq 2\theta \leq 63.2$
Index ranges	$-20 \leq h \leq 18$ $-6 \leq k \leq 6$ $-15 \leq l \leq 15$
Independent reflections	1286 [ $R(\text{int}) = 0.072$ ]
Refined parameters	89
Goodness of fit	1.057
$R_1$ (all data); $R_1 (F^2 > 2\sigma(F^2))$	0.0230, 0.0212
$wR_2$ (all data); $wR_2 (F^2 > 2\sigma(F^2))$	0.0512, 0.0505
$\Delta\rho_{\text{max}}$ , $\Delta\rho_{\text{min}}$ ( $\text{e} \text{\AA}^{-3}$ )	1.56, -2.13

The Ga-N bond-lengths range from 1.90 to 1.95 Å (Figure 3) and agree well with the sum of the ionic radii<sup>[19-21]</sup> as well as with typical Ga-N distances (e.g.  $\text{Sr}_4\text{GaN}_3\text{O}$ , Ga-N : 1.88 – 1.92 ) Similar  $[\text{GaN}_3]^{6-}$  ions have been found in  $\text{Sr}_3\text{GaN}_3$ ,  $\text{Sr}_6\text{GaN}_5$ ,<sup>[2]</sup>  $\text{Sr}_4\text{GaN}_3\text{O}$  and  $\text{Sr}_4\text{GaN}_3(\text{CN}_2)$ .<sup>[5]</sup> The coordination sphere of the trigonal planar  $[\text{GaN}_3]^{6-}$  ions can be described as three-capped trigonal prisms of  $\text{Ba}^{2+}$  atoms. In  $\text{Sr}_3\text{GaN}_3$ <sup>[2]</sup> similar trigonal prism of  $\text{Sr}^{2+}$  atoms have been observed. The  $\text{N}^{3-}$  atoms are likewise surrounded in distorted octahedrons of five  $\text{Ba}^{2+}$  and one  $\text{Ga}^{3+}$  atom.

**Table 2.** Atomic coordinates and isotropic displacement parameters ( $\text{\AA}^2$ ) of  $\text{LiBa}_5\text{GaN}_3\text{F}_5$ , standard deviations in parentheses.

Atom	Wyckoff position	x	y	z	$U_{\text{iso}}^*/U_{\text{eq}}$
Ba1	4c	0.43534 (2)	$\frac{1}{4}$	0.68180 (2)	0.0092 (1)
Ba2	4c	0.51012 (2)	$\frac{3}{4}$	0.87769 (3)	0.0090 (1)
Ba3	4c	0.34365 (2)	$\frac{3}{4}$	0.47028 (3)	0.0089 (1)
Ba4	4c	0.24513 (2)	$\frac{3}{4}$	0.77891 (3)	0.0100 (1)
Ba5	4c	0.16417 (2)	$\frac{1}{4}$	0.63252 (2)	0.0109 (1)
Ga1	4c	0.35910 (4)	$\frac{1}{4}$	0.92467 (4)	0.0076 (2)
F1	8d	0.4111 (2)	0.0121 (5)	0.3013 (2)	0.0151 (6)
F2	4a	$\frac{1}{2}$	0	$\frac{1}{2}$	0.0131 (7)
F3	4c	0.4075 (3)	$-\frac{1}{4}$	0.6854 (3)	0.0171 (8)
F4	4c	0.1779 (4)	$-\frac{1}{4}$	0.9936 (3)	0.027 (1)
N1	4c	0.4799 (4)	$\frac{1}{4}$	0.8980 (4)	0.014 (2)
N2	4c	0.2813 (4)	$\frac{1}{4}$	0.8020 (4)	0.013 (2)
N3	4c	0.3152 (4)	$\frac{1}{4}$	1.0734 (5)	0.012 (2)
Li1	4c	0.459 (2)	$\frac{1}{4}$	0.4020 (8)	0.026 (3)

$\text{Li}^+$  does not directly coordinate to the  $[\text{GaN}_3]^{6-}$  ions but is surrounded by six  $\text{F}^-$  in a distorted octahedron. The Li-F distances are ranging between 1.97 and 1.98 Å for the equatorial F2 and F1 and 2.33 to 2.39 Å for the axial F3 and F4 (cf. Figure 3).

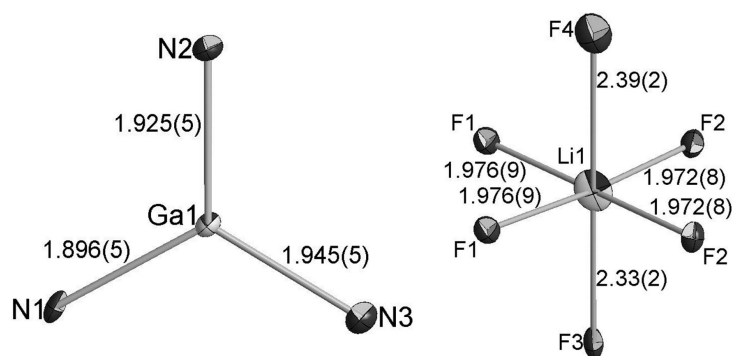


**Figure 3.** Coordination of  $\text{Ga}^{3+}$  and  $\text{Li}^+$  in thermal ellipsoids with 50 % probability.  $\text{Ga}^{3+}$  has a trigonal planar coordination by  $\text{N}^{3-}$ , six  $\text{F}^-$  coordinate  $\text{Li}^+$  (elongated octahedron).

The latter ones exceed significantly the sum of the ionic radii ( $2.06 \text{ \AA}$ )<sup>[19]</sup> while the equatorial Li-F distances are slightly shorter than reported distances in other  $\text{LiF}_6$  octahedrons ( $\text{K}_2\text{LiAlF}_6$ , Li-F :  $2.109 \text{ \AA}$ ).<sup>[22,23]</sup> In the second coordination sphere, the octahedron  $\text{LiF}_6$  is coordinated

by eight  $\text{Ba}^{2+}$  in a cubic way, comparable with the cubic  $\text{Ca}^{2+}$ -coordination of  $\text{Ti}^{4+}$  in  $\text{CaTiO}_3$ . The coordination of  $\text{F}^-$  occurs in distorted octahedrons of five  $\text{Ba}^{2+}$  and one  $\text{Li}^+$ . Only F2 is coordinated by two  $\text{Li}^+$  and four  $\text{Ba}^{2+}$ . The atomic distances Ba-F and Li-F are mentioned above. The the thermal displacement parameter  $U_{\text{iso}}^*/U_{\text{eq}}$  of F4 is considerably higher (cf. Table 3) in comparison with the other values for fluorine atoms.

**Table 3.** Selected interatomic distances [ $\text{\AA}$ ] and angles [ $^\circ$ ] of  $\text{LiBa}_5\text{GaN}_3\text{F}_5$ , standard deviations in parentheses.

Ba1-N1	2.739(5)	Ba5-F1	2.806(2)
Ba1-F2	2.8286(5)	Ga1-N1	1.896(5)
Ba2-N3	2.765(6)	Ga1-N2	1.925(5)
Ba2-F1	2.853(2)	Ga1-N3	1.945(5)
Ba3-N2	2.826(5)	Li1-F1	1.976(9)
Ba3-F3	2.816(3)	Li1-F2	1.972(8)
Ba4-N3	2.687(5)	Li1-F3	2.33(2)
Ba4-F4	2.830(4)	Li1-F4	2.39(2)
Ba5-N1	2.872(5)		
N2-Ba1-F1	132.7(1)	F2-Li1-F3	89.5(5)
N3-Ba3-F1	132.8(9)	F3-Li1-F4	179.3(5)
F3-Ba4-F4	136.1(1)	N1-Ga1-N3	120.3(2)
F4-Ba5-N1	137.6(1)	N1-Ga1-N2	118.7(2)

One reason for this observation may be the fact, that - considering the octahedron  $\text{LiF}_6$  - the F4 atom is a “free” one and does not connect to the next octahedrons. Additionally, the  $U_{11}$  value for F4 is almost three times higher than the values for the other  $\text{F}^-$ . The short distance between Ba4-F4 (2.83 Å) may be responsible for this observation. The F3 atom has an even shorter distance to Ba4 (2.76 Å) and is also a non-bridging one. Here we can also observe a little higher  $U_{\text{iso}}^*/U_{\text{eq}}$  value. The only other known Li containing nitridogallate, ( $\text{LiSrGaN}_2$ ) contains a two-dimensional network of corner sharing  $\text{GaN}_4$  tetrahedrons resulting in a tetrahedral coordination of lithium.<sup>[6]</sup> The five crystallographically different  $\text{Ba}^{2+}$  ions are sevenfold or ninefold coordinated by  $\text{N}^{3-}$  atoms of the  $[\text{GaN}_3]^{6-}$  and  $\text{F}^-$  ions, respectively (Figure 4).

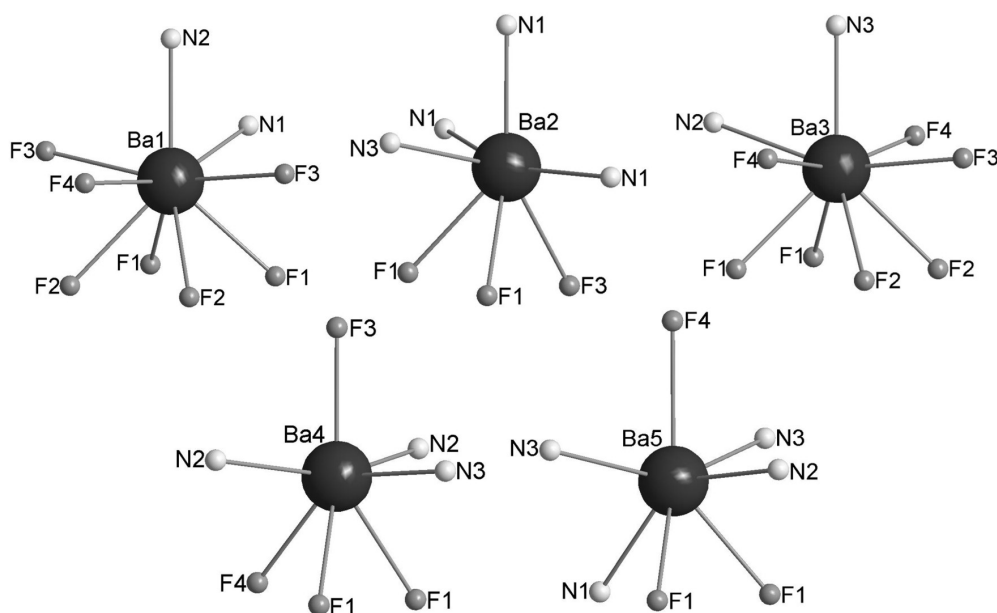


**Figure 4.** Coordination of the five crystallographically different  $\text{Ba}^{2+}$ . The  $\text{N}^{3-}$  and  $\text{F}^-$  around  $\text{Ba}^{2+}$  build trigonal or squared pyramids, respectively, with capped faces.

Coordination of the  $\text{Ba}^{2+}$  atoms occurs in form of square or trigonal pyramids, respectively, where each face of the pyramid is additionally capped by anions. The distances Ba-N and Ba-F range from 2.74 to 2.87 Å and are in good accordance to known Ba-N and Ba-F distances (e.g.  $\text{Ba}_3\text{Al}_2\text{N}_4$ , Ba-N : 2.607 - 2.873 Å;  $\text{Ba}_3\text{Cu}_2\text{Al}_2\text{F}_{16}$ , Ba-F : 2.597 - 2.957 Å).<sup>[24-27]</sup> Selected bond-lengths and angles of  $\text{LiBa}_5\text{GaN}_3\text{F}_5$  are given in Table 3. To proof the electrostatic consistency of the crystal structure MAPLE (Madelung Part of Lattice Energy) calculations of the lattice energy<sup>[28,29]</sup> were carried out (cf. Table 4). The partial MAPLE values (for  $\text{Li}^+$ ,  $\text{Ba}^{2+}$ ,  $\text{Ga}^{3+}$ ,  $\text{N}^{3-}$  and  $\text{F}^-$ ) are in good accordance to reference values. The electrostatic consistency of the refined crystal structure has been verified by comparing MAPLE

sums of different binary and ternary nitrides with the MAPLE value of  $\text{LiBa}_5\text{GaN}_3\text{F}_5$ . Both values differ only slightly by 0,19 %. The model contains the data of the theoretical binary nitride  $\text{Ba}_3\text{N}_2$ .<sup>[33,34]</sup>

**Table 4.** Partial MAPLE values and MAPLE sums [kJ/mol] of  $\text{LiBa}_5\text{GaN}_3\text{F}_5$ .

$\text{LiBa}_5\text{GaN}_3\text{F}_5$				Model
Ba1	1662	N1	970	GaN
Ba2	1760	N2	965	LiF
Ba3	1672	N3	956	BaF <sub>2</sub>
Ba4	1733	F1	108	$\text{Ba}_3\text{N}_2$ <sup>[33,34]</sup>
Ba5	1826	F2	134	
Ga	5157	F3	126	
Li	629	F4	117	
$\Sigma = 29031$				$\Sigma = 29089 \quad \Delta = 0.19 \%$

Typical partial MAPLE values [kJ/mol]:  $\text{Ba}^{2+}$ : 1600 - 2500;  $\text{Ga}^{3+}$ : 4500 - 6000;  $\text{Li}^+$ : 600 - 860;  $\text{N}^{3-}$ : 3000 - 6000;  $\text{F}^-$ : 450 - 600.<sup>[30-32]</sup>

### 6.3.2. Band Gap Determination

To specify the optical band gap the extinction of the complete spectrum, ranging from UV up to near IR was measured (Figure 5). The observed absorption represents a permitted charge transfer transition from a  $\text{N}^{3-}$  state to a metal state. With extrapolation of the linear region between 16000 and 17000  $\text{cm}^{-1}$  the optical band gap was determined to 1.9 eV. The measured energy of the optical band gap lies within the red sector of the visible spectrum and is in accordance with the observed red color of the crystals.

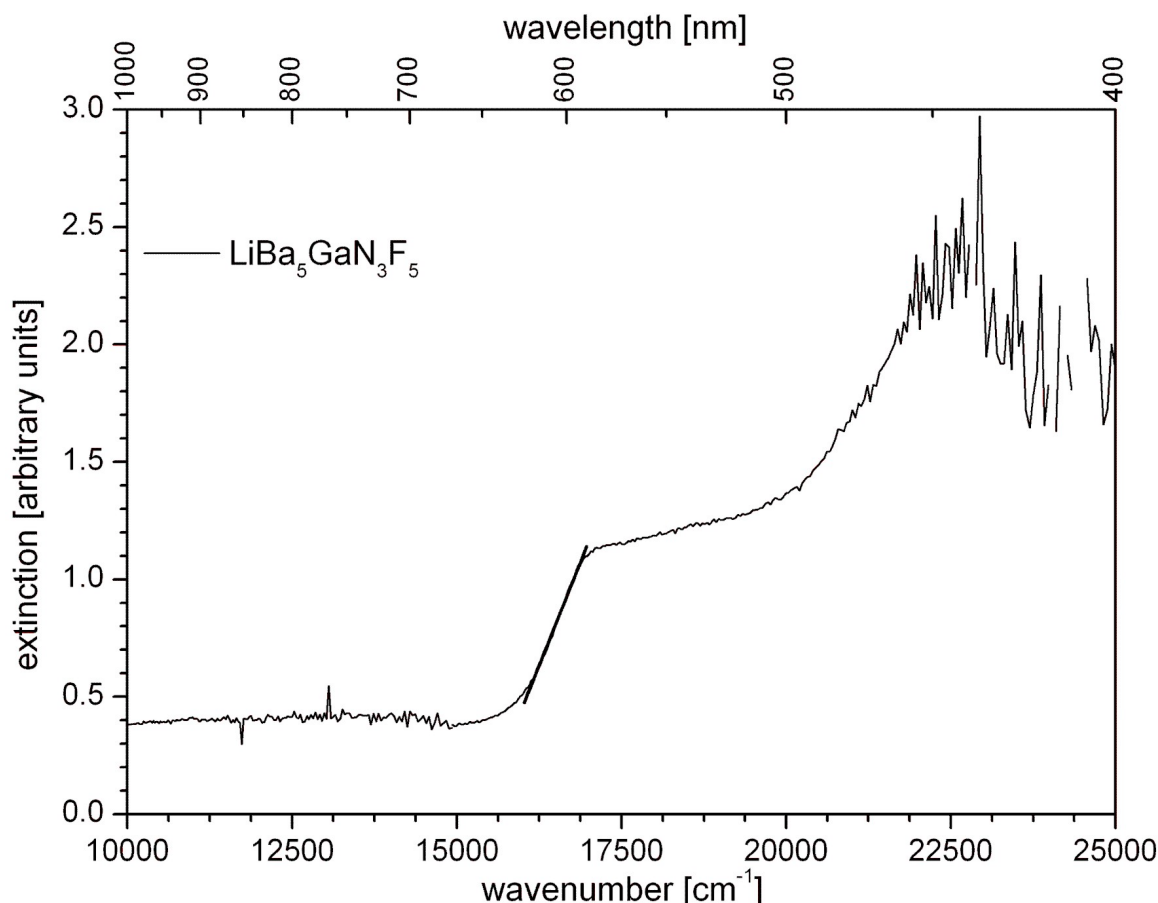
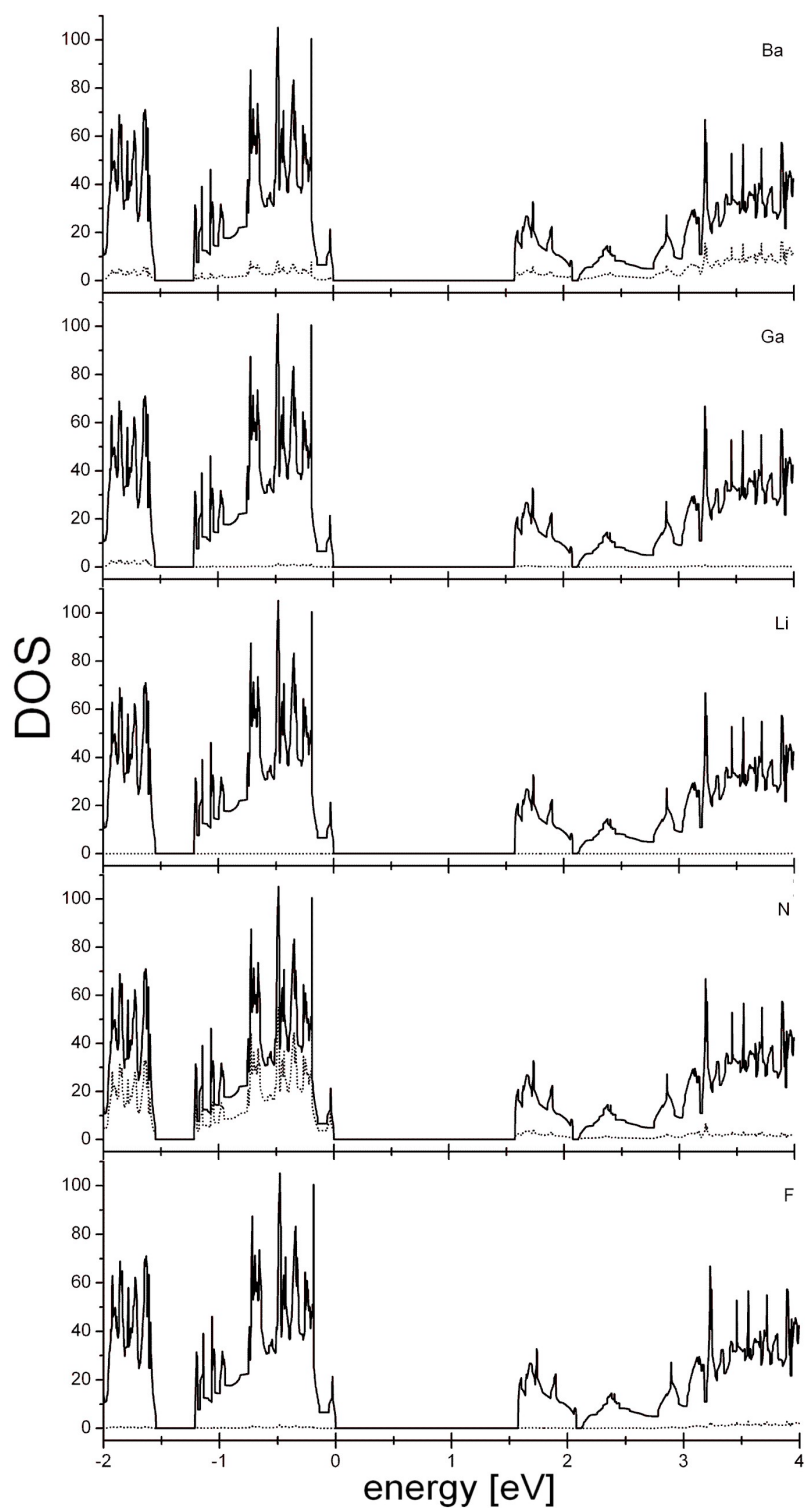


**Figure 5.** Extinction of  $\text{LiBa}_5\text{GaN}_3\text{F}_5$  from UV up to near IR. The line shows the extinction of  $\text{LiBa}_5\text{GaN}_3\text{F}_5$ . With the linear slope ( $16000\text{--}17000\text{ cm}^{-1}$ ) the energy of the band gap was determined to 1.9 eV.

The band gap of  $\text{LiBa}_5\text{GaN}_3\text{F}_5$  has also been determined by calculations of the electronic structure. Additionally, these calculations give information about the character of the band gap. The density of states (DOS) was calculated for each kind of atom as well as for the entire compound (Figure 6). The energy of the electronic band gap was calculated to 1.6 eV. The highest occupied molecular orbital consists of 57 % nitrogen. Ba and Ga have only little contribution, Li and F are not involved here. The transition occurs towards the lowest unoccupied molecular orbital, consisting of Ba and N. The overall DOS is larger than the sum of the individual DOS for each atom as seen in Figure 6. The difference to the overall DOS lies in the so-called interstitial sphere. This is evidence that some electron density could not be allocated solely to single atoms, but the electron density resides beyond the atomic spheres.

**Figure 6.** Calculated density of states (DOS) of  $\text{LiBa}_5\text{GaN}_3\text{F}_5$  with contributions of each atom.



With 1.6 eV the calculated energy of the electronic band gap is smaller than the energy from the optical measurements 1.9 eV. This observation is typical for DFT calculations which usually underestimate the band gap. Nevertheless, both values are in accordance with the observed red color of the crystals.

#### **6.4. Conclusion**

The incorporation of fluorine into nitridogallates leads to a new composition. Similarly to nitridosilicates, the usage of a mixed Li/Na flux shows an extension of the structural variety of nitridogallates. In combination with the fluorine source  $\text{EuF}_3$ , an additional structural unit, the  $\text{LiF}_6$  octahedrons could be integrated into a nitridogallate compound, probably due to the strong Li-F binding compared to the Li-N. Optical measurements on single crystals as well as calculations of the electronic structure are beneficial for band gap investigations.



## 6.5. References

- [1] H. Yamane, F.J. DiSalvo, *Acta Crystallogr. Sect. C: Cryst. Struct. Commun* **1996**, 52, 760.
- [2] D. G. Park, Z. A. Gál, F. J. DiSalvo, *Inorg. Chem.* **2003**, 42, 1779.
- [3] G. Cordier, M. Ludwig, D. Stahl, P. C. Schmidt, R. Kniep, *Angew. Chem.* **1995**, 107, 1879; *Angew. Chem. Int. Ed. Engl.* **1995**, 34, 1761.
- [4] S. J. Clarke, F. J. DiSalvo, *Inorg. Chem.* **1997**, 36, 1143.
- [5] P. M. Mallinson, Z. A. Gál, S. J. Clarke, *Inorg. Chem.* **2006**, 45, 419.
- [6] D. G. Park, Z. A. Gál, F. J. DiSalvo, *J. Alloys Compd.* **2003**, 353, 107.
- [7] D. G. Park, Y. Dong, F. J. DiSalvo, *Solid State Sci.* **2008**, 10, 1846.
- [8] P. E. Rauch, A. Simon, *Angew. Chem.* **1992**, 104, 1505; *Angew. Chem. Int. Ed.* **1992**, 31, 1519.
- [9] H. Huppertz, W. Schnick, *Chem. Eur. J.* **1997**, 3, 249.
- [10] M. Zeuner, S. Pagano, P. Matthes, D. Bichler, D. Johrendt, T. Harmening, R. Pöttgen, W. Schnick, *J. Am. Chem. Soc.* **2009**, 131, 11242.
- [11] S. Pagano, S. Lupart, M. Zeuner, W. Schnick, *Angew. Chem.* **2009**, 121, 6453; *Angew. Chem. Int. Ed.* **2009**, 48, 6335.
- [12] X-RED 32, Data reduction for STADI 4 and IPDS, Version 1.03, STOE & Cie GmbH, Darmstadt, Germany 2002.
- [13] X-SHAPE, Crystal optimization for numerical absorption correction, version 1.05, STOE & Cie GmbH, Darmstadt, Germany (1999).
- [14] G. M. Sheldrick, *Acta Crystallogr. Sect. A: Found. Crystallogr.* **2008**, 64, 112.
- [15] J. Ferguson, W. Orr, *Rev. Sci. Instrum.* **1973**, 44, 225.
- [16] E. Krausz, *Aust. J. Chem.* **1993**, 43, 1041.
- [17] E. Krausz, C. Tomkins, H. Adler, *J. Phys. E: Sci. Instrum.* **1982**, 15, 1167.
- [18] P. Blaha, K. Schwarz, G. K. H. Madsen, D. Kvasnicka, J. Luitz, WIEN 2k, An Augmented Plane Wave + Local Orbitals Program for Calculation Crystals Properties, Technical University Vienna.
- [19] R. D. Shannon, *Acta Crystallogr. Sect. A: Found. Crystallogr.* **1967**, 32, 751.
- [20] W. H. Baur, *Crystallogr. Rev.* **1987**, 1, 59.
- [21] J. C. Slater, *J. Chem. Phys.* **1964**, 41, 3199.
- [22] Y. M. Kieslev, A. I. Popov, V. B. Sokolov, S. N. Spirin, *Russ. Inorg. Chem.* **1989**, 34, 243.

- [23] J. Graulich, S. Drücke, D. Babel, *Z. Anorg. Allg. Chem.* **1998**, 624, 1460.
- [24] M. Ludwig, R. Niewa, R. Kniep, *Z. Naturforsch. B.: J. Chem. Sci.* **1999**, 54, 461.
- [25] A. Gudat, S. Haar, R. Kniep, A. Rabenau, *J. Less-Common Met.* **1990**, 159, 29.
- [26] R. Niewa, F. J. DiSalvo, *J. Alloys Compd.* **1998**, 279, 153.
- [27] P. Gredin, G. Corbel, J. P. Wright, N. Dupont, A. De Kozak, *Z. Anorg. Allg. Chem.* **2003**, 629, 1690.
- [28] R. Hoppe, *Angew. Chem.* **1966**, 78, 52; *Angew. Chem. Int. Ed.* **1966**, 5, 95.
- [29] R. Hoppe, *Angew. Chem.* **1970**, 82, 7; *Angew. Chem. Int. Ed.* **1970**, 9, 25.
- [30] K. Köllisch, Dissertation, Ludwig-Maximilians-Universität München, **2001**.
- [31] H. Höppe, Dissertation, Ludwig-Maximilians-Universität München, **2003**.
- [32] R. Lauterbach, Dissertation, University of Bayreuth, **1999**.
- [33] S. R. Römer, T. Dörfler, P. Kroll, W. Schnick, *Phys. Status Solidi B* **2009**, 246, 1604.
- [34] E. Orhan, S. Jobic, R. Brec, R. Marchand, J. Y. Saillard, *J. Chem. Mater.* **2002**, 12, 2475.

## 7. Novel Nitrido-magnesiometalates of Ga and Al

For synthesis of nitridogallates, mostly reactions of metals in sodium flux are described, using  $\text{NaN}_3$  as nitrogen source. Herein, we present several syntheses routes whereas the described nitrido-magnesiogallate is commonly synthesized. Additionally, nitrido-magnesioaluminates were obtained from a fluoride route carried out in Li-flux. In contrast to previous described incorporation of Li and F in the resulting compound, in the following products none of them is part of the crystalline nitride compounds but can be found in the side phase LiF. The formation of this side phase is the driving force for these reactions. The reported novel nitrido-magnesioaluminates and nitrido-magnesiogallates are isostructural and solid solutions in and between those two compound classes were carried out.

**Novel Nitrido-magnesioaluminates, Nitrido-magnesiogallates and Solid Solutions of  $AEMg_2Al_{2-x}Ga_xN_4$  ( $x = 0-2$ ,  $AE = Ca, Sr, Ba$ )**

**Frauke Hintze, Philipp Pust, Andreas Locher, Daniela Zitnanska, Sascha Harm and Wolfgang Schnick**

***To be published***

**Abstract:** Synthesis of the novel nitrido-magnesioaluminates, nitrido-magnesiogallates and solid solutions thereof of compositions  $Ca_{1-x}Sr_x[Mg_2Al_2N_4]$ ,  $Sr_{1-x}Ba_x[Mg_2Al_2N_4]$ ,  $Sr[Mg_2Al_{1.95}Ga_{0.05}N_4]$ ,  $Sr_{1-x}Ba_x[Mg_2Al_{1.95}Ga_{0.05}N_4]$  and  $Ba[Mg_2Al_{1.9}Ga_{0.1}N_4]$  are reported employing arc-welded Ta- or Nb-ampoules, respectively. Most suited was the fluoride route, an expansion of the Li-flux method where metal-fluorides have been added to the metallic melt. The novel nitrides were obtained as single crystals. Additionally, synthesis of  $Ba[Mg_2Ga_2N_4]$  and  $Sr_{1-x}Ba_x[Mg_2Ga_2N_4]$  was carried out using metals as starting materials.  $Ca[Mg_2Al_2N_4]$  and  $Eu[Mg_2Al_2N_4]$  were obtained by using  $NH_4N_3$  as nitrogen source. All compounds are isostructural crystallizing in the  $UCr_4C_4$ -structure type (space group  $I4/m$  (no. 87),  $a = 8.0655(11) - 8.3654(12)$ ,  $c = 3.2857(7) - 3.4411(7)$  Å). The crystal structure is built up of edge-sharing tetrahedra, miscellaneously occupied by  $Mg^{2+}$  and  $Al^{3+}$ , by  $Mg^{2+}$  and  $Ga^{3+}$  or by all three elements, respectively. The alkaline-earth ion or  $Eu^{2+}$  is located in channels of the tetrahedral network. The structural variability of the  $UCr_4C_4$ -structure type is nicely demonstrated with the reported compounds.

### 7.1. Introduction

Binary nitrides e.g.  $\text{Mg}_3\text{N}_2$ ,  $\text{AlN}$  and  $\text{GaN}$  find various industrial applications. For example  $\text{Mg}_3\text{N}_2$  can be utilized as catalyst for synthesis of nitride ceramic materials.<sup>[1]</sup>  $\text{AlN}$  is employed as substrate material for fabrication of semiconductors, as heat conductor, and is a promising candidate for optoelectronic devices.<sup>[2,3]</sup>  $\text{GaN}$  is one of the most thoroughly investigated compounds nowadays due to its application as direct wide band gap semiconductor for high-performance LEDs.<sup>[4-6]</sup>

Only a small number of ternary and higher nitrides with group 2 metals deriving from these binary nitrides are known so far. Only two ternary alkaline-earth magnesium nitrides, namely  $\text{CaMg}_2\text{N}_2$  and  $\text{SrMg}_2\text{N}_2$  have been reported in literature.<sup>[7,8]</sup> In the compound class of nitridoaluminates, ternary compounds  $\text{AE}_3\text{Al}_2\text{N}_4$  ( $\text{AE} = \text{Ca}, \text{Sr}, \text{Ba}$ ) and  $\text{Ca}_3\text{AlN}_3$  are known.<sup>[9-11]</sup> Ternary nitridogallates occur more frequently and have been studied recently.<sup>[12-14]</sup> However, only few higher nitrides with elemental combination  $\text{Mg/Ga}$  or  $\text{Mg/Ge}$  are known.<sup>[15,16]</sup> Higher nitrides of  $\text{Al}$  containing  $\text{Mg}$  are not known so far. All of these nitridometalate compounds are built up of tetrahedral building units  $\text{MN}_4$  (with  $M = \text{Mg}, \text{Al}, \text{Ga}$ ). Since ionic radii of fourfold coordinated  $\text{Ga}^{3+}$  and  $\text{Mg}^{2+}$  (0.47 and 0.57 Å, respectively)<sup>[17]</sup> are comparable, mixed occupation of these elements on tetrahedral sites is possible and thus miscellaneously occupied  $(\text{Mg/Ga})\text{N}_4$ -tetrahedra occur in  $\text{Sr}[\text{Mg}_2\text{Ga}_2\text{N}_4]$  and  $\text{Ca}_2[\text{Ga}_3\text{MgN}_5]$ .<sup>[15,16]</sup> Those tetrahedral units can be connected via common vertices and/or edges building 0D-, 1D-, 2D- or 3D-anionic substructures.<sup>[11,13,16]</sup>

Recently, the isostructural compounds  $\text{Sr}[\text{Mg}_2\text{Ga}_2\text{N}_4]$  and  $\text{Sr}[\text{Mg}_3\text{GeN}_4]$  have been described by *DiSalvo* crystallizing in the  $\text{UCr}_4\text{C}_4$ -structure type with space group  $I4/m$  (no. 87).<sup>[16]</sup> Therein, only one alkaline-earth metal site was reported, coordinated by eight N-atoms in a cube-like subunit. Additionally, a single tetrahedral site, miscellaneously occupied by  $\text{Mg/Ga}$  or  $\text{Mg/Ge}$  has been found.<sup>[16]</sup>

In this contribution novel nitrido-magnesiocaluminates  $\text{Ca}[\text{Mg}_2\text{Al}_2\text{N}_4]$ ,  $\text{Sr}[\text{Mg}_2\text{Al}_2\text{N}_4]$  and  $\text{Eu}[\text{Mg}_2\text{Al}_2\text{N}_4]$  are presented as well as a novel nitrido-magnesiogallate  $\text{Ba}[\text{Mg}_2\text{Ga}_2\text{N}_4]$  and solid solutions  $\text{AE}[\text{Mg}_2\text{Al}_{2-x}\text{Ga}_x\text{N}_4]$  ( $x = 0-2$ ,  $\text{AE} = \text{Ca}, \text{Sr}, \text{Ba}$ ). All quaternary compounds and the solid solutions are isotypic, crystallizing in  $\text{UCr}_4\text{C}_4$ -structure type and the solid solutions are substitutional variants on one or two crystallographic sites. Detailed structure investigations of the pure phases as well as of solid solutions are

performed. These compounds are nicely illustrating the structural variability of the  $\text{UCr}_4\text{C}_4$ -structure type and structural relationships between multinary nitridoaluminates and nitridogallates.

## 7.2. Experimental Section

For synthesis of  $M[\text{Mg}_2\text{Al}_{2-x}\text{Ga}_x\text{N}_4]$  ( $x = 0-2$ ,  $M = \text{Ca}, \text{Sr}, \text{Ba}, \text{Eu}$ ) different approaches have been employed. All manipulations were carried out under Ar-atmosphere in a glove box (Unilab, MBraun, Garching;  $\text{O}_2 < 1$  ppm,  $\text{H}_2\text{O} < 1$  ppm).

*Metal route.* In this synthetic approach mixtures of the respective metals and  $\text{NaN}_3$  as nitrogen source are used in a sodium melt. This route was used for synthesis of  $\text{Ba}[\text{Mg}_2\text{Ga}_2\text{N}_4]$  and the solid solution of  $\text{Sr}_{1-x}\text{Ba}_x[\text{Mg}_2\text{Ga}_2\text{N}_4]$ . Typically, 0.31 mmol  $\text{NaN}_3$  (20.1 mg, Acros, 99 %), 0.064 mmol Mg (1.53 mg, Alfa Aesar, 99.9 %), 0.245 mmol Ga (17.1 mg, Sigma Aldrich, 99.99 %) and 1.95 mmol Na-melt (44.9 mg, Sigma Aldrich, 99.95 %) were used. Furthermore, 0.063 mmol alkaline-earth metal (Ba: Sigma Aldrich, 99.99 %; Sr: Smart Elements, 99.99 %) or the respective molar amount was added. The starting materials were filled into Ta- or Nb-ampoules (30 mm length, 10 mm diameter, 0.5 mm wall thickness). The ampoules were weld shut by arc melting under Ar atmosphere and placed in quartz tubings under vacuum to prevent oxidation of the ampoules. The respective reaction mixtures were heated in a tube furnace with  $50^\circ/\text{h}$  to  $760^\circ\text{C}$ , maintained at that temperature for 48 h and then cooled down to  $200^\circ\text{C}$  with a rate of  $3.4^\circ/\text{h}$ . After reaction, the ampoules were opened in a glove box and Na was separated from the reaction products by sublimation at  $320^\circ\text{C}$  under vacuum for 10 h.

*Fluoride route.* For a faster reaction compared to the metal route, the following synthesis technique was used. Herein, the metal fluorides together with  $\text{Mg}_3\text{N}_2$  were used. To capture the  $\text{F}^-$ -ions, syntheses took place in a Li-melt with  $\text{LiN}_3$  as nitrogen-source. Synthesis of  $\text{Ca}_{1-x}\text{Sr}_x[\text{Mg}_2\text{Al}_2\text{N}_4]$ ,  $\text{Sr}_{1-x}\text{Ba}_x[\text{Mg}_2\text{Al}_2\text{N}_4]$ ,  $\text{Sr}[\text{Mg}_2\text{Al}_{1.95}\text{Ga}_{0.05}\text{N}_4]$ ,  $\text{Sr}_{1-x}\text{Ba}_x[\text{Mg}_2\text{Al}_{1.95}\text{Ga}_{0.05}\text{N}_4]$  and  $\text{Ba}[\text{Mg}_2\text{Al}_{1.9}\text{Ga}_{0.1}\text{N}_4]$  was possible with this route. The molar ratio of starting materials was  $\text{AEF}_2$  ( $\text{AE} = \text{Ca}, \text{Sr}, \text{Ba}$ ;  $\text{CaF}_2$ : Sigma Aldrich, 99.99 %,  $\text{SrF}_2$ : Sigma Aldrich, 99.99 %,  $\text{BaF}_2$ : Sigma Aldrich, 99.99 %) :  $\text{TF}_3$  ( $T = \text{Al}, \text{Ga}$ ;  $\text{AlF}_3$ : ABCR, 99.5 %,  $\text{GaF}_3$ : Sigma Aldrich, 99.99 %) = 0.3 : 0.6 mmol. Moreover, 0.21 mmol  $\text{Mg}_3\text{N}_2$  (21.0 mg, Sigma Aldrich, 99.5 %), 0.30 mmol  $\text{LiN}_3$  (14.7 mg,

synthesized according to *Fair et al.*)<sup>[18]</sup> and 3.0 mmol Li (20.8 mg, Sigma Aldrich, 99.9 %) were added. The respective mixture of starting materials was filled into Ta-ampoules and sealed by arc-melting under argon. The ampoules were placed in quartz tubes and heated in tube furnaces to 900 °C with 200 °/h, maintained at that temperature for 24 h and subsequently cooled down to 500 °C with a rate of 10 °/h. After reaction, the furnace was turned off and the Ta-ampoules were opened in a glove box.

*Synthesis of Ca[Mg<sub>2</sub>Al<sub>2</sub>N<sub>4</sub>].* For synthesis of Ca[Mg<sub>2</sub>Al<sub>2</sub>N<sub>4</sub>] the fluoride route was slightly modified since 0.30 mmol NH<sub>4</sub>N<sub>3</sub> (18.0 mg, synthesized according to *Fearson*)<sup>[19]</sup> were used as nitrogen source instead of LiN<sub>3</sub>. The further procedure was as described above.

*Synthesis of Eu[Mg<sub>2</sub>Al<sub>2</sub>N<sub>4</sub>].* For synthesis of Eu[Mg<sub>2</sub>Al<sub>2</sub>N<sub>4</sub>] 0.30 mmol Eu (45.6 mg, Smart Elements, 99.99 %), 0.6 mmol AlF<sub>3</sub> (50.4 mg, ABCR, 99.5 %), 0.20 mmol Mg<sub>3</sub>N<sub>2</sub> (20.0 mg, Sigma Aldrich, 99.5 %) and 0.30 mmol NH<sub>4</sub>N<sub>3</sub> (18.0 mg, synthesized according to *Fair et al.*)<sup>[18]</sup> were mixed with 3.00 mmol Li-melt (20.8 mg, Sigma Aldrich, 99.9 %). The reaction mixture was filled into Ta-ampoules that were sealed under Ar-atmosphere by arc melting. Placed in a quartz tubing, the Ta-ampoule was heated to 900 °C in 200 °/h, held at this temperature for 12 h and cooled down to 500 °C in 10 °/h. Subsequently, the furnace was turned off and Ta-ampoules were opened in a glove box.

Scanning electron microscopy was performed on a JEOL JSM 6500 F equipped with a field emission gun at a maximum acceleration voltage of 30 kV. Synthesized samples were prepared on adhesive conductive carbon pads and coated with a likewise conductive carbon film. The chemical compositions were confirmed by EDX spectra (Detector: Oxford instruments), each recorded on an area limited to one crystal face to avoid influence of possible contaminating phases.

Single-crystal X-ray data of small single crystals were collected on a Nonius Kappa-CCD diffractometer with graded multilayer X-ray optics and Mo-K<sub>α</sub> radiation ( $\lambda = 0.71073 \text{ \AA}$ ). X-ray diffraction data of bigger single crystals were collected on a STOE IPDS I diffractometer using monochromated Mo-K<sub>α</sub> radiation ( $\lambda = 0.71073 \text{ \AA}$ ). Absorption correction was done using WinGX or X-RED.<sup>[20,21]</sup>

The structures were solved by direct methods implemented in SHELXS-97.<sup>[22,23]</sup> Refinement of crystal structures was carried out with anisotropic displacement parameters for all atoms by full-matrix least-squares calculation on  $F^2$  in SHELXL-97.<sup>[23,24]</sup> Further details of the structure investigations are available from the Fachinformationszentrum Karlsruhe, D-76344 Eggenstein Leopoldshafen, Germany (fax: +49-7247-808-666; email: crysdata@fiz.karlsruhe.de) on quoting the depository numbers CSD-425319 (Ca[Mg<sub>2</sub>Al<sub>2</sub>N<sub>4</sub>]), CSD-425321 (Sr[Mg<sub>2</sub>Al<sub>2</sub>N<sub>4</sub>]), CSD-425320 (Eu[Mg<sub>2</sub>Al<sub>2</sub>N<sub>4</sub>]), and CSD-425318 (Ba[Mg<sub>2</sub>Ga<sub>2</sub>N<sub>4</sub>]).

### 7.3. Results and Discussion

With the synthesis methods described above a series of new compounds was obtained, namely Ca[Mg<sub>2</sub>Al<sub>2</sub>N<sub>4</sub>], Sr[Mg<sub>2</sub>Al<sub>2</sub>N<sub>4</sub>], Eu[Mg<sub>2</sub>Al<sub>2</sub>N<sub>4</sub>], Ba[Mg<sub>2</sub>Ga<sub>2</sub>N<sub>4</sub>], Sr<sub>x</sub>Ba<sub>1-x</sub>[Mg<sub>2</sub>Al<sub>2</sub>N<sub>4</sub>], Ca<sub>x</sub>Sr<sub>1-x</sub>[Mg<sub>2</sub>Al<sub>2</sub>N<sub>4</sub>], Sr<sub>1-x</sub>Ba<sub>x</sub>[Mg<sub>2</sub>Al<sub>1.95</sub>Ga<sub>0.05</sub>N<sub>4</sub>], and Ba[Mg<sub>2</sub>Al<sub>1.9</sub>Ga<sub>0.1</sub>N<sub>4</sub>]. The presented nitrido-magnesioaluminates are to the best of our knowledge the first reported. Since all compounds are isotypic, only Eu[Mg<sub>2</sub>Al<sub>2</sub>N<sub>4</sub>] will be described in the following section for reasons of clarity. Further crystallographic information on remaining compounds are available in the supplementary part.

#### **Crystal Structure Description**

*Nitrido-magnesioaluminates and nitrido-magnesiogallates.* Eu[Mg<sub>2</sub>Al<sub>2</sub>N<sub>4</sub>] was solved and refined in the tetragonal space group *I4/m* (no. 87) with  $a = 8.1539(12)$ ,  $c = 3.3430(7)$  Å. The crystallographic data of Eu[Mg<sub>2</sub>Al<sub>2</sub>N<sub>4</sub>] are listed in Table 1, the atomic coordinates and displacement parameters are given in Table 2. Eu[Mg<sub>2</sub>Al<sub>2</sub>N<sub>4</sub>] crystallizes in the UCr<sub>4</sub>C<sub>4</sub>-structure type<sup>[25]</sup> forming a three-dimensional network of (Mg/Al)N<sub>4</sub>-tetrahedra (Figure 1). The framework contains strands of edge-sharing tetrahedra which are connected to each other, forming *vierer* rings along [001] (Figure 2). The Eu<sup>2+</sup>-site is located in every second *vierer*-ring strand, centered in face-sharing cuboid like polyhedra (Figures 1 and 2) with a bond-length Eu-N of 2.832(2) Å. Compared to the sum of the ionic radii a slight deviation is observed.<sup>[17]</sup> An elongation of this bond is also observed in all other compounds we report here as well as in Sr[Mg<sub>2</sub>Ga<sub>2</sub>N<sub>4</sub>] which crystallizes in the UCr<sub>4</sub>C<sub>4</sub>-structure type as well.<sup>[16]</sup>



**Table 1.** Crystallographic data of Eu[Mg<sub>2</sub>Al<sub>2</sub>N<sub>4</sub>].

Formula	Eu[Mg <sub>2</sub> Al <sub>2</sub> N <sub>4</sub> ]
Crystal system	tetragonal
Space group	<i>I</i> 4/ <i>m</i> (no. 87)
Lattice parameters /Å	<i>a</i> = <i>b</i> = 8.1539(12) <i>c</i> = 3.3430(7)
Cell volume /Å <sup>3</sup>	222.26(7)
Formula units /cell	2
$\rho_{\text{calcd.}} / \text{g} \cdot \text{cm}^{-3}$	4.64
$\mu / \text{mm}^{-1}$	14.637
T /K	293(2)
F(000)	282
Diffractometer	STOE IPDS I
Radiation,	Mo-K $\alpha$
	( $\lambda$ = 0.71073 Å),
monochromator	graphite
Absorption correction	multi scan
Max. / min. transmission	0.3894 / 0.3644
$\theta$ range /°	3.1 - 40.3
Index ranges	$-11 \leq h \leq 11$ $-11 \leq k \leq 11$ $-4 \leq l \leq 4$
Independent reflections	179 ( $R_{\text{int}}$ = 0.0415)
Refined parameters	16
Goodness of fit	1.105
$R_1$ (all data)	0.0152
$R_1$ ( $F^2 > 2\sigma(F^2)$ )	0.0152
$wR_2$ (all data)	0.0333
$wR_2$ ( $F^2 > 2\sigma(F^2)$ )	0.0333
Max. / min. residual electron density /e·Å <sup>-3</sup>	2.06 / -0.94

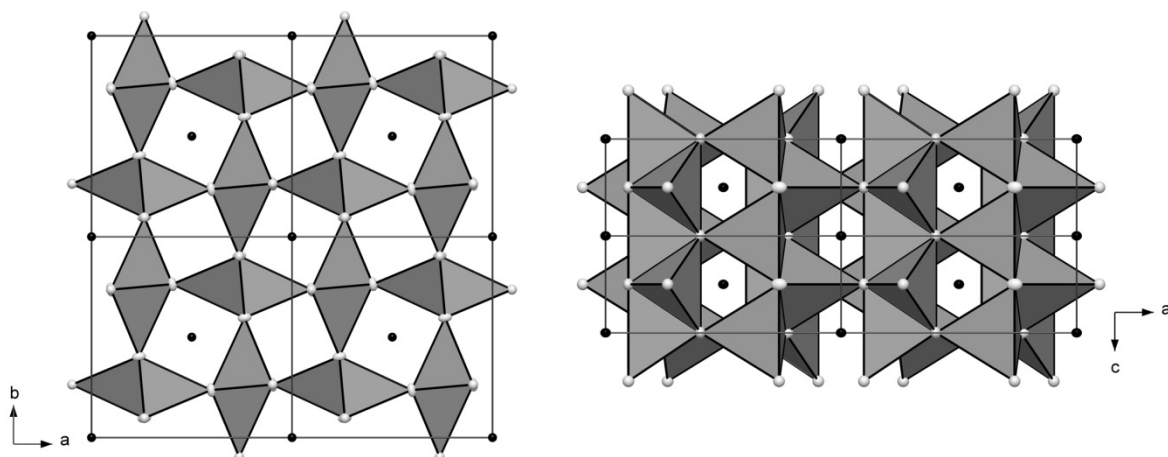


**Figure 1.** Figure 1: Crystal structure of  $\text{Eu}[\text{Mg}_2\text{Al}_2\text{N}_4]$ .  $(\text{Mg}/\text{Al})\text{N}_4$ -tetrahedra gray, nitrogen atoms bright gray and  $\text{Eu}^{2+}$ -ions black. Left: viewing direction along  $[001]$ , right: viewing direction along  $[010]$ .

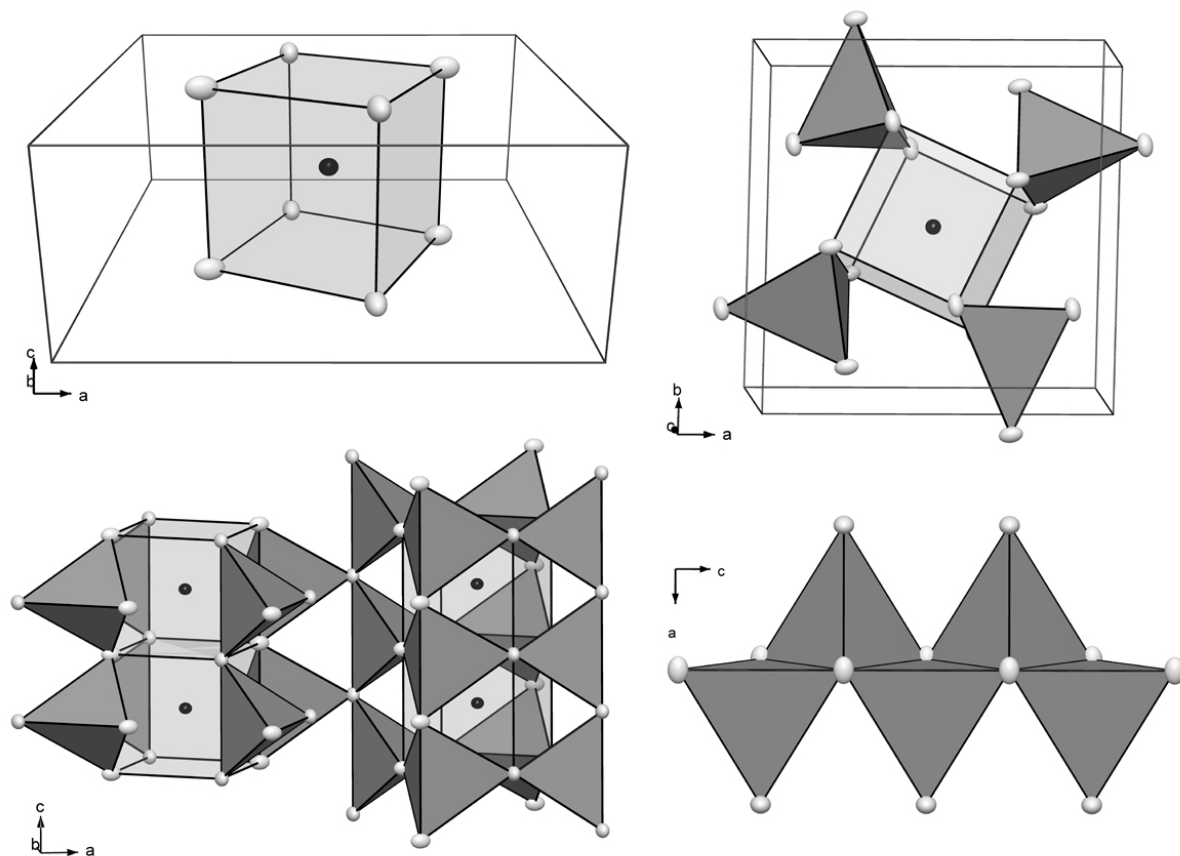


**Figure 2.** Structural details of  $\text{Eu}[\text{Mg}_2\text{Al}_2\text{N}_4]$ , all atoms are shown as ellipsoids with 50 % probability. Top left: cuboid-like coordination of  $\text{Eu}^{2+}$  (black) by eight nitrogen atoms (gray); top right: coordination of the  $\text{Eu}^{2+}$  centered polyhedra by  $(\text{Mg}/\text{Al})\text{N}_4$ -tetrahedra; bottom left: structure assembly and conjunction of  $(\text{Mg}/\text{Al})\text{N}_4$ -tetrahedra; bottom right: edge sharing of  $(\text{Mg}/\text{Al})\text{N}_4$ -tetrahedra strands.

$(\text{Mg}^{2+}/\text{Al}^{3+})$ -atoms on the tetrahedrally coordinated site are statistically disordered. Since those atoms on tetrahedral position  $(\text{Mg}^{2+}/\text{Al}^{3+})$  exhibit the same electron density in X-ray diffraction data the atomic ratio  $\text{Mg} : \text{Al}$  was additionally confirmed by EDX-analysis. The bond length of  $(\text{Mg}/\text{Al})\text{-N}$  varies between 1.95 and 2.06 Å.

Comparable values for Al-N and Mg-N distances appear in the structures  $\text{Sr}_3\text{Al}_2\text{N}_4$  (Al-N: 1.86 - 1.96 Å) and  $\text{CaMg}_2\text{N}_2$  (Mg-N: 2.13 - 2.30 Å),<sup>[8,9]</sup> while the reported bond length of (Mg/Al)-N in  $\text{Eu}[\text{Mg}_2\text{Al}_2\text{N}_4]$  correspond with the average of these distances.

**Table 2.** Atomic coordinates and isotropic displacement parameters / Å<sup>2</sup> of  $\text{Eu}[\text{Mg}_2\text{Al}_2\text{N}_4]$ , standard deviations in parentheses.

Atom	x	y	z	$U_{\text{iso}}^*/U_{\text{eq}}$
Eu	0	0	0	0.01207(18)
Al	0.18343(14)	0.36371(13)	0	0.0105(2)
Mg	0.18343(14)	0.36371(13)	0	0.0153(2)
N	0.2365(5)	0.5973(4)	0	0.0207(6)

For the reported gallium containing compounds similar results were obtained. Although  $\text{Ga}^{3+}$  and  $\text{Mg}^{2+}$  exhibit different electron density in X-ray diffraction data no ordering of the atoms on tetrahedral position was observed and the elemental distribution was confirmed by EDX-analysis as well.

Rietveld refinement of powder-diffraction data validates the structure of  $\text{Eu}[\text{Mg}_2\text{Al}_2\text{N}_4]$  obtained from single-crystal diffraction data (see Table 3 and Figure 3). Besides the  $\text{Eu}[\text{Mg}_2\text{Al}_2\text{N}_4]$  structure, also some amount of LiF can be found as byproduct. This stems from reaction in Li-flux, using the fluoride route where the formation of LiF is the driving force of the reaction. This result has been confirmed by EDX-analysis where also fluorine was detected but could be identified as contaminations and thus was not incorporated into the single crystals.

A comparison of all synthesized quaternary compounds and their crystal structure parameters is summarized in Table 4. The lattice parameters  $a$  and  $c$  shift as expected to larger values with increasing cation size. Surprisingly, a difference between  $\text{Sr}[\text{Mg}_2\text{Al}_2\text{N}_4]$  and  $\text{Eu}[\text{Mg}_2\text{Al}_2\text{N}_4]$  in lattice parameters and volume can be observed although ionic radii of eightfold coordinated  $\text{Sr}^{2+}$  (1.26 Å) and  $\text{Eu}^{2+}$  (1.25 Å) are nearly equal.<sup>[17]</sup> The relative difference of ionic radii between the alkaline-earth ions  $\text{Ca}^{2+}$  and  $\text{Sr}^{2+}$  is smaller than the relative difference between  $\text{Al}^{3+}$  and  $\text{Ga}^{3+}$  and therefore, the volume change from nitrido-magnesioaluminate to nitrido-magnesiogallate is larger (5.5 % increase from  $\text{Sr}[\text{Mg}_2\text{Al}_2\text{N}_4]$  to  $\text{Sr}[\text{Mg}_2\text{Ga}_2\text{N}_4]$ ) than

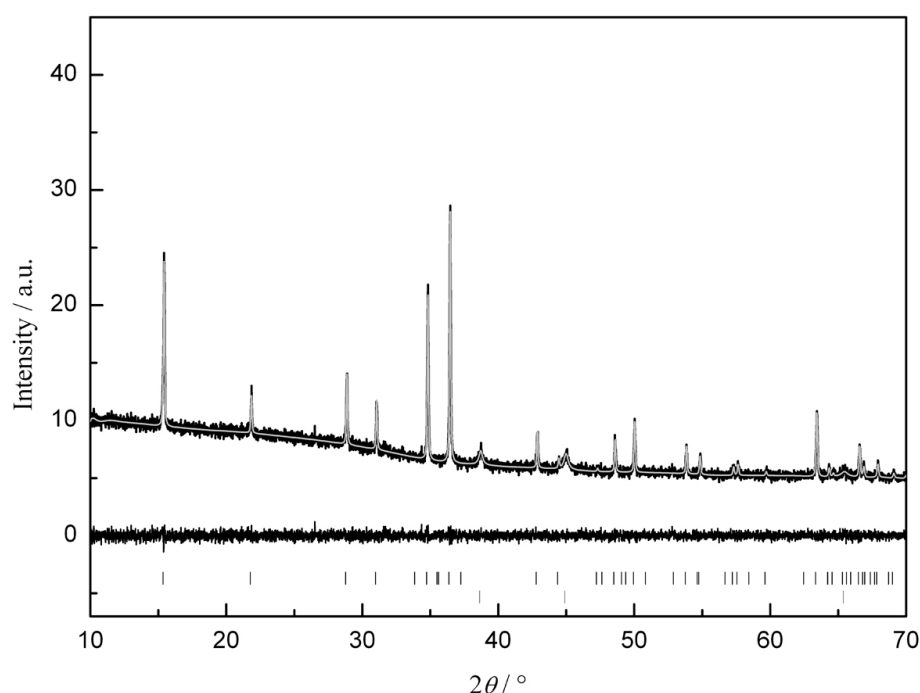
**Table 3.** Crystallographic data of Rietveld refinement of Eu[Mg<sub>2</sub>Al<sub>2</sub>N<sub>4</sub>].

Formula	Eu[Mg <sub>2</sub> Al <sub>2</sub> N <sub>4</sub> ]
Crystal system	tetragonal
Space group	<i>I4/m</i> (no. 87)
Lattice parameters (Å)	<i>a</i> = <i>b</i> = 8.16004(13), <i>c</i> = 3.35036(7)
Cell volume (Å <sup>3</sup> )	223.088(8)
Formula units per unit cell	2
Density (g · cm <sup>-3</sup> )	4.623
T (K)	293(2)
Diffractometer	STOE STADI P
Radiation (Å)	Cu-K <sub>α1</sub> ( <i>λ</i> = 1.54056)
Profile range	5.0 ≤ <i>θ</i> ≤ 35.0
Data points	6000
Total number of reflections	33
Refined parameters	57
Background function	Shifted Chebyshev (36 parameters)
<i>R</i> values	<i>R</i> <sub>P</sub> = 0.0273, <i>wR</i> <sub>P</sub> = 0.0345, <i>R</i> ( <i>F</i> <sup>2</sup> ) = 0.0374

the change of volume in nitrido-magnesiometalates, depending on alkaline-earth ion (2.1 % increase from Ca[Mg<sub>2</sub>Al<sub>2</sub>N<sub>4</sub>] to Sr[Mg<sub>2</sub>Al<sub>2</sub>N<sub>4</sub>]). Accordingly, the influence of different atom types positioned on the tetrahedral position on lattice parameters is larger than the influence of the metal atom in the channels of the *vierer* rings.

**Table 4.** Comparison of crystallographic data of quaternary nitrido-magnesioaluminates and nitrido-magnesiogallates.

Formula	Lattice Parameters / Å		Volume / Å <sup>3</sup>
	<i>a</i>	<i>c</i>	
Ca[Mg <sub>2</sub> Al <sub>2</sub> N <sub>4</sub> ]	8.0655(11)	3.2857(7)	213.74(7)
Sr[Mg <sub>2</sub> Al <sub>2</sub> N <sub>4</sub> ]	8.1008(11)	3.3269(7)	218.32(8)
Eu[Mg <sub>2</sub> Al <sub>2</sub> N <sub>4</sub> ]	8.1529(12)	3.3430(7)	222.26(8)
Sr[Mg <sub>2</sub> Ga <sub>2</sub> N <sub>4</sub> ] <sup>[17]</sup>	8.2925(7)	3.3585(5)	230.95(4)
Ba[Mg <sub>2</sub> Ga <sub>2</sub> N <sub>4</sub> ]	8.3654(12)	3.4411(7)	240.81(7)

**Figure 3.** Observed (black) and calculated (bright gray) X-ray powder diffraction pattern as well as difference profile for the Rietveld refinement of Eu[Mg<sub>2</sub>Al<sub>2</sub>N<sub>4</sub>]. The first line of vertical bars indicate possible peak positions. The second line of vertical bars indicates the reflections of the byproduct LiF.

**Solid solutions.** Besides the described quaternary phases, some substitutions on the alkaline-earth site, on the tetrahedral site or on both sites were achieved. Mixture on alkaline-earth site was obtained by using Sr and Ba metal, SrF<sub>2</sub> and CaF<sub>2</sub>, or SrF<sub>2</sub> and BaF<sub>2</sub>, respectively, depending on the synthesis route. The tetrahedral site is already miscellaneously occupied by Mg and Al or Mg and Ga as mentioned above. However, a mixture on tetrahedral site with Mg, Al and Ga was achieved by using Mg<sub>3</sub>N<sub>2</sub> together with AlF<sub>3</sub> and GaF<sub>3</sub> in the starting material mixture. After reaction at 900 °C needle shaped crystals could be isolated from inhomogeneous product.

Single-crystal X-ray data always revealed crystal structures in the  $\text{UCr}_4\text{C}_4$ -type as described above. Addition of the larger alkaline-earth ion  $\text{Sr}^{2+}$  on the  $\text{Ca}^{2+}$ -site in  $\text{Ca}_{1-x}\text{Sr}_x[\text{Mg}_2\text{Al}_2\text{N}_4]$  or  $\text{Ba}^{2+}$  on the  $\text{Sr}^{2+}$ -site in  $\text{Sr}_{1-x}\text{Ba}_x[\text{Mg}_2\text{Al}_2\text{N}_4]$  leads to an increase of lattice parameters  $a$  and  $c$  as expected. Incorporation of  $\text{Ga}^{3+}$  on the tetrahedral site of  $\text{Sr}[\text{Mg}_2\text{Al}_2\text{N}_4]$  is quite difficult, only 5 % of Ga were incorporated, independently of the weighted amount of Ga. Surprisingly, we were able to obtain a phase with 10 % of Ga additional to Al and Mg on tetrahedral site with Ba as alkaline-earth ion ( $\text{Ba}[\text{Mg}_2\text{Al}_{1.9}\text{Ga}_{0.1}\text{N}_4]$ ) even though no Ba-phase of nitrido-magnesioaluminate is known so far. Therefore, the little amount of Ga incorporated on tetrahedral position changes the crystal lattice as already seen from comparison of crystallographic data of the quaternary phases. Presumably, the change in lattice parameters made it possible for Ba to be introduced on the alkaline-earth site. Regarding mixture of alkaline earth and tetrahedral site, experiments with the fluoride route and with Ga metal instead of  $\text{GaF}_3$  were carried out. As alkaline-earth fluorides, only  $\text{SrF}_2$  and  $\text{BaF}_2$  were used,  $\text{CaF}_2$  was not considered. The experiments were performed at 900 °C but EDX-results show that no incorporation of both alkaline-earth metals (Sr, Ba) and three elements on tetrahedral position (Mg, Al, Ga) in one crystal was possible. Investigation of powdered products gave some first hints that all atom types (Sr, Ba, Mg, Al, Ga) are part of the product but not as a single crystal phase. Mostly, in crystalline products no Ga or no Al was incorporated and solid solutions of nitrido-magnesioaluminates  $\text{Sr}_{1-x}\text{Ba}_x[\text{Mg}_2\text{Al}_2\text{N}_4]$  or nitrido-magnesiogallates  $\text{Sr}_{1-x}\text{Ba}_x[\text{Mg}_2\text{Ga}_2\text{N}_4]$ , respectively were obtained. This is not surprising since because this is a hexanary system. Therefore, inhomogeneous products were expected and also the crystals from one reaction can differ in their amount of the respective elements. These solid solutions show the possibility of three elements miscellaneously occupied on one single crystallographic site, and stable refinement of all three atoms on this position is possible. Nevertheless, controlled synthesis of these compounds is rather difficult but the reported ones nicely demonstrate the broad variability in the  $\text{UCr}_4\text{C}_4$ -structure type and the strong structural relationship between nitrido-magnesioaluminates and nitrido-magnesiogallates.

*MAPLE calculations.* To confirm the crystal structures, MAPLE calculations on quaternary compounds and on solid solutions were carried out. The electrostatic consistency of the crystal structures were proven by comparison of MAPLE values for each atom type was well as the MAPLE sum, compared with the sum of constituting

nitrides. Comparison with MAPLE data reported before shows good agreement of the calculated values. The results of MAPLE investigations are exemplarily listed for Ba[Mg<sub>2</sub>Ga<sub>2</sub>N<sub>4</sub>] and Sr[Mg<sub>2</sub>Al<sub>1.95</sub>Ga<sub>0.05</sub>N<sub>4</sub>] in Table 5.

**Table 5.** MAPLE values in [kJ/mol] for Ba[Mg<sub>2</sub>Ga<sub>2</sub>N<sub>4</sub>] and Sr[Mg<sub>2</sub>Al<sub>1.95</sub>Ga<sub>0.05</sub>N<sub>4</sub>].

Ba[Mg <sub>2</sub> Ga <sub>2</sub> N <sub>4</sub> ]	calculated MAPLE value	Δ	Sr[Mg <sub>2</sub> Al <sub>1.95</sub> Ga <sub>0.05</sub> N <sub>4</sub> ]	calculated MAPLE value	Δ
Ba	1614.36		Sr	1721.26	
Mg/Ga	3673.89		Mg/Al/Ga	3716.06	
N	4776.03		N	4886.93	
Ba[Mg <sub>2</sub> Ga <sub>2</sub> N <sub>4</sub> ]	35430.98		Sr[Mg <sub>2</sub> Al <sub>1.95</sub> Ga <sub>0.05</sub> N <sub>4</sub> ]	36151.30	
model:			model:		
BaMg <sub>2</sub> <sup>[27]</sup>			0.3 Sr <sub>3</sub> Al <sub>2</sub> N <sub>4</sub> <sup>[9]</sup>		
+ 2 Ba <sub>3</sub> Ga <sub>2</sub> N <sub>4</sub> <sup>[29]</sup>			+ 0.05 GaN <sup>[28]</sup>		
- 2 GaN <sup>[28]</sup>			+ 0.1 SrMg <sub>2</sub> N <sub>4</sub> <sup>[7]</sup>		
- 2 Ba <sub>3</sub> N <sup>[30]</sup>			+ 0.6 Mg <sub>3</sub> N <sub>2</sub> <sup>[7]</sup>		
	35250.06	0.5 %	+ 1.35 AlN <sup>[31]</sup>	36677.88	1.5 %

Typical partial MAPLE values [kJ/mol]: Sr<sup>2+</sup>:1500-2100; Ba<sup>2+</sup>:1500-2000; Mg<sup>2+</sup>: 2100 – 2400; Al<sup>3+</sup>:5500-6000; Ga<sup>3+</sup>:4500 - 6000; N<sup>3-</sup>:4300 – 6000.<sup>[32-34]</sup>

## 7.4. Conclusion

In this contribution we present the first nitrido-magnesiometalates, a novel nitrido-magnesiogallate and solid solutions as substitutional variants thereof. All presented compounds are isostructural, exemplarily discussed on Eu[Mg<sub>2</sub>Al<sub>2</sub>N<sub>4</sub>]. The number of compounds in UCr<sub>4</sub>C<sub>4</sub>-structure type is significantly increased and substitutional variants of nitrido-magnesiometalates and nitrido-magnesiogallates are demonstrated. This points out that with an expansion of the Li-flux method by introducing fluorides in the metallic melt a multitude of quaternary and higher compounds are accessible. Since formation of LiF is the driving force of the reaction, not only thermodynamic products can be obtained easily since reaction temperatures up to 900 °C are quite moderate for solid-state reactions. Furthermore, with this expansion of the Li-flux method reaction time can be decreased in comparison to reactions starting from metals. The synthesized products were investigated by single-crystal X-ray diffraction and EDX-analysis as well as Rietveld refinement of powdered samples. To prove electrostatic consistency of the products, MAPLE calculations were carried out and confirm also the triply mixed occupation on tetrahedral site in the crystal structure.

## 7.5. References

- [1] T. Murata, K. Itatani, F. Scott Howell, A. Kishioka, M. Kinoshita, *J. Am. Ceram. Soc.* **1993**, 76, 2909-2911.
- [2] R. Niewa, F. J. DiSalvo, *Chem. Mater.* **1998**, 10, 2733-2752.
- [3] G. A. Slack, R. A. Tanzilli, R. O. Pohl, J. W. Vandersande, *J. Phys. Chem. Solids* **1987**, 48, 641-647.
- [4] S. Nakamura, *Science* **1998**, 281, 956-961.
- [5] S. Nakamura, S. Pearton, G. Fasol, *The Blue Laser Diode*, Springer Verlag, Berlin, **2000**.
- [6] D. Ehrentraut, E. Meißner, M. Bockowski, *Technology of Gallium Nitride Crystal Growth*, Springer, Berlin, Heidelberg, **2010**, Vol. 133.
- [7] O. Reckeweg, F. J. DiSalvo, *Z. Anorg. Allg. Chem.* **2001**, 627, 371-377.
- [8] V. Schultz-Coulon, W. Schnick, *Z. Naturforsch.* **1995**, 50b, 619-622.
- [9] W. Blase, G. Cordier, M. Ludwig, R. Kniep, *Z. Naturforsch. B: J. Chem. Sci.* **1994**, 49, 501-505.
- [10] M. Ludwig, J. Jäger, R. Niewa, R. Kniep, *Inorg. Chem.* **2000**, 39, 5909-5911.
- [11] M. Ludwig, R. Niewa, R. Kniep, *Z. Naturforsch. B: J. Chem. Sci.* **1999**, 54, 461-465.
- [12] F. Hintze, F. Hummel, P. J. Schmidt, D. Wiechert, W. Schnick, *Chem. Mater.* **2012**, 24, 402-407.
- [13] S. J. Clarke, F. J. DiSalvo, *Inorg. Chem.* **1997**, 36, 1143-1148.
- [14] D. G. Park, Z. A. Gál, F. J. DiSalvo, *Inorg. Chem.* **2003**, 42, 1779-1785.
- [15] F. Hintze, W. Schnick, *Z. Anorg. Allg. Chem.* **2012**, 638, 2243-2247.
- [16] D. G. Park, Y. Dong, F. J. DiSalvo, *Solid State Sci.* **2008**, 10, 1846-1852.
- [17] R. D. Shannon, *Acta Crystallogr., Sect. A: Found. Crystallogr.* **1976**, 32, 751-767.
- [18] H. D. Fair, R. F. Walker, *Energetic Materials 1, Physics and Chemistry of the Inorganic Azides*, New York, London, **1997**.
- [19] W. J. Fieser, *Inorg. Syntheses* **1946**, 2, 136-138.
- [20] L. J. Farrugia, *J. Appl. Crystallogr.* **1999**, 32, 837-838.
- [21] X-RED 32, 1.03; STOE & Cie GmbH Darmstadt, **2002**.
- [22] SHELXS, G. M. Sheldrick Universität Göttingen, **1997**.



- [23] G. M. Sheldrick, *Acta Crystallogr. Sect. A: Found. Crystallogr.* **2008**, 64, 112-122.
- [24] SHELXL, G. M. Sheldrick Universität Göttingen, **1997**.
- [25] L. G. Akselrud, O. I. Bodak, E. P. Marusin, *Sov. Phys. Crystallogr. (Engl. Transl.)* **1989**, 34, 289-290.
- [26] E. Hellner, F. Laves, *Z. Kristallogr.* **1943**, 105, 134-143.
- [27] M. Roos, J. Wittrock, G. Meyer, S. Fritz, J. Strähle, *Z. Anorg. Allg. Chem.* **2000**, 626, 1179-1185.
- [28] H. Yamane, F. J. DiSalvo, *Acta Crystallogr. Sect. C: Cryst. Struct. Commun.* **1996**, 52, 760-761.
- [29] U. Steinbrenner, A. Simon, *Z. Anorg. Allg. Chem.* **1998**, 624, 228-232.
- [30] H. Schulz, K. H. Thiemann, *Solid State Commun.* **1977**, 23, 815-815.
- [31] M. Zeuner, S. Pagano, W. Schnick, *Angew. Chem.* **2011**, 123, 7898-7920; *Angew. Chem. Int. Ed.* **2011**, 50, 7754-7775.
- [32] H. A. Höpfe, *Doctoral Thesis*, Ludwig-Maximilians-Universität München **2003**.
- [33] K. Köllisch, *Doctoral Thesis*, Ludwig-Maximilians-Universität München **2001**.

## **8. Ammonothermal Synthesis and Crystal Structure of $\text{BaAl}_2(\text{NH}_2)_8 \cdot 2 \text{NH}_3$**

For synthesis of  $\text{BaAl}_2(\text{NH}_2)_8 \cdot 2 \text{NH}_3$  supercritical  $\text{NH}_3$  was used as nitrogen source. The ammonothermal reaction procedure was presented in the beginning. With this synthesis method, the binary amide  $\text{BaAl}_2(\text{NH}_2)_8 \cdot 2 \text{NH}_3$  could be obtained from reaction of an alloy of both metals in supercritical ammonia at 550 °C. Single crystals were isolated from an Al-substrate and are stable at temperatures lower than -35 °C. X-ray diffraction was carried out under continuous cooling with liquid nitrogen. The crystal structure could be solved and refined and is described in the following. Due to synthesis with supercritical ammonia  $\text{NH}_3$ -molecules are incorporated in channels of the crystal structure. Surprisingly, the crystal structure is completely different from isoelectronic  $\text{CaAl}(\text{NH}_2)_8$ , published before.

## Ammonothermal Synthesis and Crystal Structure of $\text{BaAl}_2(\text{NH}_2)_8 \cdot 2\text{NH}_3$

Philipp Pust, Sebastian Schmiechen, Frauke Hintze and Wolfgang Schnick

**published in:** *Z. Anorg. Allg. Chem.* **2013**, 639, (in press).

**Keywords:** Ammonothermal, Ternary Amide, High-Pressure Autoclave, Substrate, Aluminum

**Abstract:**  $\text{BaAl}_2(\text{NH}_2)_8 \cdot 2 \text{NH}_3$  was synthesized starting from an intermetallic phase with nominal composition  $\text{Al}_2\text{Ba}$  under ammonothermal conditions in a stainless-steel autoclave at 823 K and 245 MPa. Single crystals were grown on aluminum substrates and prepared under low-temperature conditions. The crystal structure ( $R\text{-}3c$  (no. 167),  $a = 15.7370(17)$ ,  $c = 28.804(6)$  Å,  $Z = 1$ , 1829 reflections, 65 parameters,  $wR_2 = 0.07$ ) was solved on the basis of single-crystal X-ray diffraction data.  $\text{BaAl}_2(\text{NH}_2)_8 \cdot 2 \text{NH}_3$  contains isolated  $\text{Al}(\text{NH}_2)_4$ -tetrahedra forming two different types of channels along [001].

### 8.1. Introduction

Synthesis of ternary or multinary nitride materials can be carried out with a broad range of synthetic approaches. Due to the high kinetic stability of nitrogen ( $\text{N}_2$ ) regular high-temperature routes starting from metals and nitrogen require typically rather high temperatures above  $1000^\circ\text{C}$ . Unfortunately, such reactions lead frequently to non phase-pure products.<sup>[1,2]</sup> We have recently reported on another approach for nitrides starting from binary amides and imides as precursor compounds to form nitridosilicates.<sup>[3,4]</sup> In such amides or imides the proximity of nitrogen and the corresponding metal ions on an atomic level facilitates a significant reduction of synthesis temperature. Employment of thermally less stable ternary amides could lead to further reduction of temperatures and may enable access to kinetically controlled nitridic products. This method could be of interest, especially in the nitridoaluminate system with respect to the thermodynamically very stable binary compound  $\text{AlN}$ .

*Rouxel et al.* were the first to report on ternary alkaline-earth aluminum amides.<sup>[5-7]</sup> The syntheses were performed in liquid ammonia in sealed glass tubes starting from an alkaline-earth electride solution and an excess of metallic aluminum. A stoichiometric formula  $\text{M}^{\text{II}}\text{Al}_2(\text{NH}_2)_8$  ( $\text{M}^{\text{II}} = \text{Sr}, \text{Ba}$ ) was derived from elemental analysis and IR-spectroscopy as well as thermal decomposition measurements have been performed. The compounds showed a rapid decomposition after being extracted from ammonia atmosphere and thus it was not possible to determine the crystal structure.<sup>[5-7]</sup>

Another method to access ternary aluminum amides has been demonstrated by *Peters et al.* employing ammonothermal conditions.<sup>[8]</sup> To increase the solubility of aluminum in supercritical  $\text{NH}_3$  ammonobasic mineralizers like  $\text{K}$  or  $\text{K}(\text{NH}_2)_2$  are useful. Formation of intermediate  $\text{KAl}(\text{NH}_2)_2$  and subsequent thermal decomposition induces the generation of  $\text{AlN}$ .

We adapted this technique to our needs and performed the ammonothermal synthesis of an alkaline-earth aluminum amide employing stainless-steel autoclaves. Crystal structure determination was achieved by low-temperature single-crystal preparation and measurement.

## 8.2. Results and Discussion

$\text{BaAl}_2(\text{NH}_2)_8 \cdot 2 \text{NH}_3$  was synthesized starting from an intermetallic phase with nominal composition  $\text{Al}_2\text{Ba}$  and dry ammonia in a stainless-steel autoclave at 823 K and 245 MPa under supercritical conditions. Colorless crystals, which exhibited a high sensitivity towards hydrolysis and thermal decomposition under ambient conditions, were grown on an aluminum substrate and isolated under low-temperature conditions (213 K).

The crystal structure of  $\text{BaAl}_2(\text{NH}_2)_8 \cdot 2 \text{NH}_3$  was solved from single-crystal diffraction data and refined in trigonal space group  $R\bar{3}c$  (no. 167) with  $a = 15.7370(17)$  and  $c = 28.804(6)$  Å. The crystallographic data of  $\text{BaAl}_2(\text{NH}_2)_8 \cdot 2 \text{NH}_3$  are summarized in Table 1, atomic coordinates and isotropic displacement parameters are listed in Table 2.

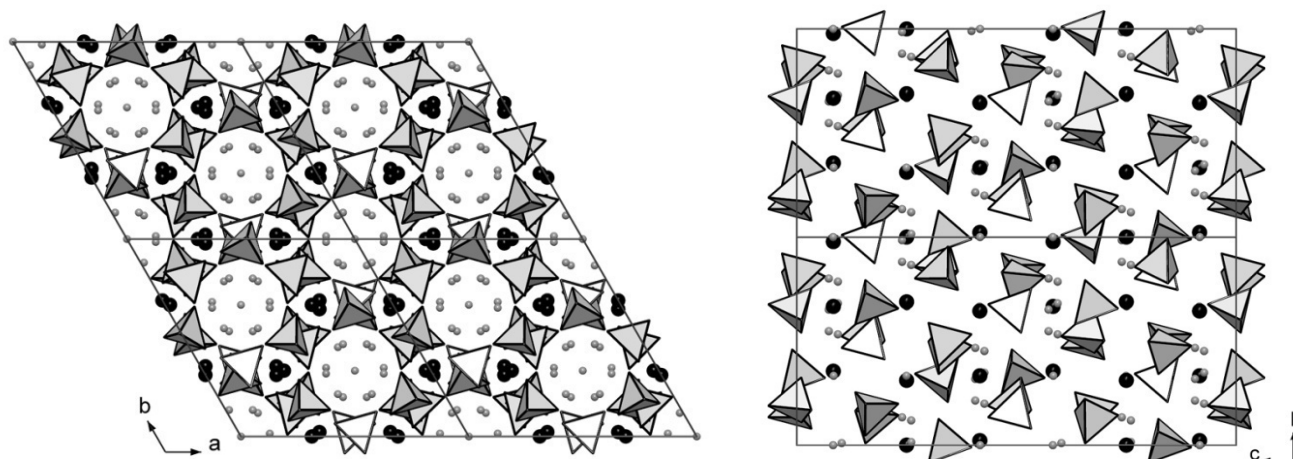


**Figure 1.** Crystal structure of  $\text{BaAl}_2(\text{NH}_2)_8 \cdot 2 \text{NH}_3$ .  $\text{Al}(\text{NH}_2)_4$ -tetrahedra gray,  $\text{Ba}^{2+}$  black, ammonia nitrogen atoms bright gray. Hydrogen atoms of the amide groups and of the ammonia molecules are not displayed. Top: Viewing direction along [001], bottom: Viewing direction along [100].

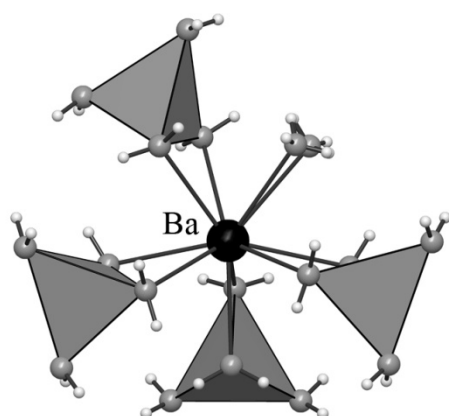


**Figure 2.** Coordination of  $\text{Ba}^{2+}$  in  $\text{BaAl}_2(\text{NH}_2)_8 \cdot 2 \text{NH}_3$ .  $\text{Al}(\text{NH}_2)_4$ -tetrahedra gray,  $\text{Ba}^{2+}$  black, N bright gray, H white.

**Table 1.** Crystallographic data of  $\text{BaAl}_2(\text{NH}_2)_8 \cdot 2 \text{NH}_3$ .

Formula	$\text{BaAl}_2(\text{NH}_2)_8 \cdot 2\text{NH}_3$
Crystal system	trigonal
Space group	$R\bar{3}c$ (no. 167)
Lattice parameters /Å	$a = b = 15.7370(17)$ $c = 28.804(6)$
Cell volume /Å <sup>3</sup>	6177.7(16)
Formula units /cell	1
$\rho_{\text{calcd.}} / \text{g} \cdot \text{cm}^{-3}$	1.673
$m / \text{mm}^{-1}$	3.004
T /K	200(2)
F(000)	3036
Diffractometer	Kappa CCD
Radiation, monochromator	Mo-K $\alpha$ ( $\lambda =$ 0.71073 Å), graphite
Absorption correction	multi-scan <sup>[12]</sup>
Max. / min. transmission	0.4322 / 0.2100
$\theta$ range /°	3.2 - 29.6
Index ranges	$-21 \leq h \leq 21$ $-21 \leq k \leq 21$ $-37 \leq l \leq 39$
Independent reflections	1829 ( $R_{\text{int}} = 0.0685$ )
Refined parameters	65
Goodness of fit	1.021
$R_1$ (all data); $R_1 (F^2 >$ $2\sigma(F^2))$	0.0280, 0.0246
$wR_2$ (all data); $wR_2 (F^2$ $> 2\sigma(F^2))$	0.0700, 0.0674
Max. / min. residual electron density /e·Å <sup>-3</sup>	0.84 / -1.51

The crystal structure of  $\text{BaAl}_2(\text{NH}_2)_8 \cdot 2 \text{NH}_3$  is built up of isolated  $\text{Al}(\text{NH}_2)_4$ -tetrahedra forming two different types of channels along [001] (see Figure 1).  $\text{Ba}^{2+}$ -ions are located in the smaller voids, whereas the bigger channels are occupied by ammonia molecules. Volume calculations with PLATON<sup>[9]</sup> delivered a pore volume of  $1242.5 \text{ \AA}^3$  in the larger tubes, leading to sufficient space to enclose two  $\text{NH}_3$  molecules per unit cell.

**Table 2.** Atomic coordinates and isotropic displacement parameters /  $\text{\AA}^2$  of  $\text{BaAl}_2(\text{NH}_2)_8 \cdot 2 \text{NH}_3$ , standard deviations in parentheses.

Atom	x	y	z	$U_{\text{eq}}$
Ba1	0.35543(1)	$\frac{1}{3}$	0.8333	0.02367(9)
Al1	0.35806(6)	0.15825(5)	0.00234(2)	0.02902(17)
N1	0.24822(18)	0.07955(19)	-0.03310(9)	0.0404(5)
N2	0.3991(2)	0.28800(17)	-0.01122(8)	0.0407(6)
N3	0.3232(2)	0.13391(17)	0.06434(7)	0.0377(5)
N4	0.45903(18)	0.13427(18)	-0.01033(8)	0.0368(5)
N5	0.5474(6)	0.3481(10)	0.0731(4)	0.070(3)
N6	0	0	-0.0832(4)	0.143(5)

The shortest distance between ammonia molecules and surrounding amide groups ( $2.885(13) \text{ \AA}$ ) is too large to form stabilizing hydrogen bonds, resulting in high mobility of the enclosed molecules and large isotropic displacement parameters. Therefore hydrogen atoms bound to ammonia nitrogen N6 were disregarded in the crystal structure refinement assuming severe rotational disorder in the  $\text{NH}_3$  molecules.

$\text{Al}(\text{NH}_2)_4$ -tetrahedra show interatomic distances (Al-N) of  $1.85 \text{ \AA}$ , which correspond with Al-N distances in nitridoaluminates like  $\text{LiCaAlN}_2$  (Al-N:  $1.92\text{--}1.96 \text{ \AA}$ )<sup>[10]</sup> or  $\text{Ba}_3\text{Al}_2\text{N}_4$  (Al-N:  $1.91\text{--}1.98 \text{ \AA}$ ).<sup>[2]</sup>

$\text{Ba}^{2+}$ -ions are aligned in the smaller tubes along [001] (see Figure 1). The  $\text{Ba}^{2+}$ -site is coordinated by eight amide groups and one ammonia molecule with Ba-N distances ranging from  $2.93$  to  $2.98 \text{ \AA}$  (see Figure 2). Comparable values can also be observed in  $\text{Ba}(\text{NH}_2)_2$  (Ba-N:  $2.79\text{--}3.17 \text{ \AA}$ ).<sup>[11]</sup>

### 8.3. Conclusions

In this contribution it was possible to elucidate the crystal structure of  $\text{BaAl}_2(\text{NH}_2)_8 \cdot 2 \text{NH}_3$  and to confirm the assumed stoichiometric formula given by *Rouxel et al.*<sup>[6]</sup> The structure shows tube like pores with a calculated volume of  $1242.5 \text{ \AA}^3$  leaving space for incorporation of two  $\text{NH}_3$  molecules per unit cell.  $\text{BaAl}_2(\text{NH}_2)_8 \cdot 2 \text{NH}_3$  may be a suitable precursor material for nitridoaluminate synthesis since constituting atoms are already arranged on an atomic level and a ternary compound in the system Ba-Al-N may be formed by thermal treatment and evolution of  $\text{NH}_3$ .

### 8.4. Experimental Section

**Synthesis:** All manipulations were performed with rigorous exclusion of oxygen and moisture in flame-dried Schlenk-type glassware on a Schlenk line interfaced to a vacuum ( $10^{-4}$  mbar) line or in an argon-filled glove box (Unilab, MBraun, Garching,  $\text{O}_2 < 1$  ppm,  $\text{H}_2\text{O} < 1$  ppm). Ammonia was purified using a cleaning cartridge (Micro Torr MC400-702FV, SAES Pure Gas Inc., San Luis Obispo, CA).

The synthesis of  $\text{BaAl}_2(\text{NH}_2)_8 \cdot 2 \text{NH}_3$  was performed in specially designed autoclaves made from Inconel stainless steel (no. 2.4668), sustaining a maximum pressure of 300 MPa and a maximum temperature of 873 K (development and design of the autoclaves was performed by the workgroup of *Prof. Dr.-Ing. E. Schlücker* and *Dr.-Ing. Dipl.-Wirt.-Ing. N. Alt* within the DFG-Forschergruppe FOR1600 “Chemie und Technologie der Ammonothermal-Synthese von Nitriden”). 191.3 mg (1.00 mmol) of an intermetallic phase with nominal composition  $\text{Al}_2\text{Ba}$ , synthesized from the elements at 1423 K, were placed into the autoclave together with aluminum substrates. Substrates were cut from an aluminum foil and surface-ground with a rasp. A volume of 44 mL ammonia was condensed onto the compounds at 200 K, reaching a filling degree of 45 Vol.-% inside the autoclave. The autoclave was positioned vertically in a tube furnace. The autoclave lid protruded from the furnace resulting in a measured temperature gradient of 100 K from bottom to top. Within 3 h temperature was raised to 823 K, maintained for 700 h, gaining a measured pressure of 245 MPa, and quenched down to room temperature by switching of the furnace.



**Single-crystal preparation:** For the crystal preparation, we adapted the technique described by *Stalke et al.*<sup>[13]</sup> to our needs. After reaction the ammonia within the autoclave was recondensed at 200 K, the aluminum substrate was extracted and directly put into perfluoroether (Galden), which was cooled by an ethanol/dry-ice freezing mixture and a stream of cooled nitrogen to 213 K. Colorless, block-shaped single crystals grown on the aluminum substrate were isolated under a microscope, collected on the tip of a glass fiber, immediately submerged in liquid nitrogen and transferred to the diffractometer.

**Single-crystal X-ray diffraction:** Single-crystal diffraction data were collected on a Nonius Kappa CCD diffractometer (Mo- $\text{K}_\alpha$  radiation, graphite monochromator) at 200 K. A spherical absorption correction using the program SADABS<sup>[12]</sup> was applied. The crystal structure was solved by using direct methods with SHELXS.<sup>[14]</sup> The refinement of the structure was carried out by the method of least-squares using SHELXL.<sup>[14]</sup> The atomic ratio Ba:Al was confirmed by energy-dispersive X-ray spectroscopy (EDX) using a JSM-6500F scanning microscope (Jeol) equipped with an EDX detector 7418 (Oxford Instruments). An atomic ratio Ba:Al = 1:1.9 was measured by EDX analysis and agrees with the composition of  $\text{BaAl}_2(\text{NH}_2)_8 \cdot 2 \text{NH}_3$ . As a result of the high sensitivity at ambient temperature of the compound the nitrogen ratio was not determinable.

Hydrogen positions of the  $\text{Al}(\text{NH}_2)_4$ -tetrahedra could be determined by difference Fourier syntheses and were refined isotropically using restraints for nitrogen-hydrogen distances, all other atoms were refined anisotropically.

Further details of the crystal structure investigations can be obtained from the Fachinformationszentrum Karlsruhe, 76344 Eggenstein-Leopoldshafen, Germany (Fax: +49-7247-808-666; E-Mail: [crysdata@fiz-karlsruhe.de](mailto:crysdata@fiz-karlsruhe.de)) on quoting the depository number CSD-425323.

## 8.5. References

- [1] M. Ludwig, J. Jaeger, R. Niewa, R. Kniep, *Inorg. Chem.* **2000**, 39, 5909.
- [2] M. Ludwig, R. Niewa, R. Kniep, *Z. Naturforsch. B: Chem. Sci.* **1999**, 54, 461.
- [3] M. Zeuner, F. Hintze, W. Schnick, *Chem. Mater.* **2009**, 21, 336.
- [4] M. Zeuner, S. Pagano, W. Schnick, *Angew. Chem.* **2011**, 123, 7898; *Angew. Chem. Int. Ed.* **2011**, 50, 7754.
- [5] P. Palvadeau, A.-M. Trélohan, J. Rouxel, *Compt. Rend.* **1969**, 269C, 126.
- [6] J. Rouxel, P. Palvadeau, *Compt. Rend.* **1971**, 272C, 63.
- [7] P. Palvadeau, M. Drew, G. Charlesworth, J. Rouxel, *C. R. Seances Acad. Sci. (Ser. C)* **1972**, 275.
- [8] D. Peters, *J. Cryst. Growth* **1990**, 104, 411.
- [9] A. L. Spek, PLATON - A Multipurpose Crystallographic Tool, v1.07, Utrecht University, Utrecht, Netherlands, **2003**.
- [10] P. Pust, S. Pagano, W. Schnick, *Eur. J. Inorg. Chem.* **2012**, DOI:10.1002/ejic.201201283.
- [11] H. Jacobs, C. Hadenfeldt, *Z. Anorg. Allg. Chem.* **1975**, 418, 132.
- [12] G. M. Sheldrick, SADABS, v2, Multi-Scan Absorption Correction, University of Göttingen, Germany, **2001**.
- [13] T. Kottke, D. Stalke, *J. Appl. Crystallogr.* **1993**, 26, 615.
- [14] G. M. Sheldrick, *Acta Crystallogr., Sect. A: Found. Crystallogr.* **2008**, 64, 112.

## 9. Discussion and Outlook

### 9.1. Nitrides

In this thesis a number of novel Ga containing compounds has been presented. All of them derive from the binary nitride GaN. This nitride has been synthesized in supercritical ammonia at elevated pressure and temperature. To realize these reaction conditions, the use of specially designed autoclaves was necessary. Those pressure vessels were developed by engineers from University of Erlangen and are able to stand pressures up to 3000 bar and temperatures of 600 °C. Starting from metallic Ga and a GaN feedstock, together with a mixture of ammonobasic and ammonoacidic mineralizers it was possible to obtain GaN in hexagonal modification.<sup>[1]</sup> During reaction, the pressure must be high enough on the one hand to make sure supercritical state is achieved. On the other hand, reaction pressure has to be within the pressure limits of the vessel. Therefore, an ammonia filling device was built where the autoclave can be evacuated and filled with a certain amount of ammonia and the filling degree can be monitored. Since the working of all technical equipment was demonstrated by synthesis of GaN powder, still some challenges for further syntheses of binary and higher nitrides are present. Even if the amount of ammonia at the beginning of the reaction is defined, the resulting pressure can only be estimated roughly. Ammonia is not only the solvent but also starting material in these reactions and acts as nitrogen source. Therefore, nitrogen is consumed and hydrogen develops during reaction. The resulting pressure, constituted of ammonia and hydrogen is mostly much higher than the expected pressure from filling degree. Careful monitoring of pressure during reaction is indispensable to make sure that the pressure limits are properly followed. Furthermore, corrosion of autoclave material must be taken into account. Especially in the ammonoacidic regime contaminations of products with Cr or Ni from autoclave material are known. Therefore, a suitable liner material is required. A material chemically and mechanically stable under the given reaction conditions is hard to find. The use of Pt liners is reported in literature,<sup>[2,3]</sup> but due to high costs of raw materials they are expensive. Nevertheless, this reaction method is very promising to find access to novel nitrogen based materials with interesting properties like high hardness or luminescence for example.

Further nitride materials were presented in chapter 3 with  $\text{Eu}^{2+}$ -doped  $\text{Mg}_3\text{N}_2$  and the double nitride  $\text{Mg}_3\text{GaN}_3$ . Syntheses were carried out in tantalum ampoules, starting from the elements using sodium azide as nitrogen source in a sodium flux. *Verdier* reported a compound with sum formula  $\text{Mg}_3\text{GaN}_3$  earlier in 1970<sup>[4]</sup> but crystal structure was unknown yet. With the synthesis in sodium flux single crystals of  $\text{Mg}_3\text{GaN}_3$  could be obtained and elucidation of crystal structure was carried out. The double nitride is comprised of mixed occupied  $(\text{Mg}/\text{Ga})\text{N}_4$  and  $\text{MgN}_4$  tetrahedra, building an uncharged three-dimensional network by vertex- and corner sharing. Doping of this compound with  $\text{Eu}^{2+}$  led to luminescence properties that were investigated in detail. The band emission showed maximum intensity at 578 nm and full width at half maximum of 132 nm. This is the first time, luminescence of a double nitride was reported. Furthermore, the well-known binary nitride  $\text{Mg}_3\text{N}_2$  showed comparable luminescence properties upon doping with  $\text{Eu}^{2+}$ . In both nitrides, the  $\text{Mg}^{2+}$  or the  $\text{Mg}^{2+}/\text{Ga}^{3+}$  sites respectively are too small to be occupied by  $\text{Eu}^{2+}$ . In the respective crystal structure, interstitial sites were found, surrounded by six nitrogen atoms in an octahedral arrangement. In these voids,  $\text{Eu}^{2+}$  could be located with reasonable Eu-N distances. Lately, different approaches were attempted to elucidate the distribution and concentration of activator ion in host lattices. To understand the origin and the quality of luminescence properties, detailed knowledge of local surrounding of activator ions is necessary. If this can be achieved, prediction of luminescence properties due to structural characteristics may be possible.

The double nitride was further investigated to determine the band gap of this compound. Therefore, soft X-ray absorption and emission spectroscopy was carried out and compared to DFT calculations. In very good agreement, both methods predict  $\text{Mg}_3\text{GaN}_3$  to be a semiconductor with a direct band gap of 3.0 eV. In comparison, GaN has a direct wide band gap of 3.5 eV.<sup>[5]</sup> Unfortunately, lattice mismatch between those two compounds is too large to make  $\text{Mg}_3\text{GaN}_3$  a suitable substrate material for GaN crystal growth. Furthermore, the rather broad emission band makes an application in phosphor converted LEDs unfavorable yet.

## 9.2. Nitridogallates

In contrast to previously mentioned nitrides most nitridogallates are comprised of  $\text{GaN}_4$  tetrahedra, building an anionic substructure, typically charge balanced by alkaline earth ions like  $\text{Ca}^{2+}$ ,  $\text{Sr}^{2+}$  or  $\text{Ba}^{2+}$ .

A novel ternary compound,  $\text{Ba}_3\text{Ga}_3\text{N}_5$  was presented in chapter 4. Herein, a hitherto unknown structural motif was found. Highly condensed tetrahedra are building strands running along [010]. This one-dimensional substructure is quite unexpected for such a high degree of condensation. This shows the broad structural variability of nitridogallates. Furthermore, a high degree of condensation stands in most cases for a stable network and therefore such compounds seem to be favorable for luminescence properties upon doping with  $\text{Eu}^{2+}$ . This was confirmed by doping of  $\text{Ba}_3\text{Ga}_3\text{N}_5$  and the observed emission at 638 nm after irradiation with UV to blue light. This was the first reported luminescent nitridogallate. Surprisingly, the isoelectronic Sr-compound  $\text{Sr}_3\text{Ga}_3\text{N}_5$ <sup>[6]</sup> exhibits a different crystal structure, containing a three-dimensional network of corner sharing  $\text{GaN}_4$ -tetrahedra. Since the degree of condensation is the same, similar properties can be expected. Synthesizing this compound doped with  $\text{Eu}^{2+}$  was possible, but no luminescence was observed. DFT calculations of both compounds revealed a band gap of 1.46 eV for  $\text{Ba}_3\text{Ga}_3\text{N}_5$  and 1.53 eV for  $\text{Sr}_3\text{Ga}_3\text{N}_5$ . The strong red shifted emission of  $\text{Ba}_3\text{Ga}_3\text{N}_5\text{:Eu}^{2+}$  illustrates the potential of nitridogallates as possible phosphor materials in phosphor converted LEDs and was the first reported luminescent nitridogallate.

But a high degree of condensation does not always lead to luminescence properties like the nitridogallate  $\text{Ca}_2\text{Ga}_3\text{MgN}_5$  demonstrates. In this compound, the tetrahedral building units contain Ga and Mg, both occupying one site. These tetrahedra are connected via vertices and edges building a three-dimensional network. In hexagonal channels  $\text{Ca}^{2+}$  atoms are located. The crystal structure can be related to  $\text{Sr}_2\text{Si}_5\text{N}_8$ ,<sup>[7]</sup> a red phosphor material used in phosphor converted LEDs when it is doped with  $\text{Eu}^{2+}$ .<sup>[8]</sup> Although, the degree of condensation is quite high in  $\text{Ca}_2\text{Ga}_3\text{MgN}_5$  (atomic ratio (Ga,Mg) : N = 4 : 5), even higher than in the nitridosilicate (5 : 8), no luminescence was observed. Mixed occupation of the tetrahedra center is already known from  $\text{Sr}(\text{Mg}_2\text{Ga}_2)\text{N}_4$ , published by *DiSalvo* et al.<sup>[9]</sup> This compound crystallizes in the  $\text{UCr}_4\text{C}_4$  structure type.<sup>[10]</sup> In the latter, only one tetrahedral site and a single further metal site is reported. The tetrahedral site in the nitridogallate is occupied by

Mg and Ga and the further metal site is occupied by the alkaline-earth metal. A number of compounds were found, crystallizing also in this structure type (see chapter 7), all of them with a mixed occupation, varying from mixed Mg/Ga (nitrido-magnesiogallates) to mixed Mg/Al (nitrido-magnesioaluminates). The variability of this structure type was shown, since additionally solid solutions were synthesized, mixing the alkaline-earth site, the tetrahedral site with Mg, Ga and Al or mixing both sites. Most of these compounds were obtained by using a Li-flux and  $\text{LiN}_3$  as nitrogen source. Furthermore, the respective fluorides and  $\text{Mg}_3\text{N}_2$  were used as starting materials. The driving force of these reactions is the formation of LiF. Therefore, not only thermodynamic products are accessible and temperatures can be moderate for solid-state reactions ( $900\text{ }^\circ\text{C}$ ) as well as reaction duration is decreased in comparison to syntheses starting from metals. On the other site, LiF is part of the product mixture and cannot easily be removed. When single crystals are desired the side phase can be sorted out but in powdered products LiF is always obtained as a byproduct. Nevertheless, Li must not be incorporated in the crystal structure of the target compound but with modification of fluxing agents, Li can be incorporated as demonstrated with  $\text{LiBa}_5\text{GaN}_3\text{F}_5$ . Here a mixed flux of Na and Li was used. Together with the fluoride from starting material  $\text{EuF}_3$  Li and F build edge-sharing octahedra in the crystal structure. In this compound, no  $\text{GaN}_4$  tetrahedra are found but trigonal planar  $\text{GaN}_3$  units. These units are not connected to each other, so regarded as a nitridogallate the crystal structure is zero-dimensional. Such trigonal planar  $\text{GaN}_3$  units were observed earlier in  $\text{Sr}_3\text{GaN}_3$  for example.<sup>[11]</sup> The single crystals of this Li-containing compound are deeply red. Therefore, the band gap was measured on single crystals and calculated by DFT methods. The measurement reveals a band gap of 1.9 eV, according to DFT calculations the band gap is 1.6 eV. This deviation arises since such calculations always underestimate the band gap and the measured value of 1.9 eV is reasonable and in accordance to the observed color of the crystals.

Most of the previously presented reactions started from metals or fluorides and were carried out in a metallic flux. The ammonothermal synthesis route offers a lot of potential for nitride materials and amides or imides could be synthesized and used as starting materials. For synthesis of nitridoaluminates,  $\text{BaAl}_2(\text{NH}_2)_8 \cdot 2\text{NH}_3$  seems to be a promising precursor. Synthesis was performed in previously presented autoclaves. Isolation of single crystals from the Al-substrate was rather difficult since the compound decomposes very rapidly and must be kept under low temperature

conditions. In the crystal structure,  $\text{Al}(\text{NH}_2)_4$  tetrahedra are observed, not connected to each other but stabilized by hydrogen bonds. Furthermore,  $\text{NH}_3$  molecules are found in pores of the crystal structure. Starting from this material, building of  $\text{AlN}_4$  tetrahedra and forming a nitridoaluminate seems to be reasonable. Unfortunately, the high sensitivity of the compound impeded further reactions with  $\text{BaAl}_2(\text{NH}_2)_8 \cdot 2\text{NH}_3$  yet. But the postulated sum formula from *Rouxel et al.*<sup>[12]</sup> was confirmed and the crystal structure could be elucidated. Further synthesis and research may bring access to suitable precursor materials for synthesis of nitridoaluminates or nitridogallates as well.

### 9.3. Outlook

In the previous paragraph, synthesis of a precursor material was discussed. For synthesis of nitridogallates different starting materials than metals are conceivable. For example digallides  $\text{SrGa}_2$  and  $\text{BaGa}_2$  can easily be synthesized from their constituting metals at 1000 or 900 °C, respectively.<sup>[13,14]</sup> To form a nitridogallate, nitridation of the alloy material is necessary. Therefore, Further reaction with azides (i.e.  $\text{Ba}(\text{N}_3)_2$ ) or in nitrogen or ammonia atmosphere at elevated temperatures is possible. First attempts in this direction were unsuccessful yet and further optimizations of reaction conditions have to be made for synthesis of nitridogallates starting from alloys. In the digallides, a preorganization of the alkaline-earth metal and Ga is achieved. Another precursor material could already include a nitrogen to metal bond like in alkaline earth-azides (i.e.  $\text{Sr}(\text{N}_3)_2$ ) or amides  $\text{Ba}(\text{NH}_2)_2$  for example. First investigations with  $\text{Ba}(\text{NH}_2)_2$  as starting material revealed  $\text{Ba}_3\text{Ga}_2\text{N}_4$ <sup>[15]</sup> in form of yellow single crystals. This compound is already known, but the published synthesis started from the metals. This demonstrates, that synthesis of nitridogallates is possible starting from nitrogen containing precursor materials like amides. Therefore, also novel compounds could be accessible by a modified starting material mixture.

All presented nitrogen-gallium compounds with luminescence properties nicely show the possibility of application in phosphor converted LEDs. All investigations of the band gap illustrate that the band gap is slightly too small for such an application. To increase the band gap, an additional element introduced to nitridogallates. Structurally related to nitridogallates are nitridosilicates. Since in this compound

class, also luminescence properties are observed and some representatives find already use in phosphor converted LEDs a combination of these two compound classes seems to be promising. Starting from an alloy material, for example  $\text{Ba}_8\text{Ga}_{10}\text{Si}_{36}$ <sup>[16]</sup> or  $\text{CaGaSi}$ <sup>[17]</sup> nitridation could be achieved with a nitrogen source like azides, heated up under nitrogen atmosphere at elevated temperatures or with supercritical ammonia in autoclaves. Additionally, “ $\text{Si}(\text{NH})_2$ ” or  $\text{Si}_3\text{N}_4$  could be used as starting materials and Si-source, well known from nitridosilicate syntheses.<sup>[8]</sup> Independently from starting material mixture, syntheses of nitridogallates seem to work only in a metallic melt like a Na-flux for example. All investigations without a flux revealed no crystalline products yet.

Many isoelectronic compounds are known in the field of nitridogallates like  $\text{Sr}_3\text{Ga}_3\text{N}_5$ <sup>[6]</sup> and  $\text{Ba}_3\text{Ga}_3\text{N}_5$  or  $\text{Sr}(\text{Mg}_2\text{Ga}_2)\text{N}_4$ <sup>[9]</sup> and  $\text{Ba}(\text{Mg}_2\text{Ga}_2)\text{N}_4$ , but they sometimes show considerable structural differences and exhibit different properties. Therefore, exchange of alkaline earth element in known nitridogallates could lead to novel compounds with different crystal structures and properties as well. Since  $\text{Ca}_2\text{Ga}_3\text{MgN}_5$  exhibits a highly condensed network but does not show luminescence properties, the respective Sr or Ba compound would be of interest. Using Sr or Ba metal instead of Ca was unsuccessful yet but revealed a novel compound  $\text{Sr}_2\text{GaMg}_3\text{N}_{4.33}$  with different structural features.<sup>[18]</sup>

In some reactions it was observed that additional metals in the starting material mixture improved crystallinity of the product but were not incorporated into the crystals. In the synthesis of  $\text{Ba}_3\text{Ga}_3\text{N}_5$  for example, additional Sr and Mg improved crystallinity as well as additional Ca is required for the successful synthesis of  $\text{Mg}_3\text{GaN}_3$ . Therefore, so far unsuccessful syntheses could be improved by adding further metals.

Synthesis in supercritical ammonia is also very promising to obtain novel, highly condensed nitridogallates. Furthermore, the larger reaction volume can lead to bigger product volumes than a few single crystals, obtained from reaction in tantalum ampoules. On the other hand, crystal growth of larger single crystals is possible in autoclaves as well. This synthesis method can not only be used for nitridogallates, but also synthesis of nitridoaluminates or other nitride based materials is possible.



In this thesis, a number of novel Ga-N compounds was presented and their respective properties were investigated in detail. Luminescence properties in nitridogallates were reported for the first time and therefore, a novel compound class is accessible for use in phosphor converted LEDs. Nevertheless, further research effort has to be made to adjust synthesis and reaction conditions to obtain products, applicable in that technology. Furthermore, nitridogallates or the double nitride  $\text{Mg}_3\text{GaN}_3$  are promising candidates as substrate materials for GaN crystal growth if lattice mismatch is suitable. The performed investigations on the band gap of several nitridogallates, gives a detailed insight into the physical background of this material class.

## 9.4. References

- [1] W. Paszkowicz, S. Podsiadlo, R. Minikayev, *J. Alloys Compd.* **2004**, 382, 100.
- [2] D. Ehrentraut, Y. Kagamitani, T. Fukuda, F. Orito, S. Kawabata, K. Katano, S. Tereda, *J. Cryst. Growth* **2008**, 310, 3902.
- [3] D. Ehrentraut, Y. Kagamitani, A. Yoshikawa, N. Hoshino, H. Itoh, S. Kawabata, K. Fujii, T. Yao, T. Fukuda, *J. Mater. Sci.* **2007**, 43, 2270.
- [4] P. Verdier, R. Marchand, J. C. Lang, *R. Acad. Sci. Ser. C.* **1970**, 271, 1002.
- [5] R. Niewa, F. J. DiSalvo, *Chem. Mater.* **1998**, 10, 2733.
- [6] S. J. Clarke, F. J. DiSalvo, *Inorg. Chem.* **1997**, 36, 1143.
- [7] T. Schlieper, W. Milius, W. Schnick, *Z. Anorg. Allg. Chem.* **1995**, 621, 1380.
- [8] M. Zeuner, S. Pagano, W. Schnick, *Angew. Chem.* **2011**, 123, 7898; *Angew. Chem. Int. Ed.* **2011**, 50, 7754.
- [9] D. G. Park, Y. Dong, F. J. DiSalvo, *Solid State Sci.* **2008**, 10, 1846.
- [10] L. G. Akselrud, O. I. Bodak, E. P. Marusin, *Sov. Phys. Crystallogr. (engl. Transl.)* **1989**, 34, 289.
- [11] D. G. Park, Z. A. Gál, F. J. DiSalvo, *Inorg. Chem.* **2003**, 42, 1779.
- [12] J. Rouxel, P. Palvadeau, *Compt. Rend.* **1971**, 272 C, 63.
- [13] W. Harms, M. Wendorff, C. Röhr, *Z. Naturforsch., B: J. Chem. Sci.* **2006**, 62, 117.
- [14] F. Haarmann, K. Koch, D. Grüner, W. Schnelle, O. Pecher, R. Cardoso-Gil, H. Borrmann, H. Rosner, Y. Grin, *Chem. Eur. J.* **2009**, 15, 1673.
- [15] H. Yamane, F. J. DiSalvo, *Acta Crystallogr., Sect. C: Cryst. Struct. Commun.* **1996**, 52, 760.
- [16] D. Nataraj, J. Nagano, *J. Solid State Chem.* **2004**, 177, 1905.
- [17] A. Czybulka, B. Pungner, H.-U. Schuster, *Z. Anorg. Allg. Chem.* **1989**, 579, 151.
- [18] C. Pösl, *Master Thesis*, Ludwig-Maximilians-Universität München, **2013**.

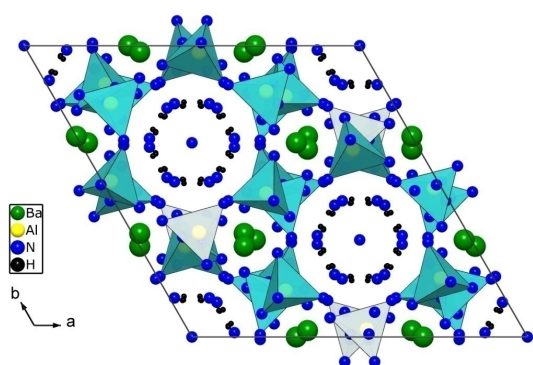
## 10. Summary

### 10.1. Ammonothermal reactions

#### Chapter 2, page 9 and chapter 8, page 105

The ammonothermal synthesis method was established. Therefore, novel autoclaves suitable for reaction conditions of supercritical ammonia up to 600 °C and 3000 bar were developed from engineers at university of Erlangen. For controlled filling of autoclaves with ammonia a filling device was built at which the filling degree can be determined and the resulting pressure can be estimated by additional knowledge of temperature. To proof the system, synthesis of GaN was carried out. In addition to Ga-metal, GaN powder was used as feedstock. A mixture of ammonobasic (Na) and ammonoacidic (NH<sub>4</sub>Cl) mineralizer was used. The autoclave was filled with 40 ml, this corresponds to 41 % filing degree. During reaction at 550 °C 1805 bar pressure were achieved. Since this value is higher than expected a chemical reaction takes place and H<sub>2</sub> is produced by decomposition of NH<sub>3</sub> and responsible for the higher pressure. The obtained product consist of GaN and NaNH<sub>2</sub> due to high amount of Na in the starting material mixture.

In a further reaction in supercritical ammonia, an alloy of Ba and Al was used as starting material for synthesis of BaAl<sub>2</sub>(NH<sub>2</sub>)<sub>8</sub> · 2 NH<sub>3</sub>. By the use of an Al-substrate,

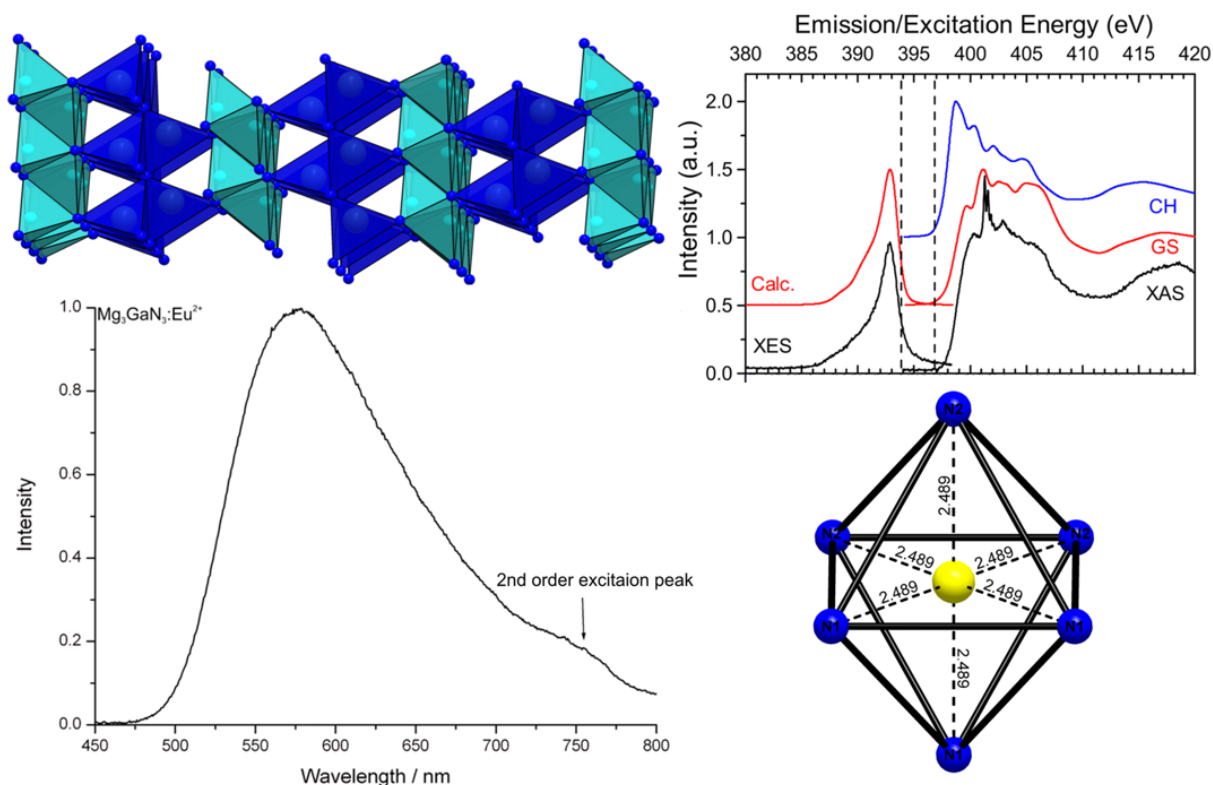


single crystals of acceptable size could be obtained. The crystals are stable at temperatures lower than -35 °C in ammonia atmosphere. Single-crystal X-ray diffraction was performed and the structure could be solved and refined in the space group  $R\bar{3}c$  (no. 167) with  $a = 15.7370(17)$  and  $c = 28.804$  Å. The crystal structure of the amide is built up of isolated Al(NH<sub>2</sub>)<sub>4</sub>-

tetrahedra, stabilized through hydrogen-bonds. In the resulting channels in the structure, Ba atoms are located, coordinated by 9 N-atoms whereof two of them belong to disordered NH<sub>3</sub>-molecules. Additionally, free NH<sub>3</sub>-molecules are inside channels as well, further stabilizing the crystal structure.

## 10.2. Magnesium Nitrides with Luminescence Properties $\text{Mg}_3\text{GaN}_3:\text{Eu}^{2+}$ and $\text{Mg}_3\text{N}_2:\text{Eu}^{2+}$

Chapter 3, page 24



The double nitride  $\text{Mg}_3\text{GaN}_3$  was obtained from reaction of the metals in Na-flux with  $\text{NaN}_3$  as nitrogen source. The crystal structure ( $R\bar{3}m$  (no. 166),  $a = 3.3939(5)$  and  $c = 25.854(5)$  Å) contains  $\text{MgN}_4$ -tetrahedra as well as miscellaneously occupied (Mg/Ga) $\text{N}_4$ -units. These tetrahedra are sharing common corners and edges whereby a three-dimensional network derives. This network is uncharged and all atoms are part of the tetrahedral network. Therefore,  $\text{Mg}_3\text{GaN}_3$  is a double nitride. with MAPLE calculations, the crystal structure was confirmed. Upon doping with  $\text{Eu}^{2+}$   $\text{Mg}_3\text{GaN}_3$  shows luminescence ( $\lambda_{\text{Em.}} = 578$  nm,  $\text{FWHM} = 4052$   $\text{cm}^{-1}$  (132 nm),  $x = 0.491$ ,  $y = 0.498$ ,  $\text{LE} = 132$  lm/W). It is assumed that  $\text{Eu}^{2+}$  occupies interstitial, octahedral voids of the crystal structure. Band gap was determined by soft X-ray absorption and emission measurements and compared to theoretical values from first principle DFT calculations. In good agreement of both methods,  $\text{Mg}_3\text{GaN}_3$  reveals a band gap of 3.0 eV.

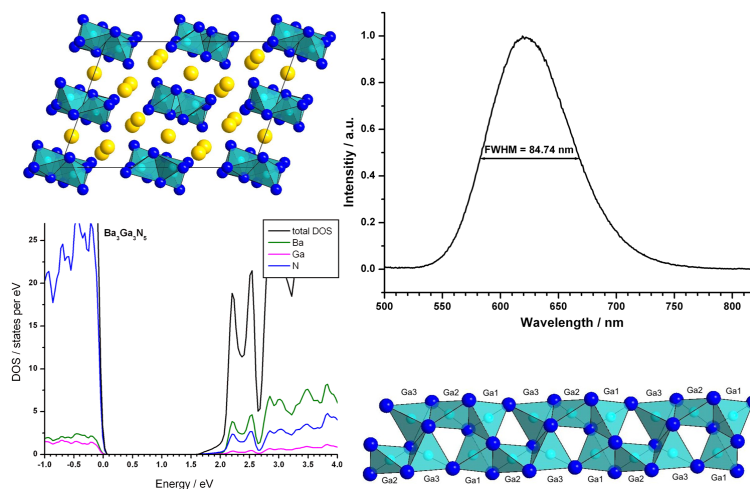
In an analogue synthesis  $\text{Mg}_3\text{N}_2$  could be obtained from Mg-metal in Na-flux. Additionally, Sr and Ge were part of starting material mixture and seem to improve

crystallinity of the product. Single crystals were obtained, investigated by X-ray diffraction. The refined lattice parameters ( $Ia\bar{3}$  (no. 206),  $a = 9.9550(11) \text{ \AA}$ ) and crystal structure comply with values from data reported before.  $\text{Eu}^{2+}$ -doped samples show also luminescence ( $\lambda_{\text{Em.}} = 589 \text{ nm}$ ,  $\text{FWHM} = 4056 \text{ cm}^{-1}$  (147 nm),  $x = 0.509$ ,  $y = 0.480$ ,  $\text{LE} = 317 \text{ lm/W}$ ) when irradiated with UV to blue light.

### 10.3. Ternary Novel Nitridogallate $\text{Ba}_3\text{Ga}_3\text{N}_5$

Chapter 4, page 47

The ternary nitridogallate  $\text{Ba}_3\text{Ga}_3\text{N}_5$  was obtained as single crystals after reaction of Ba and Ga in Na-flux with  $\text{NaN}_3$  at  $760^\circ\text{C}$ . Sr and Ge were also present in the starting materials mixture but were not part of the crystalline product. The crystal structure was solved and refined in space group  $C2/c$  (no. 15) with  $a = 16.801(3)$ ,  $b = 8.3301(2)$ ,  $c = 11.623(2) \text{ \AA}$  and  $\beta = 109.92(3)^\circ$ . The  $\text{GaN}_4$ -tetrahedra are highly condensed, building strands running along  $[010]$ . The coordination number of the Ba-atoms varies from 4 to 8. Therefore, the crystal structure differs strongly from isoelectronic compound  $\text{Sr}_3\text{Ga}_3\text{N}_5$ . Calculations of the electronic structure were carried out and revealed an

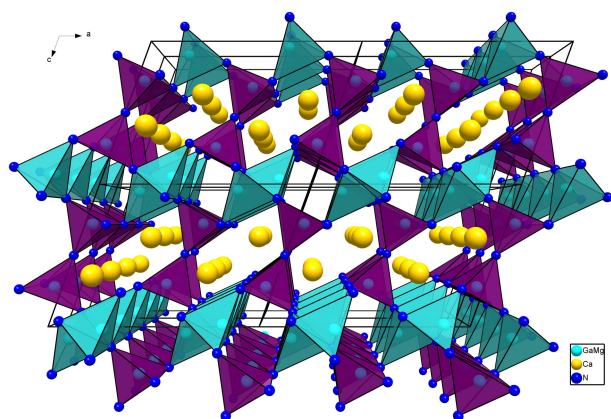


electronic band gap of 1.46 eV for  $\text{Ba}_3\text{Ga}_3\text{N}_5$  and 1.53 eV for  $\text{Sr}_3\text{Ga}_3\text{N}_5$ .  $\text{Eu}^{2+}$ -doped samples of  $\text{Ba}_3\text{Ga}_3\text{N}_5$  show luminescence ( $\lambda_{\text{Em.}} = 638 \text{ nm}$ ,  $\text{FWHM} = 2123 \text{ cm}^{-1}$  (84.7 nm),  $x = 0.644$ ,  $y = 0.347$ ,  $\text{LE} = 173 \text{ lm/W}$ ) when irradiated with 365 nm. Due to luminescence characteristics it is assumed that  $\text{Eu}^{2+}$  is located on octahedrally coordinated sites.

### 10.4. Quaternary Nitrido-magnesiogallate $\text{Ca}_2\text{Ga}_3\text{MgN}_5$

Chapter 5, page 63

A novel quaternary nitridogallate is reported, crystallizing in monoclinic spacegroup  $C2/m$  (no. 12,  $a = 11.160(2)$ ,  $b = 3.2965(7)$ ,  $c = 8.006(2)$  Å and  $\beta = 109.93(3)^\circ$ ). In this magnesio-nitridogallate, miscellaneously occupied (Mg/Ga) $N_4$ -tetrahedra are found since the ionic radii of fourfold coordinated  $Ga^{3+}$  and  $Mg^{2+}$  are comparable. These miscellaneously occupied tetrahedra are connected via vertices or edges and vertices, building a three-dimensional network. Along [010] hexagonal and quadratic rings are observed, stacked in this direction forming channels. In these hexagonal rings, the Ca-atoms of the crystal structure are incorporated. These features of the crystal structure of  $Ca_2Ga_3MgN_5$  resemble to the crystal structure of  $Sr_2Si_5N_8$  and both are compared.

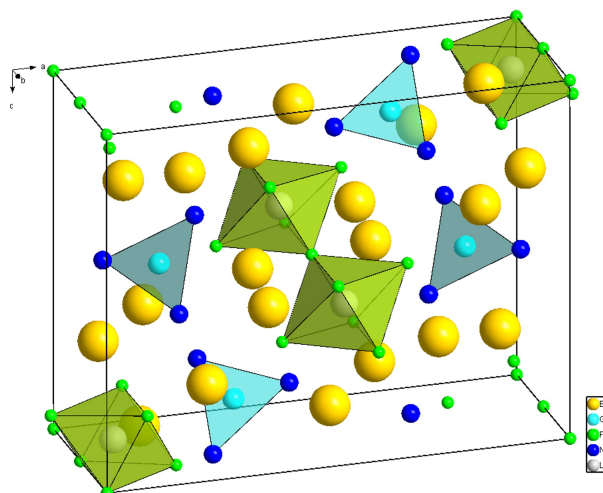


rings are observed, stacked in this direction forming channels. In these hexagonal rings, the Ca-atoms of the crystal structure are incorporated. These features of the crystal structure of  $Ca_2Ga_3MgN_5$  resemble to the crystal structure of  $Sr_2Si_5N_8$  and both are compared.

### 10.5. Nitridogallate Fluoride $LiBa_5GaN_3F_5$

Chapter 6, page 76

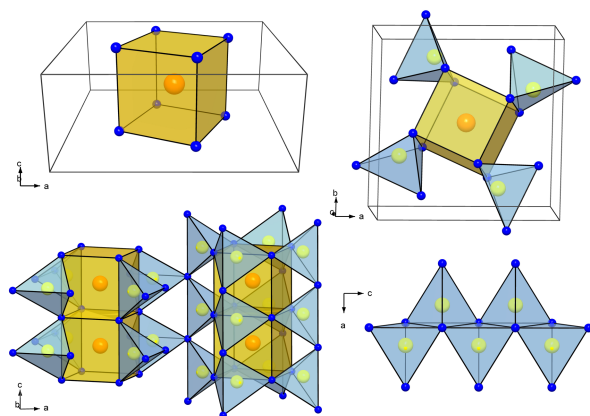
The lithium and fluorine containing compound  $LiBa_5GaN_3F_5$  was obtained by variation of fluxing agent using a mixed Li and Na-melt.  $EuF_3$  served as F-source and was initially employed for doping reasons. After reaction of the metals Ba and Ga with  $NaN_3$  and the starting materials mentioned above at  $760^\circ C$  red needle shaped crystals were obtained. The crystal structure ( $Pnma$  (no. 62),  $a = 15.456(3)$ ,  $b = 5.707(1)$  and  $c = 12.259(3)$  Å) contains  $LiF_6$ -octahedrons, sharing vertices and zigzag chains are built, running along [010]. Ga is coordinated by three N-atoms in isolated trigonal planar units, perpendicular to the chains of octahedrons. Investigations of the band gap were performed on  $LiBa_5GaN_3F_5$  by calculations of the electronic structure (1.6 eV) as well as extinction measurements on single crystals (1.9 eV).



## 10.6. Novel Nitrido-magnesiometalates of Ga and Al

Chapter 7, page 90

Several novel nitride-magnesioaluminates ( $A[Mg_2Al_2N_4]$ ,  $A = \text{Eu, Ca, Sr}$ ) and a novel nitride-magnesiogallate ( $Ba[Mg_2Ga_2N_4]$ ) are presented as well as solid solutions in and between those two compound classes. All of them crystallize in tetragonal space



group  $I4/m$  (no. 87). The tetrahedra in the respective crystal structures are miscellaneously occupied by Al and Mg or Ga and Mg. The atoms of the electropositive elements (Ca, Sr, Ba, Eu) are coordinated by eight N-atoms in a nearly cubic surrounding. By edge and corner sharing the tetrahedra are building a three-dimensional network

with quadrangular channels, partly filled with atoms of the electropositive elements. Solid solutions were carried out on nitride-magnesiogallates, mixing Sr and Ba and nitride-magnesioaluminates mixing Ca and Sr. Additionally, the tetrahedral site was occupied by all three elements Mg, Al and Ga. To obtain these compounds, different synthesis routes were used and are described as well as crystal structure elucidation.

## 11. Appendix

### 11.1. List of Publications within this thesis

**Magnesium Double Nitride  $\text{Mg}_3\text{GaN}_3$  and Binary Nitride  $\text{Mg}_3\text{N}_2$  as New Host Lattices for  $\text{Eu}^{2+}$ -Doping – Synthesis, Structural Studies, Luminescence and Band Gap Determination**

F. Hintze, N. W. Johnson, M. Seibald, D. Muir, A. Moewes W. Schnick, *Chem Mater.* **2013** (accepted).

*For this publication synthesis of the samples, literature research, formulation of the manuscript main part, MAPLE calculations, and localization of vacancies for  $\text{Eu}^{2+}$  in the crystal structure were done by Frauke Hintze as well as crystal structure determination with assistance of Markus Seibald. Synchrotron experiments and analysis of these data were done by Neil W. Johnson and David Muir in the group of Alexander Moewes. Luminescence investigations were done in LDC Aachen by Detlef Wiechert and Dr. Peter Schmidt.*

**Novel Nitrido-magnesiogallates, Nitrido-magnesiogallates and Solid Solutions of  $\text{AE}[\text{Mg}_2\text{Ga}_{2-x}\text{Al}_x\text{N}_4]$  ( $x = 0-2$ ,  $\text{AE} = \text{Ca}, \text{Sr}, \text{Ba}$ )**

Frauke Hintze, Philipp Pust, Andras Locher, Daniela Zitnanska, Sascha Harm, Wolfgang Schnick, (to be submitted).

*Synthesis of novel nitrido-magnesiogallates, crystal structure investigation, comparisons to nitrido-magnesiogallates and formulation of parts of the manuscript were done by Frauke Hintze. Philipp Pust synthesized with assistance of Andreas Locher, Daniela Zitnanska and Sascha Harm novel nitrido-magnesiogallates. He also wrote parts of the manuscript, carried out single crystal and powder diffraction investigations on nitrido-magnesiogallates and produced the pictures included in this manuscript.*



**Ammonothermal Synthesis and Crystal Structure of  $\text{BaAl}_2(\text{NH}_2)_8 \cdot 2 \text{NH}_3$**

Philipp Pust, Sebastian Schmiechen, Frauke Hintze, Wolfgang Schnick, *Z. Anorg. Allg. Chem.* **2013**, 639, 1185.

*For this publication, Frauke Hintze developed and installed the used autoclaves and the filling device. Synthesis and crystal structure determination were carried out by Philipp Pust. Sebastian Schmiechen also assisted in installing the filling device.*

**$\text{Ca}_2\text{Ga}_3\text{MgN}_5$  – A Highly Condensed Nitridogallate**

F. Hintze, W. Schnick, *Z. Anorg. Allg. Chem.* **2012**, 638, 2243.

*For this publication, Frauke Hintze carried out synthesis of  $\text{Ca}_2\text{Ga}_3\text{MgN}_5$ , crystal structure investigations, MAPLE calculations and comparison to nitridosilicate as well as formulation of the manuscript.*

**$\text{Ba}_3\text{Ga}_3\text{N}_5$  – A Novel Host Lattice for  $\text{Eu}^{2+}$ -Doped Luminescent Materials with Unexpected Nitridogallate Substructure**

F. Hintze, F. Hummel, P.J. Schmidt, D. Wiechert, W. Schnick, *Chem. Mater.* **2012**, 24, 402.

*Frauke Hintze carried out synthesis of  $\text{Ba}_3\text{Ga}_3\text{N}_5$ , crystal structure investigations and formulation of the manuscript. DFT calculations were done by Franziska Hummel, luminescence investigations were done by Detlef Wiechert and Peter J. Schmidt at the LDC Aachen.*

**A Novel Nitridogallate Fluoride  $\text{LiBa}_5\text{GaN}_3\text{F}_5$  – Synthesis, Crystal Structure, and Band Gap Determination**

F. Hintze, W. Schnick, *Solid State Sci.* **2010**, 12, 1368.

*For this publication, Frauke Hintze carried out synthesis of  $\text{LiBa}_5\text{GaN}_3\text{F}_5$ , crystal structure investigations and formulation of the manuscript. DFT calculations were carried out in cooperation with Daniel Bichler at LMU Munich (group of Prof. Johrendt). Band-gap measurements were carried out in the group of Prof. Glaum, Bonn.*

## 11.2. Publications published prior to this thesis

### Utilising Metal Melts of Low-Melting Metals as a Novel Approach for MOF

#### Synthesis: The 3D-Imidazolate $^3_\infty[\text{Ga}_2(\text{Im})_6\text{ImH}]$ from Gallium and Imidazole

A. Zurawski, F. Hintze, K. Müller-Buschbaum, *Z. Anorg. Allg. Chem.* **2010**, 636, 1333.

### Low Temperature Precursor Route for Highly Efficient Spherically Shaped LED-Phosphors $\text{M}_2\text{Si}_5\text{N}_8:\text{Eu}^{2+}$ (M = Eu, Sr, Ba)

M. Zeuner, F. Hintze, W. Schnick, *Chem. Mater.* **2009**, 21, 336.

## 11.3. CSD Numbers

Crystallographic data were deposited with the Fachinformationszentrum Karlsruhe (76344 Eggenstein-Leopoldshafen, Germany, fax: (+49)7247-808-666; e-mail: [crysdata@fiz-karlsruhe.de](mailto:crysdata@fiz-karlsruhe.de)) and are available on quoting the respective CSD depository number.

Compound	CSD-number	Compound	CSD-number
$\text{Mg}_3\text{GaN}_3$	425108	$\text{BaAl}_2(\text{NH}_2)_8$	425323
$\text{Mg}_3\text{N}_2$	425109	$\text{CaMg}_2\text{Al}_2\text{N}_4$	425319
$\text{Ba}_3\text{Ga}_3\text{N}_5$	423521	$\text{SrMg}_2\text{Al}_2\text{N}_4$	425321
$\text{Ca}_2\text{Ga}_3\text{MgN}_5$	425083	$\text{EuMg}_2\text{Al}_2\text{N}_4$	425320
$\text{LiBa}_5\text{GaN}_3\text{F}_5$	421592	$\text{BaMg}_2\text{Ga}_2\text{N}_4$	425318

#### 11.4. Conference contributions

*„Synthesis approach to promising nitride host lattices“* (poster)

D. Durach, F. Hintze, C. Pösl, W. Schnick

XIth International Krutyn Summer School 2012, “Cutting-Edge Luminescent Materials: Shifting the Frontiers” 23.09 – 29.09.2012, Krutyn, Polen

*„Hochkondensierte Nitridogallate als Wirtsgitter für  $\text{Eu}^{2+}$ -Dotierung“* (poster)

F. Hintze, W. Schnick

Vortragstagung Fachgruppe Festkörperchemie und Materialforschung GDCh  
17.09. – 19.09.2012, Darmstadt, Deutschland

*„Synthesis and Analysis – Strategies for New Phosphor Materials“* (poster)

F. Hintze, M. Seibald, P. Pust, S. Schmiechen, W. Schnick

Phosphor Global Summit 20.03. – 22.03.2012, Scottsdale AZ, USA

*„Nitride Phosphor Materials - Research, Application and Pertinence“* (poster)

S. Schmiechen, F. Hintze, M. Seibald, P. Pust, W. Schnick

Phosphor Global Summit 20.03. – 22.03.2012, Scottsdale AZ, USA

*„GaNz schön verkantet“* (oral presentation)

F. Hintze, W. Schnick

Hemdsärmelkolloquium, 08.03. – 10.03.2012, Oldenburg, Deutschland

*„Nitridogallat“* (oral presentation)

F. Hintze, W. Schnick

Festkörper-Seminar Hirschegg, 03.06. – 06.06.2010, Hirschegg, Österreich

## 11.5. Curriculum Vitae

### Personal Data

---

Name: Frauke Charlotte Hintze  
 Date of birth: 13. April 1985  
 Place of Birth: Munich, Germany  
 Nationality: German

### Academic Career

---

since 03/2013	Scientist at OSRAM, Research and Development
since 09/2009	PhD thesis in inorganic chemistry topic: Synthetic Strategies to Novel Multinary Nitrides of Gallium
02/2009 – 07/2009	Master thesis at the chair of inorganic chemistry Supervisor: Prof. Dr. W. Schnick Topic: „Synthesis and Characterization of novel Nitridogallates and Structure Investigations of Nitridogermanates“
10/2007 – 07/2009	Study Master of Science, Chemistry
06/2007 – 10/2007	Bachelor thesis at the chair of inorganic chemistry Supervisor: Prof. Dr. W. Schnick Topic: „About the Formation of Nitridosilicates using Nitrogen Containing Precursors and their Influence on Morphology and Luminescence Properties
10/2004 – 10/2007	Study Bachelor of Science, Chemistry

## **Education**

---

06/2004	Allgemeine Hochschulreife (A-Levels)
09/1995 – 06/2004	High-school education at Gymnasium Grafing
09/1991 – 07/1995	Primary school education at Grundschule Pöding

## **Advanced Qualification**

---

10/2010	Project management course (Dr. L. von Hippel, Allessa Chemie)
04/2011	European Patent Academy „Chemistry and patents – success for innovation“ (R. Lutz, European Patent Office)
06/2012	„Constructive conflict resolution“ (People management LMU)